TAL
TECH

DOCTORAL THESIS

Research and Development of Measurement Solution and Methodology for Assessment of Light Reflection from Surfaces

Toivo Varjas

Research and Development of Measurement Solution and Methodology for Assessment of Light Reflection from Surfaces

TOIVO VARJAS

TALLINN UNIVERSITY OF TECHNOLOGY
School of Engineering
Department of Electrical Power Engineering and Mechatronics
This dissertation was accepted for the defence of the degree 14/11/2021

Supervisor: Tenured Associate Professor Argo Rosin, Dr.Sc.Eng.
                                          School of Engineering
                                          Tallinn University of Technology
                                          Tallinn, Estonia

Opponents: Docent (Optical Metrology), Senior University Lecturer
                                          Petri Olavi Kärhä, Dr.Sc.
                                          School of Electrical Engineering
                                          Department of Signal Processing and Acoustics
                                          Aalto University
                                          Helsinki, Finland

                                          Associate Professor, Anna Mutule, Dr.Sc.ing.
                                          Faculty of Electrical and Environmental Engineering
                                          Institute of Power Engineering
                                          Riga Technical University
                                          Riga, Latvia

Defence of the thesis: 15/12/2021, Tallinn

Declaration:
Hereby I declare that this doctoral thesis, my original investigation and achievement, submitted for the doctoral degree at Tallinn University of Technology has not been submitted for doctoral or equivalent academic degree.

Toivo Varjas

_____
                                          signature

European Union
European Regional
Development Fund

Investing
in your future

Mõõtelahenduse ja -metoodika uurimine ning arendamine pindadelt valguse peegeldumise hindamiseks

TOIVO VARJAS

Contents

List of publications

The list of author's publications, on the basis of which the thesis has been prepared:

I Kuusik, M.; Varjas, T.; Rosin, A. (2016). Case Study of Smart City Lighting System with Motion Detector and Remote Control. Proceedings of the IEEE International Energy Conference (EnergyCon): 2016 IEEE International Energy Conference (ENERGYCON), Leuven, Belgium, 4-8 April 2016. Leuven, Belgium: IEEE, 1–5. 10.1109/ENERGYCON.2016.7513906.

II Armas, J.; Ivanov A.; Varjas T. (2017). Short-Circuit Currents Calculations in Street Lighting Networks. 58th International Scientific Conference on Power and Electrical Engineering of Riga Technical University, RTUCON 2017, Riga, Latvia, 2017-November. IEEE, 1–9, doi: 10.1109/RTUCON.2017. 8124758

III Varjas, T.; Kuusik, M.; Armas, J.; Rosin, A. (2018). Assessment of pedestrian crossings measuring parameters and implementation of new measuring methods in Estonia. 59th International Scientific Conference on Power and Electrical Engineering of Riga Technical University: 2018 IEEE 59th International Scientific Conference on Power and Electrical Engineering of Riga Technical University (RTUCON), Riga, Latvia, 12-13 November 2018. IEEE, 1–4, doi: 10.1109/RTUCON.2018.8659822

IV Korõtko, T.; Rosin, A.; Varjas, T.; Ahmadiahangar, R. (2020). Awareness of BSR Municipalities about Sustainable Urban Lighting and Green Public Procurements. 2020 IEEE International Conference on Environment and Electrical Engineering and 2020 IEEE Industrial and Commercial Power Systems Europe (EEEIC / I&CPS Europe). Madrid, Spain: IEEE, 1–6. doi: 10.1109/EEEIC/ICPSEurope49358.2020.9160761.

V De Luca, F.; Sepulveda, A; Varjas, T. (2021). Static Shading Optimization for Glare Control and Daylight. Towards a New, Configurable Architecture, Proceedings of the 39th eCAADe Conference: eCAADe 2021 - Towards a New, Configurable Architecture, Faculty of Technical Sciences, University of Novi Sad, Novi Sad, Serbia, 8-10 September 2021. Ed. Stojakovic, V.; Tepavcevic, B. Education and research in Computer Aided Architectural Design in Europe, 419–428.

VI Sepulveda, A.; De Luca, F.; Varjas, T. (2021). Influence of daylight modeling decisions on daylight provision and glare protection. Proceedings of the Symposium on Simulation for Architecture and Urban Design (SimAUD): 2021 Symposium on Simulation for Architecture and Urban Design, A. Chronis, G. Wurzer, W.E. Lorenz, C.M. Herr, U. Pont, D. Cupkova, G. Wainer, Online, 15-17 April 2021. ACM Digital Library [forthcoming].

VII Varjas, T.; Laaneots, R.; Rosin, A. (2021). European Patent Application no EP3839482 (A1) Method and Device for Measuring Charcteristics of Refelection of Light on Surfaces. Available: https://espacenet.com. Publication 2021-06-23.

Author's contribution to the publications

Contribution to the papers in this thesis are:

I   Main co-author; paper writing, responsible for the literature overview, data collection, measurements, calculations and analysis.

II   Main co-author; paper writing, responsible for data collection and methodology analysis.

III Main author; paper writing, responsible for the literature overview, data collection, measurements, calculations and analysis. Presentation of the paper at the 2018 IEEE 59th International Scientific Conference on Power and Electrical Engineering of Riga Technical University (RTUCON) in Riga.

IV   Main co-author; paper writing, responsible for the literature review, data collection and analysis.

V   Main co-author; responsible for the literature overview, experimental measurements, analysis and co-authored writing.

VI   Main co-author; responsible for the literature overview, experimental measurements, analysis and co-authored writing.

VII Main author; drafting the patent claim, responsible for the literature review, data collection, development of a new measurement experimental instrument prototype, measurements, development and analysis of measurement methodologies.

Abbreviations

BMC	Best measurement capability; minimum possible expanded uncertainty
CIE	Commission Internationale de l'Eclairage International Commission on Illumination
CEN	European Committee for Standardization
DIALux	Lighting design software
EN	European National (Standards)
EMPIR	European Metrology Programme for Innovation and Research
GUM	Guide to the expression of uncertainty in measurement
HPS	High-pressure sodium
LabSoft	Lighting measurement software
LED	Light-emitting diode
ILMD	Image luminance measuring device
M1 – M6	European lighting class
MPE	Maximum permissible measurement error
RELUX	Lighting design software
SSL	Solid-state lighting

Symbols

a	Limit value for a distribution; variation limit
a_{xj}	Limit value for a measurement error or uncertainty contributor in the units of the result of measurement; variation limit
a^*_{xj}	Limit value for an error or uncertainty contributor in the unit of the influence quantity; variation limit
b	Ratio; distribution factor
β	Angle between the oriented vertical planes through the observer to the point of observation and from the point of observation through the luminaire (with respect to luminance coefficient)
c	Sensitivity factor from a_{xj} to a_{jx}
CCT	Correlated colour temperature [K]
d	Resolution of a measurement instrument; step of the last decimal place of the number; rounded value of the result of measurement; step of rounding; etc.
ε	Angle between the light path at a point on a surface and the normal to the surface
$\bar{E}$	Average illuminance (on a road area) horizontal illuminance averaged over a road area [lx]
E_{min}	Minimum illuminance (on a road area) lowest illuminance on a road area [lx]
E_v	Vertical plane illuminance (at a point) illuminance on a vertical plane [lx]
$E_{v\,min}$	Minimum vertical plane illuminance (at a plane above a road area) lowest vertical plane illuminance on a plane at a specified height above the road area [lx]
f	Function of multiple input quantities, ie $f(X_1, X_2, \ldots X_j, \ldots X_N)$
f_{TI}	Threshold increment TI (of an object at the road surface)
Φ	Luminous flux [lm]
$\Phi(\lambda)$	Spectral radiant power [W nm^{-1}]
h	Hysteresis
i	Order markings of dimensions; order of readings
I	Luminous intensity distribution
IR	Infrared
j	Sequence identifier of the input quantity; sequence identifier of combined standard uncertainty component
k	Coverage factor
l	Length
L	Average road surface luminance (of a carriageway of a road) luminance of the road surface averaged over the carriageway. Unit is candelas per square meter [cd/m^2]
L_{av}	Average luminance [cd/m^2]
L_{max}	Maximum luminance [cd/m^2]
L_{min}	Minimum luminance [cd/m^2]

m	Sequence number of the approximate number of cycles
n	Total number of dimensions; total number of values
N	Total input quantity x_j
p	Number of independent combined standard uncertainty components
q	Number of dependent combined standard uncertainty components
q_L	Luminance coefficient; quotient of the luminance of a surface element in a given direction by the illuminance on the surface element
r	Correlation factor
r_L	Reduced luminance coefficient; luminance coefficient of a surface element multiplied by the cube of the cosine of the angle of incidence of the light on the surface element
$s(x_j)$	Standard deviation of the jth set of measured quantity values
$s(x_j)_i$	Standard deviation of sample i
$s(\bar{x}_j)$	Standard deviation of the arithmetic mean of the measured quantity values of the j input quantity
S/P	Ratio of Scotopic to Photopic lumens
t	Student's margin calculated from the t-distribution
t_i	Margin factor for the ith sample
ΔT	Temperature difference
TI	Threshold increment [%]
u	Standard uncertainty
u_{jL}	Standard uncertainty of the jth combined standard uncertainty component
u_{xj}	Standard uncertainty of the value of the jth input quantity (influence quantity)
u_{xjt}	Actual standard uncertainty of the jth input quantity
$u(y)$	Combined standard uncertainty of the result of measurement
U	Expanded uncertainty of the result of measurement
U_l	Longitudinal uniformity (of road surface luminance of a carriageway); lowest of the longitudinal uniformities of the driving lanes of the carriageway
U_0	Overall uniformity (of road surface luminance, illuminance on a road area or hemispherical illuminance) ratio of the lowest to the average value
UV	Ultraviolet
$V(\lambda)$	CIE photopic spectral luminous efficiency function
$V(\lambda')$	CIE scotopic spectral luminous efficiency function

1 Introduction

Urban lighting is required to have a central role in the design of future smart cities. The term urban lighting refers to both, street and other lighting installations (e.g., recreational areas, infrastructure etc.). Substantial part of energy consumption in Europe originates from urban areas that produce notable emissions of greenhouse gasses. Over 90 million lighting poles worldwide count for more than 50% of public energy consumption and about 60% of relative costs [1]. By 2050, nearly 70% of the world's population will live in urban areas, creating challenges and opportunities for municipalities and industries, where digital technology will function as a catalyst for urban transformation towards more efficient and livable cities [2]. In future cities, street lighting will play an essential role in security and life quality. Modern lighting control systems are capable of adapting lighting conditions to suit the user, thus improving personal wellbeing and perceived quality of life [3]. Modern luminaires and control systems provide effective street lighting, which can reduce crime and traffic collisions, but also encourage socio-economic activities at night and improve the perception of personal safety and security [4]. Innovations in lighting, such as solid-state light emitting diodes (LED), promise energy savings of about one half and a notable reduction of maintenance costs [1].

Electricity consumed by lighting accounts for approximately 20% of world electricity consumption [5]. Therefrom, an estimated 5% is used by public lighting like street lighting, parking lots lighting, pedestrian area lighting, and park lighting [6]. Continual rise in electric energy price has put municipalities in a situation where they need to find possibilities for saving, also in street lighting. It is common that after peak hours some luminaires are switched off. This does indeed considerably reduce electric energy consumption, but it also creates inferior lighting solutions and significantly diminishes traffic safety in urban areas. Although it could be assumed that classical lighting technologies are now ready, the light efficiency of light sources, together with light quality indicators, has not yet reached its limits. It is especially important to increase the reliability of lighting systems and their efficiency through control systems. It has also become important to improve the quality of visible light in the nocturnal movement environment, taking into account human scotopic and mesopic vision, which is significantly different from daytime photopic vision [III]. Also, it is required to take into account the current revolutionary developments in solid-state lighting (SSL) and the introduction of new measuring devices for night vision.

Over the last decade, significant energy savings have been achieved in road lighting by replacing an obsolete lighting system with a new LED system. In the long run, it is already understood that energy savings will not increase in the coming years. In the future, savings will be made on switching to LED luminaires. The number of lighting points in urban areas is often increasing and the infrastructure needs to be replaced. Additional savings are seen to be achieved through the development of smart lighting systems. In addition to intelligent management aimed at energy saving, the Smart Cities solution requires the goal of lighting quality, better visibility and thus the safety of the traffic environment. Future street lighting solutions must allow for improved control and management capabilities, as well as sophisticated measurement capabilities, the integration of different control systems and the use of large-scale information networks. Intelligent control systems are mostly applied to reduce energy consumption by controlling the level of lighting according to user needs, environmental conditions and system maintenance. However, new design paradigms and metrics addressing these new

objectives are needed to ensure the same or even better safety for road users, to improve the quality of the lighting environment, and therefore it is not only necessary to measure the energy part but also the lighting quality [7].

The most important lighting parameters on which designers in most European Union countries base their outdoor lighting planning are presented in the standards CEN/TR 13201-1: 2014 and EN 13201 series [8]-[12]. These modern normative documents and measurement methodologies are based on photopic vision, which does not really appreciate the dominant mesopic environment in outdoor lighting. In recent years, measuring devices have been introduced to evaluate the mesopic photometry system [13], [14]. Modern road surface luminance measurement techniques based on ILMD (Image Luminance Measuring Device) photometry [15], [16] and measurement methods according to the standard EN 13201-4: 2015 have been applied to the measurement of road lighting [11]. These measuring devices allow us to evaluate the luminance and luminance distribution more efficiently and to offer safer solutions when implementing management systems in conflict areas.

At present, the introduction of new lighting solutions in street lighting is of great interest as a research topic and with numerous experiments in the design of new lighting systems. So far, road weighted q-data (r-tables) that are more than 30 years old have been used in road calculation programs. It is important to assess the modern lighting solutions and the quality characteristics of the light generated for reflection of the light of the characteristic quantities of the hitherto used and improve the measurement methods to simplify the mobile measuring device that is used on different sizes of road pavements to assess operatively the reflected beam, and the diversity of their size, while reducing the intensity of the measurements and increasing the accuracy of the measurement.

1.1 Motivation for this thesis

About 40 years ago, The Commission Internationale de l'Eclairage (CIE) launched the concept of developing and evaluating the luminance of road lighting through a number of methods [17]. In 1984, the CIE adopted a technical report on the relationship between the photomeric properties (reflective properties) of pavements and their construction (composition and texture) [18]. The material was primarily intended as a guide for outdoor lighting designers and road builders. This defined the so-called R-classification. The standard reflection classes R1, R2, R3 and R4 assigned to dry pavements were described as reflection tables or r-tables containing reduced luminosity coefficients. Internationally, several years after the publication of the r-tables, several scientific articles reported that road pavements have changed or that the aggregates used in different countries are different. [6]

In Estonia, from 1980 to 2004, there was some confusion in the design of street lighting due to the lack of a corresponding Estonian or European Union standard. Both USSR standards and international CIE standards were used. The CEN technical report CEN/TR 13201-1, translated by the Estonian Center for Standardization in 2004, provided a clearer basis for future guidelines for the design of outdoor lighting.

The r-tables in the CIE technical report were based on pavement reflectance measurements made more than 50 years ago. For the most part, no control measurements were performed in Estonia, and the use of correct input data from light calculations was a free choice for lighting designers. In 2007, CIE established new reporterships R4-32: Reflection Properties of Road Surfaces and R4-24 Definition of an

Eye Sensitivity Function in the Mesopic Region to be Used for the Calculation of Road Lighting Levels [14].

The perceived need is an important paradigm shift in the field of outdoor lighting design. The normative documents on which road construction is based have become obsolete, changes have taken place in the materials of road pavements. During the last decade, a revolutionary development has taken place in the technological advancement of luminaires. In addition, significant developments have emerged in the lighting measurement and control technology. Lighting at night and in dim conditions significantly affects a person's vision in these environments, and taking this into account, the creation and evaluation of surrounding lighting environment has become an important priority.

The Lighting Engineering Laboratory of the Department of Electrical Power Engineering and Mechatronics of Tallinn University of Technology, in cooperation with the largest local governments in Estonia, has promoted outdoor lighting research to create energy-efficient and safer environments. The vast majority of research focuses on the inspection of lighting installations using standard measurement techniques, the assessment and optimization of the energy efficiency of control systems, and topologies [19]-[21].

In the last decade, marked attention has been paid to update the values of luminance factors standardized for lighting simulation programs in the design and construction of road pavements and lighting installations. Constant innovations in the technologies of road surface and their lighting with modern lighting solutions have led to the assessment of values of light reflection from new points of view. Operational measurement of light reflection quantities from road pavement surfaces, such as luminance, luminance factor, reduced luminance factor, as well as light color temperature and color coordinates, allow for the development of more energy efficient and safer solutions.

It is required to implement modern technical solutions and develop new measurement methods that would ensure the use of optimized measurement geometry with pre-standardized instructions for environmental conditions and lighting solutions. The aim is to ensure the reliability and mobility of measurement results by reducing the measurement intensity and enabling the measurement of different sizes of pavement reflections, eliminating the effects of instantaneous properties of road lighting installations, weather and ambient conditions and extraneous and disturbing light and increasing measurement accuracy.

In summary, the following paradigm shift has been introduced in the design of outdoor lighting:

- Changes in lighting technology, pavement materials and lighting measurement;
- Changes in lighting quality aspects to create more energy-efficient and safer solutions;
- Demand to implement of novel technical solutions and develop measurement methods that ensure the use of optimized measurement geometry with standardized guidelines for environmental conditions and lighting solutions.

1.2 Thesis objectives

The main goal of this dissertation is to develop a metrological solution and methodology that allows us to evaluate human-specific lighting perceived in a dark environment, its better application in the design and management of road lighting installations. Existing measurement methodologies are addressed and new measurement technical solutions are proposed. The author set up a goal to offer a set of measurement tools for light quality aspects with a novel methodology for its implementation and evaluation of the uncertainty of measurement results.

1.3 Hypotheses

The main hypotheses of this dissertation are:
- More precise determination of lighting measurement uncertainty components such that the upper limit of the uncertainty component will ensure increased reliability of the measurement results.
- The developed new measurement method would reduce the measurement time and improve the measurement accuracy at least three times, minimize the effects of the ambient conditions and instantaneous properties.
- The new measurement method proposed will minimize the proportion of uncertainty components, which could reduce the expanded uncertainty of the measurement results of the lighting technical quantities of the pavement surface.
- The new measuring instrument designed will consider the effect of the spectral composition of the visual light and could improve the accuracy and time-saving of measurements.

1.4 Research tasks

The main research tasks of this dissertation are:
- State of the art analysis of the relationships between the most important lighting parameters that affect scotopic and mesopic lighting in a traffic environment; mesopic photometry and measurement applications; existing lighting measurement applications and methodologies used to evaluate outdoor lighting;
- Investigation of the difference between the results obtained when measuring the illuminance of outdoor lighting and developing a new simplified calculation methodology to assess the uncertainty of the results;
- Research and development of uncertainty management methodology for lighting measurements;
- Practical assessment of uncertainty using the developed management methodology- for lighting measurements;
- Development of an innovative measuring instrument and measurement methodology for the values characterizing reflection of light from surfaces;
- Validation of the developed measurement method and instrument.

1.5 Novelty

The scientific and practical novelty of this dissertation is:

1. Analysis and classification of current lighting measurement applications and measurement methodologies for outdoor lighting assessment;
2. Development of a new calculation methodology for estimating the difference in measurement results and all components of measurement uncertainty of outdoor lighting measurement applications;
3. Development of a new measurement application and creation of a measurement methodology;
4. Creation of a prototype of a patented invention and application of a measurement methodology for more efficient analysis of the lighting properties of various lighting solutions and road surfaces;
5. Introduction of a patented measuring instrument that would significantly reduce the volume of measurements for the evaluation of lighting parameters.

1.6 Contribution and dissemination

This research is recommended for outdoor lighting designers and road builders who can use the invented method and device for various modern road pavements illuminated by traditional gas discharge luminaires and modern LED luminaires to evaluate operationally changes in pavement wear and environmental changes. Thereby it is proposed to use safer and more efficient solutions, but also to create more energy-efficient and safer environmental conditions for the replacement and modernization of lighting solutions.

The methodology developed by the thesis research and the measurement tool created for its implementation, which considers human scotopic and mesopic vision in dark and dim environments, can assess the values of pavement light reflection values with innovative control systems used in modern road lighting.

The results of this dissertation have been presented at international scientific conferences and doctoral schools. The direct practical scientific results of this dissertation have been applied in the following international R&D projects: *VIR19013 "Lighting the Baltic Sea Region - Cities accelerate the deployment of sustainable and smart urban lighting solutions" and VFP19031 "FINEST TWINS: Establishment of Smart City Center of Excellence".* Additionally, the practical results of this study have been applied in the national research and development projects (*LEEEE21065, LEEEE20099, LEP19093*, etc) commissioned by the local municipalities or companies (i.e., Enefit Connect, Elektrilevi, Tallinn, etc.) by the accredited Lighting Laboratory of Tallinn University of Technology.

2 State of the art

2.1 Growing role of street lighting

Artificial lighting plays an indispensable role in everyday life today. The energy consumption of electric light sources accounts for about 20% of global electricity consumption, of which 5% is used in general lighting, such as street and car park lighting, pedestrian lighting and park lighting [6], [22]. The constant increase in electricity consumption has encouraged local governments to find ways to save on street lighting. Often some lights are switched off after peak hours, which allows significant reduction in electricity consumption. However, it also creates poorer lighting conditions and significantly impairs road safety in urban areas. Although it could be assumed that classical lighting technologies are now ready, the light efficiency of light sources, together with light quality indicators, has not yet reached its limits. The target is to increase the reliability of lighting systems and their efficiency through control systems as well as to improve the quality of visible light in the nocturnal movement environment, taking into account human scotopic and mesopic vision, which is significantly different from photopic or daytime vision. Also, the current revolutionary developments in semiconductor light (SSL) enable the introduction of new measuring devices for night vision. [23]

Road and street lighting plays a very important role and its running costs are high, often accounting for around 30% to 50% of the city's total energy consumption. As a result, there is a strong pressure on electricity supply and environmental protection. It is estimated that by 2050, 5 billion people, or about 60% of the world population, will live in cities, and according to the International Energy Agency, by 2030, demand for lighting alone will be 80% higher than in 2005. [24], [25]

The potential for the energy efficiency improvement of outdoor lighting is substantial. The condition of the outdoor lighting network has improved in larger Estonian cities. In 2015, street lighting was renewed in seven major cities, during which more than 12 000 luminaires were installed, including the replacement of cable lines and masts.

Network reconstruction works are ongoing. Additional luminaires will also be installed on the pedestrian crossings under construction. Often, in addition to the renewal of carriageways, there are also light traffic roads, parking lots and park areas in the surrounding areas. However, high pressure sodium lamps (HPS), metal halide (MH) lamps, and low pressure sodium lamps are still used in most municipalities. For example, as of the beginning of 2021, up to 33% of the luminaires installed in Tallinn, the capital of Estonia, are modern LED luminaires. If five years ago, most installations with LED luminaires were pilot projects, now under new projects, LED luminaires have been applied. Strong emphasis is placed on the development of management systems. [6], [24]

To reduce the energy consumption of lighting, the European Union has adopted the Ecodesign Directive for energy-related products (Directive 2009/125/EC) [26], which established a framework for setting of ecodesign requirements for energy-related products. The aim of the directive is to improve the environmental performance of products throughout their whole life cycle. The Directive does not set requirements for specific product categories, but defines the requirements for product authorization procedures in implementing measures. The requirements focus on the most important environmental aspects, such as the energy consumption of energy-using products [24].

2.2 Photometry in the evaluation of street lighting

2.2.1 Fundamentals of street lighting photometry

The method for photometric characterization of pavements was developed in the 1970s and updated in 1982 and 2001 [27], [28].

The International Commission on Illumination (CIE) reports describe quantities used to characterize photometry in road lighting.

In the European series of standards, EN 13201 defines luminance as the most important and perceptible parameter for drivers. Luminance is related to the intensity of the light from the road luminaires in the observed direction and to the reflective properties of the road surfaces in the observer's direction. The light emitted from the luminaires is assessed on the basis of the spatial distribution of the luminaire's luminous intensity. The luminous intensity distribution is measured with a goniometer, the modern output of which is light distribution data that can be used in light calculation simulation programs. Luminaire manufacturers have the necessary measuring instruments in their production processes to measure the light distribution data in order to improve the useful optical properties of the luminaires and to prevent light pollution. The amount of light reflected from the road surface, in turn, depends on the direction of observation, the angles of incidence and reflection, i.e., the geometry of the light. One characteristic quantity is the luminance coefficient of the pavement marked by q_L. Luminance coefficient describes the geometry of the coating material when reflected by light. Road lighting calculations are based on the tables of q_L values of different road pavements made decades ago, which were defined as reference pavements. National and EN standards also provide recommendations for checking the condition of road installations before and after the completion of roads.

In the EN 13201 series of European standards, luminance is one of the key parameters that road lighting must meet in order to ensure adequate and safe lighting for traffic in a dark environment. The luminance and luminance uniformity of the pavement properties of the light allow perceiving the surrounding environment, road conditions and possible obstacles on the road. In order to ensure a road lighting class according to CEN/TR 13201-1 in accordance with the characteristics of the road and traffic environment, the level of luminance required by the road lighting system must be ensured. The simulation of the road lighting system takes into account the power of the luminaires, the distance between the lighting masts and the height. In modern luminaires, the optical solution of the luminaires, the color temperature of the light and the control system for creating energy efficient solutions for road lighting are of particular importance. After installation, the photometric properties of the pavements also require control measurement of compliance with the simulations. [6]-[8], [29]-[31]

The luminosity coefficient q_L is the variable that characterizes best the reflection properties of different road surface pavements. The luminance factor is the ratio of the luminance L (cd/m^2) visible to the observer of the road surface, and the illuminance $\bar{E}$ in lux, which is incident on the surface and is given by the following equation (1):

$$q_L = L/\bar{E} \tag{1}$$

where:
q_L is the luminance coefficient measured in [sr^{-1}];
L is the luminance measured in [cd/m^2];
$\bar{E}$ is the illuminance measured in [lx].

Forty years ago, the luminance factor was replaced by a reduced coefficient r table called the *r*-table, where the luminance factor *r* is given by a combination of fixed illumination angles β and tan ε (see Figure 2.1). [30]
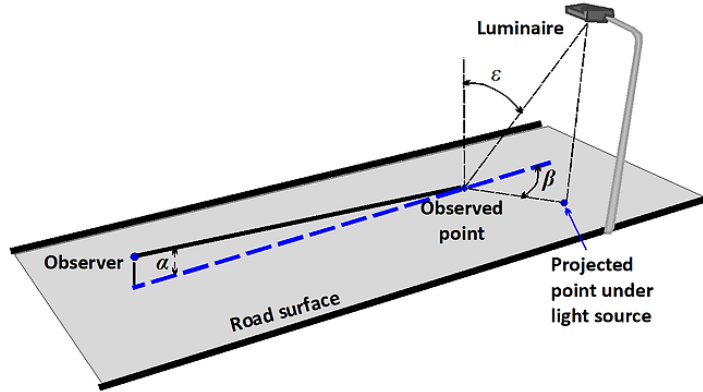
Figure 2.1 – By convention, according to CIE 066 and CIE 144, guidelines and road lighting standards, the photometric characteristics of the road surface depend on the angles of observation α (characterization of road photometry α is set at 1°), deviation β and surface. [11]

The formula for calculating the reduced luminance coefficient r_L in cd/m²/lux is derived from q_L (equation 2):

$$r_L = q_L \cos 3\varepsilon \tag{2}$$

In the standard EN13201, viewing height is 1,5 m and the viewing angle α is constant at 1°, at which the viewing distance corresponds to 86 m. In this situation, simulations and measurements are used to observe the detectable road area in front of the driver at a distance of 60 to 160 m represented in Figure 2.2. The illuminated area defined in the standard therefore applies to illuminated roads between cities where speeds are up to 90 km/h. [31]
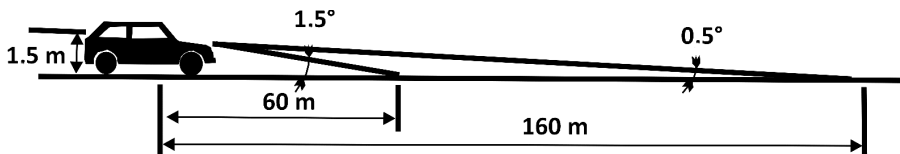
Figure 2.2 – Angle of observation at 1° (nominal value) but between 0,5° and 1,5° 60-160 m, assuming that there is no influence on road photometry.

The average luminance coefficient Q_0 represents the degree of lightness of the measured surface.

The average luminance coefficient Q_0 is computed as the average of the luminance coefficients over the specified solid angle, Ω_0 (equation 3):

$$Q_0 = \frac{1}{\Omega_0} \int q_L \, d\Omega \qquad (3)$$

As a result of the integration, the sum is obtained from the finite source data in the simulation calculations, which is close to the weighting factors corresponding to the integer angle assigned to each value $\Delta\omega$ and given to each combination of $\tan \varepsilon$ and β angles [15].

$$Q_0 = \sum q_L \times \Delta\omega \sum \Delta\omega \, Q_0 = \sum q_L \times \Delta\omega \sum \Delta\omega \qquad (4)$$

The reflection tables (r-tables) describe the reflection properties in the form of reduced luminance coefficients. The description parameters adopted by the CIE are the average luminance coefficient Q_0 and the specular factors S_1 and S_2.

The specular factor S_1 represents the degree of specularity of the observed surface. It is defined as the ratio of the reduced luminance factors (equation (5)) of two specific lighting conditions.

$$S_1 = \frac{r(\beta=0, \tan \varepsilon = 2)}{r(\beta=0, \tan \varepsilon = 0)} \qquad (5)$$
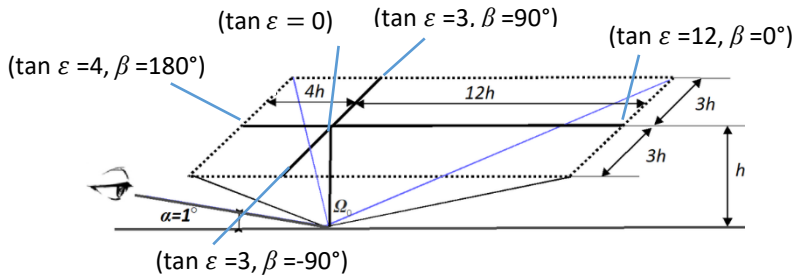
Figure 2.3 – Representation of a rectangular plane above the surface that defines [31]

- the boundaries of sight angle β and the incidence angle ε defined in CIE144 => values of the r-table

- the solid angle of integration of the coefficient Q_0.

The reflection tables in the standards used worldwide are based on the measurements made in Europe more than fifty years ago on a theoretical basis to assess the aging of pavements. The benchmarks published in the CIE technical reports have not been updated for decades and do not describe the lighting measurement uncertainty. [17], [18], [32], [33]

In recent decades, pavement materials and the binders used as well as traffic conditions, traffic regulations and behavior have changed significantly. Modern road lighting systems are designed based on existing standards using simulation software, which includes data

characterizing road pavements that do not correspond to the actual conditions or cannot be described. [34], [35]

Recent scientific studies eloquently describe the fact that using existing CIE data, we often use simulations to calculate average luminance above 50% of the actual values [36]. The technological developments in the LED luminaires used in the last decade, including dimming and innovative optical solutions with directed light distribution, have provided more energy-efficient solutions. Much attention has been paid to the estimation of measurement uncertainty. [20], [27], [37]

The EMPIR (European Metrology Program for Innovation and Research) research project SURFACE has set the goal to eliminate the shortcomings of road lighting photometry and to modernize the methodology [36].

The goal was to collect data and conduct research around the world for CIE, CEN and other road lighting communities. At the same time, the assessment paid close attention to existing measuring equipment and methods and to analyzing the safety needs of road users related to pavement reflections. The aim was to collect and submit to CIE and CEN new reference data on the most common pavements and to present new reference geometries for measuring lighting parameters. The updated data and measurement geometry should describe better the needs of road users and help to make the best use of smart LED lighting while reducing the environmental impact of road lighting equipment.

The SURFACE research project has pointed out that data collection is complex and, due to the specifics of the measurements, only a few European laboratories perform these measurements. For reasons of confidentiality, the collected r-tables are owned by the tenderer and the SURFACE consortium has undertaken not to disseminate or publish uniform r-table data. This means that CEN reference data do not consist of an identifiable r-table, but are simply representative averages. The database contains 40 tables from Switzerland, 182 from France and 18 sets of Q_0 and S_1 factors from Finland. [30]

2.2.2 Mesopic photometry

Photopic photometry has been used in lighting measurements since 1924. It has been the basis for the design of all lighting since the introduction of the photopic spectral luminance function $V(\lambda)$ [28]. Thus, all methods for estimating illuminance quantities are based on the photopic $V(\lambda)$ function. Artificial road lighting in the night environment is usually scotopic and in the dark mesopic. The spectral sensitivity of the human eye varies according to the level of light and the viewing conditions and is not uniform over the mesopic area of vision.

The International Commission on Illumination (CIE) published the technical report 191: 2010 based on visual performance of a recommended system for mesopic photometry. The new mesopic system offers, for the first time, the evaluation of illumination based on the internationally accepted mesopic photometry system. The new CIE mesopic photometric system is valid for luminosity between the scotopic and photopic regions, where the luminance is described as between 0,005 cd/m^2 and 5 cd/m^2. [13]

There are currently no guidelines for designing road lighting using mesopic photometry. European standards for average road surface luminance range from 0,3 cd/m^2 to 2 cd/m^2 located in the mesopic region. The ratio of the scotopic to the photopic luminous flux of luminaires used in road lighting should be evaluated according to the CIE scotopic spectral luminous efficiency function $V(\lambda')$. Light sources with a high S/P ratio are mesopically more efficient. Light sources that provide contrasting visibility are even more effective in mesopic conditions and can be used to reduce luminance on the road surface.

Mesopic photometry, a novel method for measuring illumination, takes into account the change in the visual response in the overlapping area of the human eye, between day vision and night vision.

With conical cells with different spectral sensitivities, human visual organs perceive colors in photopic vision mode. The central part of the retina of the eye has the highest concentration of cone cells. Stem cells are more sensitive to light but do not distinguish color. Also, rod cells are mostly found outside the fovea, which means that most of the night vision comes from the periphery.

The adaptation of the eye to dim light levels depends on the signal level of both types of photoreceptors. At low light levels, the high sensitivity of rod cells predominates. When rod cells become saturated, only cone cells detect high levels of light. Due to differences in spectral sensitivity, adaptation depends on the spectral quality of the incident light. It has also been found that adaptation occurs at different rates as light levels increase or decrease, and that adaptation occurs differently on the surface of the retina. [28], [38]

The retina consists of about six million cones, mostly located in the middle of the retina and surrounded by about 120 million rods. The cones responsible for seeing our colors work best in bright light, while the color-blind rods are responsible for seeing us at night. Scenes with an average luminance greater than about 5,0 cd/m^2 are dominated by photopic vision. The cones have an average spectral response described by the photopic light efficiency function *V(λ)* and a maximum sensitivity of 555 nm. Less than about 0,005 cd/m^2 is dominated by scotopic vision, the spectral response of the rods is described by the scotopic light efficiency function *V'(λ)*, with a maximum response of 507 nm.

Mesopic vision occurs when the average luminance of a scene is between from 0,005 to 5,0 cd/m^2, as both rods and cones contribute to what our visual system perceives.

The reason is the gradual transition to a photopically scotopic light efficiency function as the rods begin to dominate. Some publications on mesopic lighting state that the *S/P* ratio of a lamp can be estimated from its correlation-based color temperature (*CCT*), but this is incorrect, except for incandescent lamps (which have few practical applications for mesopic lighting). For example, there are two LED modules with the same *CCT* of 3500 K, but very different spectral power distributions and different *S/P* ratios. [39], [40]

2.3 Street lighting measurement

2.3.1 Reflective properties of road pavement materials

The reflective properties of the pavement material depend on the nature of the material. Pavement materials differ in the composition of the surface, the properties of the aggregate used, the color of the binder, the texture and used construction method. The used material depends to a large extent on regional availability in different countries, material quality requirements and environmental requirements. Standard *r*-tables and Q_0 values are commonly used in the design of road lighting. There is no correlation between the color temperature of light sources and pavement materials in the normative documents. This results in significant differences in road surface luminance values.

CIE Standard Publications have recommended the use of high-color, now discontinued incandescent lamps to measure the reflectance of coatings. The reflective properties of coating samples have often been studied under laboratory conditions in the light of a metal halide or a high-pressure sodium lamps. [41]-[44]

Global research has shown that newer asphalt-based and new concrete-based pavements do not meet the reflective properties given in the *r*-tables [45], [46].

For example, studies in Finland on the reflectivity of road surfaces carried out on samples of pavements cut under laboratory conditions concluded that most pavements belong to road classes R1 and R2, which are still in use today [47].

The choice of pavement materials is usually determined by mechanical strength, abrasion resistance, and slip resistance. Asphalt pavements use stone materials of different grains, mineral filters and binders, such as bitumen. The color of the asphalt pavement usually depends on the color of the aggregate and the environmental conditions. Changes in the assessment of the energy efficiency of road lighting in recent years have led to a greater focus on the reflective properties of the road surface.

The reflective properties of the road surface material significantly affect the illumination that can be achieved with a given amount of light flux from the luminaires. Darker pavements require more luminous flux from roadway luminaires than lighter pavement materials. In addition, environmental aspects and the conservation of natural resources play a key role in reducing waste. Interest in recycled materials, such as plastic waste, construction waste, tire waste, etc., has increased in road construction. [48]

2.3.2 Street lighting measurement methods and instruments

Photometric equipment for the assessment of road surfaces has been improved substantially in the last decade. Modern devices can be divided into two. Traditionally, laboratory research methods for pavements are being used, and the other direction is using portable on-site measuring instruments [30].

Comparison of measuring instruments and measurement methods:

- Laboratory instruments are used for absolute measurements and comparisons in the analysis of measurement data performed on the objects to be measured. The measurement methodology allows us to achieve less measurement uncertainty, but overlooks environmental conditions [29].

- Laboratory equipment consists of a light source, a coating sample holder and a sensor for measuring luminance. The photometry of the measurements usually takes into account the different angles of illumination specified in the *r*-table. The direction of observation is fixed in relation to the pavement sample, the lighting and the sensor for fixing the luminance can move in the selected geometry. Calibration of the (λ) curve is taken into account when measuring the luminance data. Calibrated lux meters are used to measure the luminance of the surface. The ratio of luminance to illuminance can be calculated by direct measurement using a calibrated surface. In the measurement methodology, modern measuring equipment is used. However, the mesopic environment is mainly not assessed in the measurement methodology. [VII], [47], [49]

It is estimated that laboratory measuring equipment has an uncertainty of approximately 10% - 15% and is therefore used to make reference measurements for the calibration of portable equipment. However, there is no common approach to measurement methodologies and their instruments in terms of traceability of the measurement procedure and measurement uncertainty [48].

The main disadvantage of laboratory measuring instruments is the need to take samples from pavements, which changes the geometry, environmental conditions and is costly. Therefore, changes in reflections over time and measurements at the same locations of the object cannot be monitored.

Portable equipment is used for on-site measurement of pavements. These measuring devices have a relative measuring capacity. Portable devices can be transported and used

for on-site measurements. They are usually suitable for installation in or on a vehicle and for relocation by a person. This in turn limits the weight and dimensions. [23], [30], [31]

When designing measuring instruments, trade-offs will inevitably arise, either with limited photometric possibilities or with greater measurement uncertainties. There is no uniform measurement methodology and the solutions are very different in terms of measuring instruments, lighting, mechanical and optical solutions used. Most devices do not measure the entire *r*-table or take all the necessary measurements to estimate the pavement. The dimensions of the measured illuminated field of the pavement are often limited to a smaller area than the recommended 104 mm^2. [VII]

Only the selected illumination angle (ε, β) is measured. These devices usually allow the measurement of speculative components, but not Q_0. The measured data and the resulting modeled *r*-tables are used to find the closest measured *r*-table in the database. Some compact measuring devices estimate Q_0 with two linear combinations of *r*-values, *r* (0, 0) and *r* (0, 2), which are used for the specular factor.

The devices are also used in various closed or open ambient lighting conditions.

The main advantage of portable devices is that their mobility and the object are not altered or damaged. Thus, the development of pavements can be studied over a long period of time and the information can be used to make lighting more efficient. Their measurement uncertainty may be higher, but they provide better actual pavement photometry. [30], [31], [50]

3 Development of uncertainty management procedure for lighting measurements

3.1 Review of measurement uncertainty for lighting measurements

3.1.1 Basis for estimating the developed measurement uncertainty approximation method

Uncertainty of measurement and the principles of its evaluation are important in all areas related to photometric photometric measurements. The simplified approximation method for estimating measurement uncertainty is based on GUM (Uncertainty Expression Guidance) [51] and provides guidance on how to document uncertainty information. The GUM describes detailed procedures for accurately estimating uncertainty. It is especially important to ensure that the technical specifications are followed when designing measuring instruments and applying measurement methodologies.

The developed simplified approximation method for estimating uncertainty is necessary, for example, for estimating the luminance, illuminance, color temperature or other uncertainties of lighting systems.

The purpose of the GUM-based uncertainty management method is to provide an overall uncertainty estimate and to provide an uncertainty estimate for individual measurements by comparing two or more measurements and the measurements of one or more light objects (measurement objects) within a specific specification or range. The simplified iterative approach is based on an upper bound strategy that takes into account the worst case scenario, i.e., some overestimation of the uncertainty at all levels, where the convergence cycle determines the rate of overestimation. Deliberate overestimation is necessary to avoid misstatements based on measurement results. The rate of overestimation can be adjusted by economic assessment of the situation.

The developed method is a tool to minimize the costs of metrological activities of photometric measurements and to reduce the uncertainty of measurement results.

3.1.2 General bases for estimating the uncertainty of measurement result

The developed simplified method is based on an overestimation of the uncertainties u_{xj} affecting the input variables to obtain an approximate estimate of the standard uncertainty in order to obtain $u_{xj} \geq u_{xja}$. This overestimation process provides a worst-case contribution at the upper limit of each known combined standard uncertainty component and thus ensures the outcome of the estimates. The method is based on the following principles:

- All input quantities of the measurement function that influence the measurement result are identified.
- It is decided which possible corrections should be implemented.
- The effect of each input quantity on the measurement result is evaluated.
- A convergence process is being performed.
- An assessment of the standard uncertainty of each input variable is performed.
- Using Type A or Type B assessment method. (3.4.1)
- Where possible, the B-type uncertainty estimation method is preferred in the first convergence cycle in order to obtain a coarser uncertainty estimate, to provide an overall picture and to save costs.

- Based on the standard uncertainties of all input quantities, the combined standard uncertainty is calculated from the relation of $u(y)$

$$u(y) = \sqrt{u_{x1}^2 + u_{x2}^2 + \dots + u_{xN}^2}$$ (6)

- The link (equation 6) applies only if all the components u_{xj} of combined standard uncertainty are independent (j = 1, ..., N).
- For simplification, the correlation coefficient value r is

$$r = 1, -1, 0$$ (7)

- If it is not known whether the components of combined standard uncertainty are independent, full correlation is assumed, i.e., either $r = 1$ or $r = -1$
- The expanded measurement uncertainty U is calculated by multiplying the combined standard uncertainty $u(y)$ by the coverage factor k (usually k = 2) using the relation

$$U = k \times u(y)$$ (8)

The simplified method normally consists of at least two cycles of approximation of the components of the uncertainty, as shown in the diagram in Figure 3.1.

- The purpose of the first, very coarse, simple and inexpensive approximation cycle is to identify the highest value of combined standard uncertainty components.

- The next approximation cycles, if performed, deal with providing more accurate upper limit estimates for the highest values of the combined standard uncertainty components to reduce the uncertainty estimates to $u(y)$ as a possible acceptable value.

The approximation method can be used to estimate the uncertainty of a measurement result from a given measurement operation. This method can be used for a result from a known measurement operation or for comparing several of these results, and also for developing a suitable measurement operation for managing the uncertainty of the measurement. [52]

3.2 Prerequisites for performing the uncertainty management procedure

A prerequisite for managing uncertainty and summarizing the estimates is a clearly defined measurement task that describes a measure, such as the luminance or illuminance of a surface at some point or the luminous flux of a light source. In this case, the uncertainty of measurement is the degree of compliance of a value obtained with a size measurement with the definition of quantity.

Standards define the measurand's conventional value with the help of standard chains as well as the global standards. In many cases, standards also define the ideal or conventional measurement principle, measurement procedure, measurement method, and standard reference conditions. [9]-[11], [52]

Possible deviations from standardized measurement values contribute to the uncertainty of measurement.

3.2.1 Estimation of the uncertainty of a measurement operation in the planning and development of a measurement operation

Uncertainty assessment is performed to develop the target uncertainty, taking into account the appropriate measurement operation and the uncertainty budget. The management scheme shown in Figure 3.1 is used for this purpose. According to the scheme shown in Figure 3.1, the estimation and management of the uncertainty is performed on the basis of measurement task 1 and U_S of the defined target uncertainty measured by the laboratory in box 2.

Definitions of the measurement task and the measurement required uncertainty are laboratory policy decisions that must be made at a sufficiently high level of management. A suitable measurement operation is considered to be such a measurement operation, together with the developed uncertainty aggregate, which ensures an expanded uncertainty equal to or less than the target uncertainty. If the estimated expanded uncertainty is significantly less than the target uncertainty, the measurement operation may not be economically optimal to perform the measurement task, i.e., the measurement operation is too accurate and costly.

The uncertainty management measurement operation, based on measurement task 1 and the predetermined target uncertainty U_S in box 2, shall include the following according to 3.1:

- The measurement principle 3 shall be selected on the basis of experience and possible measuring instruments available in the laboratory.
- Based on experience and capabilities known in the laboratory, the initial measurement method 4, measurement procedure 5 and measurement conditions 6 shall be established and documented.
- A first computational approximation cycle is performed, preferably based on the uncertainty estimation black box model, and an initial uncertainty aggregation as in boxes 7 to 9 is generated to give the first coarse estimate of the expanded uncertainty U_{E1} in box 10 (m = 1).
- The resulting initial expanded uncertainty estimate U_{E1} is compared to the target uncertainty U_S, as shown in oval B or C:

1) if U_{E1} is acceptable, i.e., if $U_{E1} \leq U_S$ (oval B), then the sum of the uncertainties of the first approximation cycle proves that this measurement operation A is suitable for measurement task 1, as presented in box 11 and the calculated estimate U_{E1} is the final expanded uncertainty of the measurement result;
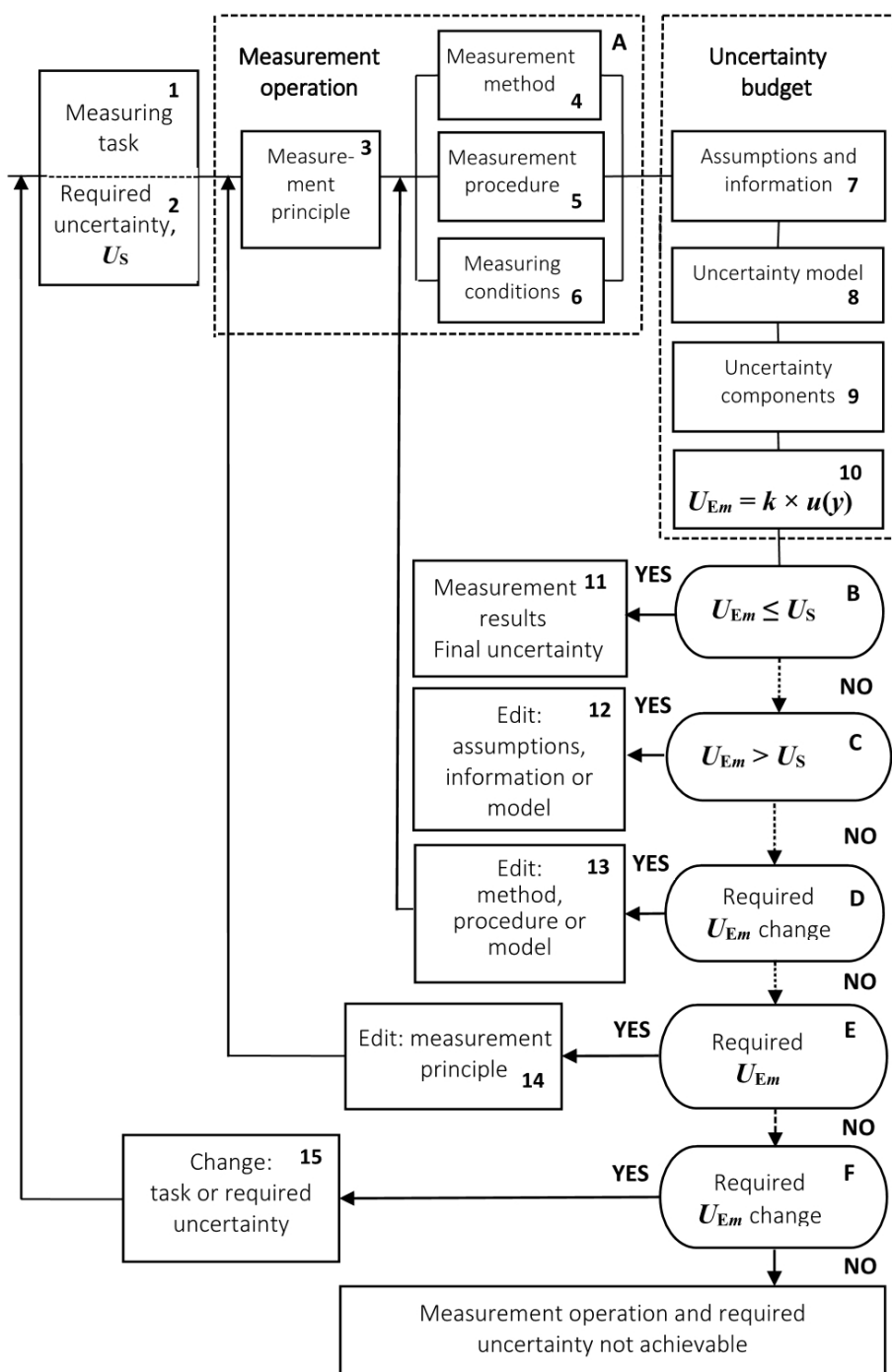
Figure 3.1 – Schematic of the procedure for estimating and managing the measurement uncertainty.

2) if $U_{E1} \ll U_S$ (oval B), then the measurement operation is technically acceptable but it may be possible to change the measurement method 4, measurement procedure 5 or measurement conditions 6 or together to make measurement operation A less accurate and cheaper by increasing the measurement uncertainty to obtain an acceptable extension to uncertainty $U_{E2} \leq U_S$. A new approximation cycle is then required to estimate the resulting new expanded uncertainty U_{E2} as described in box 10, where U_{E2} is the final expanded uncertainty of the measurement result;

3) if U_{E1} is not acceptable, i.e., if $U_{E1} > U_S$ (oval C), then the approximation process is continued with a new approximation cycle.

Before starting a new approximation cycle, the relative values of uncertainty of the components of the composite are analysed. In many cases, uncertainty values of two to three $(j = 2 \dots 3)$ components dominate the calculation of the compound uncertainty.

- If $U_{E1} > U_S$ (ovaal C, $m = 1$), the assumptions 7 or measurement model 8 are modified or the information on the uncertainty components 9 is supplemented, as described in box 12 to obtain a more accurate estimate of the dominant combined standard uncertainty components.
- A third $(m = 3)$ approximation cycle of the uncertainty pool is performed as shown in boxes 7 to 9, leading to a third smaller and more accurate estimate of the expanded uncertainty U_{E3} in box 10.
- The third expanded uncertainty estimate U_{E3} is compared to the predetermined target uncertainty U_S (oval B or C):
  1) if U_{E3} is acceptable, i.e., if $U_{E3} > U_S$ (oval B, m = 3), then the sum of the uncertainties of the third approximation cycle proved that the given measurement operation is suitable for the measurement task;
  2) if U_{E3} is not acceptable, i.e., if $U_{E3} > U_S$ (ovaal C, $m = 3$), a fourth approximation cycle (or more cycles) is required. The analysis of the uncertainty components is repeated, resulting in further changes to the assumptions, refinement of the information, modeling of possible changes as described in box 12, and focusing on the current maximum values for the uncertainty components.
- If all possibilities to find a lower and more accurate upper limit estimate have been used to obtain uncertainty estimates without achieving an acceptable expanded uncertainty in the form $U_{E3} \leq U_S$, it is necessary to change the measurement method, measurement procedure or measurement conditions, as described in box 13 to reduce the previously estimated expanded uncertainty U_{E3}. The convergence process starts again from the first convergence cycle.
- If changes in the measurement method, procedure or measurement conditions, as described in box 13, do not lead to an acceptable expanded uncertainty, it is possible to change the measurement principle 3 as described in box 14 and start the above procedure again.
- If the change of the measurement principle and the associated approximation cycles still do not lead to an acceptable expanded uncertainty, it is possible as a last resort to change the measurement task 1 or the target uncertainty 2 or both, as described in box 15 and start the above procedure again.

- If it is not possible to change measurement problem 1 or uncertainty 2, it is an indication that there is no measurement operation suitable for solving the measurement problem with the given uncertainty, see box 16. [52]

3.3 Measurement errors and their types

3.3.1 Measuring instrument

When measuring lighting measuring quantities, the readings of the measuring system or measuring instrument always have measurement deviations within certain limits. These measurement tolerances constitute an estimate of the uncertainty of the readings of the measuring instrument given in the certificate of linearity of the measuring range, the values of the corrections specific to the readings and their calibration with extension uncertainties, or given in the specification of that measuring instrument. In addition to the measurement error, the use of a measuring system or measuring instrument may give rise to measurement deviations in such characteristic quantities as:

- spectral sensitivity, which is the difference between the spectrum of the calibration source and the spectrum actually obtained from the measurement (a correction and its expanded uncertainty may be used to compensate for this difference in the spectrum of incident light);
- position and directional sensitivity of the measuring instrument;
- display resolution;
- changing the measuring range;
- noise and blind current (sensor noise and blind current values).

3.3.2 Measurement procedure

Input values of the measurement uncertainty for photometric measurements are:

- point definition, if road markers are used where measurement is affected by the accuracy of the direction and position of the markers;
- measuring field, which is the effective measuring field for spot measurement;
- actual arrangement of the measuring device (sensor), which differs from its nominal position and nominal inclination.

In addition, when using a dynamic measurement system, the inputs to the uncertainty summary associated with the measurement procedure are vehicle speed and measurement collection time, which may reduce directional sensitivity and increase the area to be measured.

3.3.3 Surrounding measurement environment

In most cases, when measuring the illuminance and luminance of the road surface in a measuring object such as an outdoor working environment, the climatic conditions, i.e., the surrounding measuring environment (temperature, humidity), are the most important input of the uncertainty set. Climatic quantities cause atmospheric light absorption and thus measurement deviations, which define the standard uncertainty of these quantities. For example, it occurs in the case of illuminance measurements, the light reaching the surface and, in the case of luminance measurements, the light reaching the luminance meter [16]. Additional parameters characterizing the measuring environment may include:

- condition of the subject: wet, dry, humid;
- relatively high or low surrounding temperature, which affects the calibration of light measuring instruments, as well as the light output of heat-sensitive lamps and luminaires;

- moisture or condensation on the light transmitting surfaces of the measuring instruments or their electrical circuits affects their accuracy.
- strong winds, which may cause vibration or oscillation of measuring instruments and lighting facilities;
- pulsating light from the measuring environment.

3.3.4 Measurer

The person taking the measurement is not stable because there are differences in physical and emotional state between days and there can often be quite large changes during the day. Consequently, the quantities due to a meter that may give rise to uncertainty are his/her education, knowledge, experience, training, correctness, honesty, dedication, and physical ability.

3.3.5 Measuring object

In an outdoor environment, the measuring object is usually the road surface within two lighting masts, where all operating conditions must be taken into account when measuring the illuminance and luminance. The values that characterize the properties over the distance between the two lighting installations affect the uncertainty of the measurement result. These inputs to the uncertainty summary are:
- road geometry values such as mast spacing and the width of the road and lane;
- non-uniformity of the measured size (illuminance, luminance, etc.) of the measured object;
- height of the light-sensitive surface of the sensor above the road surface;
- power supply conditions.

3.3.6 Measurements, calculations and software

Important attention must be paid to the number of decimal places in the values, which may have an effect on the measurement result. In general, the use of measurements, calculations and software (DIALux, RELUX, LabSoft etc.) influences the measurement result through the selection of a set of measures, algorithms, their validation, implementation and correction, the number of value points used in the calculations, error operation, and rounding, which contribute to the standard uncertainty of these inputs. [II, III]

3.3.7 Constants and transmission factors

In-depth knowledge of the distribution of constants and values of the transfer factors in the aggregate plays an important role in the estimation of standard uncertainties in the input to the uncertainty summary. In the case of photometric measurements, the constants and the transmission factors are the attenuation coefficient in the measurement of the luminous flux of the lamp, the linear coefficient of expansion of the masts and luminaires, the correction factor for the attenuation of light, etc.

3.4 Evaluation of the standard uncertainty summary input quantity and the evaluation of combined standard and expanded measurement uncertainty results

3.4.1 Evaluation of the input quantities of uncertainty summary

The standard uncertainties of the input quantities for the uncertainty summary may be estimated using the Type A or Type B uncertainty estimation method. The Type A estimation method can be used to characterize the components of uncertainty u_{xj} by the statistical distributions and standard deviations of the sets of measures. The components u_{xj} that are to be evaluated by the Type B method, can also be characterized by standard deviations, which, however, are based on expected probability distributions. They are based, for example, on information related to a reliably published value, or derived from a calibration certificate and cut-off values based on personal experience, or otherwise. Both methods are based on probability distributions and the standard uncertainty values of the inputs to the uncertainty aggregate obtained by both methods are usually given by standard deviation estimation.

In most cases, the Type A estimation method provides more accurate estimates of the combined standard uncertainty components than the Type B method, but requires extensive measurements and calculations. Therefore, the B method is usually selected for the approximation method unless there is an overriding need to estimate the standard uncertainty using the A method. In many situations, there is no option other than the use of the Type B assessment method. [52], [53]

3.4.2 Type A evaluation method of the standard uncertainty

For the uncertainty component u_{xj} in the Type A estimation method, the re-measurement dimensions are required. The arithmetic mean, standard deviation, and standard deviations of arithmetic mean of the measurements, irrespective of the type of statistical distribution, are calculated according to [53] from the following relationships:
The arithmetic mean $\bar{x}_j$ of the measured values $x_{ji} (i = 1, 2, \ldots n)$, which is an estimate of the mean, is found in the relation

$$\bar{x}_j = \frac{1}{n} \sum_{i=1}^{n} x_{ji} \tag{9}$$

The standard deviation $s(x_j)$ based on the measured values $x_{ji} (i = 1, 2, \ldots n)$, which is the evaluation σ, is obtained from the relation

$$s(x_j) = \sqrt{\frac{1}{n-1} \sum_{i=1}^{n} (x_{ji} - \bar{x}_j)^2} \tag{10}$$

The standard deviation of arithmetic mean $s(\bar{x}_j)$ of $x_{ji} (i = 1, 2, \ldots n)$ is found to be equal to the standard deviation of the amount divided by the square root of the number of measurements

$$s(\bar{x}_j) = \sqrt{\frac{1}{n(n-1)} \sum_{i=1}^{n} (x_{ji} - \bar{x}_j)^2} = s(x_j)/\sqrt{n} \tag{11}$$

If the arithmetic mean of the relation (7) and consequently the standard deviation of the equation (8) is based on very few repetitions, i.e., with the number of measurements

$n < 10$, the estimated standard deviation values may be inappropriate and possibly too small. Therefore, a back-up factor t is used. The reserve factor t is calculated from the *Student's t*-distribution. If the result of the measurement is obtained from the results of a single measurement, then the standard deviation $s(x_j)_i$ of the sample is used as the value of u_{xj} in the uncertainty aggregate, which is multiplied by the suitable back-up factor t_i.

$$u_{xj} = s(x_j)_i \times t_i \qquad (12)$$

If the result is obtained using an arithmetic mean of several inputs of this magnitude, such as i = 2 ... 5, then the standard uncertainty measurements u_{xj} of the arithmetic mean standard deviation $s(\bar{x}_j)_i$ is used in the uncertainty budget. This is multiplied by the appropriate value, meaning that

$$u_{xj} = s(\bar{x}_j)_i \times t_{i,\{s(\bar{x}_j)_i\}} \qquad (13)$$

3.4.3 Type B evaluation method of the standard uncertainty

Estimating the standard uncertainty of an input to an uncertainty summary by any means other than statistical is often limited to using past experience or *simply guessing* what value that standard uncertainty could have. Experience shows that people do not understand or cannot directly assess standard deviations. Experience also shows that people remember or derive limits of dimensional distribution (deviation limiting value) using logical arguments or laws of physics. Often specifications are known as limiting values. This knowledge can be developed into a systematic method for deriving standard uncertainties from limiting values.

If the distribution size a_{xj} of the input size or agent of the uncertainty distribution limit is given, then for all (limited) distributions there is a definite ratio b between its standard deviation and the one-sided distribution limit a_{xj}. Thus, if the distribution limit (hereinafter limit value) a_{xj} and the type of distribution are known, a standard deviation can be calculated. The limit designation is selected for symmetric divisions as $-a_{xj}$ and $+a_{xj}$. Standard uncertainty based on the above is

$$u_{xj} = a_{xj} \times b \qquad (14)$$

Experience shows that in most cases, three types of distribution are sufficient to convert the distribution limits into standard uncertainty. In Figure 3.2, these three distributions are presented together with the conversion limit of the uncertainty aggregate input size distribution to standard uncertainty u_{xj}.

In the normal distribution, the limit is twice the standard deviation value in $2 \times s$. From experience, it is known that a person remembers the value 2 as the limit of a dataset subject to normal distribution. For the three types of distribution in Figure 3.2, the values of the distribution factor b are as follows:
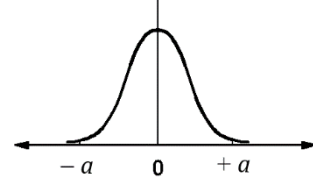
- Normal distribution b = 0,5
- Rectangular distribution b = 0,6
- Arcsin distribution b = 0,7

Estimating the standard uncertainty of the uncertainty aggregate using the Type B method requires a reasonable *guess* or knowledge of the limit a_{xj}. In order to ensure an

overestimation, a plausible assumption must be made to determine the limit value *a*. The next step is to assume the shape of the distribution. Often the shape of the distribution is known or evident. If not, a conservative assumption must be made. If it is not known that this is a normal distribution, either a rectangle or an arcsin distribution is selected. If it is not known that this is a rectangular distribution, the arcsin distribution is chosen as the most conservative assumption.

Normal distribution (Gauss distribution): $b = 0,5$

$$u_{xj} = a/2 \approx 0,5 \times a$$

Rectangular distribution (even distribution): $b = 0,6$

$$u_{xj} = a/\sqrt{3} \approx 0,6 \times a$$

Arcsin distribution (U distribution): $b = 0,7$

$$u_{xj} = a/\sqrt{2} \approx 0,7 \times a$$
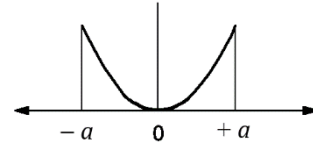
Figure 3.2 – The three types of distributions used to convert the boundary a into a standard uncertainty u_{xj} .

One way to obtain reasonable standard uncertainty estimates for uncertainty aggregate inputs / agents without using statistical methods is to set a distribution threshold for aggregate input by experience or by using physical laws, and then convert its cut-off to standard uncertainty using an assumption size distribution type. [52]

3.4.4 Repeatability

Each set of uncertainties, including the set of measurement operations for photometric measurements, shall repeat at least once. In most cases, repeatability can only be assessed experimentally using the Type A estimation method. The uncertainty component is derived using relationships $s(x_j)$ and $s(\bar{x}_j)$ given in section 4.2. [52]

The repeatability based combined standard uncertainty component (standard uncertainty) may be less than the uncertainty component resulting from the instrument's resolution. In this case, the latter will be used instead of the estimate based on iteration.

3.4.5 Resolution of the measuring instrument and value of the rounding step

The resolution of the instrument, in both analogue and numeric readings, or the last decimal place of the value obtained from the measurement, or the rounding step of the rounded result of the measurement, all denoted by *d*, result in the standard uncertainty of

$$u_{xj} = d/2\sqrt{3} \approx d/2 \times 0,6 \approx 0,3 \times d \tag{15}$$

According to equation (15), the standard uncertainty is calculated from the value of d, whichever is greatest, the input quantity (resolution, rounding step) itself being determined by a rectangle having a limit of 0,5 d.

If the standard deviation estimate for repeatability is derived from experimental measurements, the effect of resolution, rounding step, etc., is included in the standard uncertainty due to repeatability if it is greater than the standard uncertainty due to resolution, rounding pitch, etc.

3.4.6 Maximum permissible measurement error of the instrument MPE

If the instrument or etalon is known to conform to the declared MPE values for all metrological output quantities, then these MPE values can be used to derive the associated combined standard uncertainty components (standard uncertainties) using the relationship

$$u_{xj} = \text{MPE} \times b \tag{16}$$

The factor b in equation (16) is chosen according to the rules in section 3.4.3 and the expected distribution pattern. When calibration certificates (proof of compliance with MPE) are available for a measuring instrument or for a number of identical measuring instruments, it is often possible to use the results of the certificates to determine the type of distribution or, in rare cases, directly estimate the standard uncertainty of the maximum permissible uncertainty as the Type A estimation using the relationships in section 3.4.2.

3.4.7 Correction

Known uncertainties Δx_j for the input quantities of the uncertainty aggregate, for which both the value and the sign (+ or −) are known, can be compensated by the correction δ_j, which is added to the uncorrected result using the relation

$$\delta_j = -\Delta x_j \tag{17}$$

Even if the correction is taken into account, the standard uncertainty of correction remains a component of the combined standard uncertainty, see also section 3.3. For a correction to have an effect on the measurement result, the standard uncertainty of the correction shall be less than the value of the correction itself.

The decision whether to apply a correction to a known measurement error must be made by the person who creates the uncertainty summary. The criteria for whether or not a known deviation is applied is based on economic grounds.

Drift can also be considered as a known error that can be corrected.

3.4.8 Hysteresis

The indication of the hysteresis h may be regarded as a symmetrical deviation around the mean value of the two hysteresis readings. If there is a sufficient number of readings, the standard uncertainty due to hysteresis can be deduced from the Type B estimation method, based on which we get

$$u_{xj} = h/2 \times b \tag{18}$$

In relation to (18), the value of b is chosen according to the rules in section 3.4.3 and the expected distribution pattern.

3.4.9 Measurement operation

The measurement operation is affected by the input quantities/factors of the large uncertainty summary, which, in turn, are related to both the measuring instrument and the measuring object (carrier of the measured quantity) or both. Common input sizes and factors that influence the measurement operation for photometric measurements include surrounding temperature, differential temperature between the instrument and the measuring object, humidity, direction of measurement, and sensor placement. These effects are expressed in units of measurement, such as °C, % and °, and using physical connections, their values of effect must be converted into units of measurement used in light technology. A value or area is often known from the factors, and the standard uncertainty of the value or area mentioned above is known through the cut-off value of this factor distribution.

The standard reference temperature for measurements is 20 °C [54]. This means that the final result of the measurement must be expressed as a reduction to 20 °C. Temperature effects on the measuring operation from the temperature itself, the difference between the temperature of the instrument and the measuring object, or the temporal and spatial variations in temperature, result in expansion in the measuring instruments, measuring set and measuring object, which cause changes in the display. The conversion of the temperature difference ΔT to the change in the linear dimension L to ΔL with the linear expansion coefficient α is given by the relation

$$\Delta L = \Delta T \times \alpha \times L \tag{19}$$

In the case of photometric measurements, the measured object's difference in temperature as well as the measuring environment's difference from the reference temperature of 20 °C are usually compensated by an electronic system built into the instrument. Since the compensation is not perfect, it gives rise to the corresponding compensation uncertainty, which is part of the measurement uncertainty.

The direction of measurement in the measurement operation is selected depending on the state of the object to be measured, such as the road surface, geometric shape, dimensions or other characteristic values. The effect of deviation from the measurement direction defined by the measurement operation can be calculated using basic trigonometric relationships, and this effect may also be due to directional effects due to other factors.

The most commonly used measurements for photometric measurements are luminous flux, illuminance and luminance, the values of which are often given as requirements in the technical specification of the measuring object. These measurements are also very often defined in the standards for photographic objects. In many cases, a measurement operation, either intentionally or by accident, is not in accordance with these definitions of measurement quantities. In such cases, these deviations in the measurement procedure will cause errors and uncertainty in the measurement result. If measurement errors are known, corrections can be applied. In practice, a measurement operation always causes measurement uncertainty when compared to the definition of a measurand.

3.4.10 Correction of the reading on the calibration certificate

Calibration certificates shall provide corrections to the values (readings) obtained when measuring the metrological output of the measuring system or measuring instrument, together with the associated uncertainties. If the calibration certificate gives the value of the correction obtained, the combined standard uncertainty component u_{xj} is as follows.

If the standard uncertainty is expressed by the expanded uncertainty U and the declared coverage factor k, it is calculated from the relation

$$u_{xj} = U/k \qquad (20)$$

Some calibration organs have a default value of k. In such cases, the coverage factor value is not reported on the certificate and the uncertainty is expressed as the expanded uncertainty U_V and a confidence level of, e.g., 95 % or 99 % is declared

$$u_{xj} = U_V/m \qquad (21)$$

In relation (21), m is the number of standard uncertainties at half-width of the confidence interval that corresponds to the declared confidence level.

Occasionally, the calibration certificate or other information includes a statement that the instrument meets certain defined specification requirements, such as those contained in a standard, a manufacturer's information sheet, or elsewhere. In this case, the nominal value of the metrological characteristic MPE is used and the uncertainty component is derived from this MPE value.

3.4.11 Measuring object

In light measurements, the measurement of the illuminance and luminance of an object, such as pavement surfaces, is made with the sensors of the measuring instruments, either in contact or at a fixed distance.

Depending on the surface properties of the measuring object, shape deviations and other errors, the current state of the illumination solution, the pavement material and its state, the measurement quantity, i.e., illuminance, luminance, etc., is uneven. This component can be evaluated by experiment, by type A evaluation, or by type B evaluation, or partly by experimentation and partly by type B evaluation. The inaccuracy of the measurement object (the carrier of the measurand) produces the corresponding uncertainty component. This component can be evaluated by experiment, by type A evaluation, or by type B evaluation, or partly by experimentation and partly by type B evaluation.

3.4.12 Manual data and constants

The values of the constants used in the uncertainty pool, such as thermal expansion coefficients, modulus of elasticity, etc., which are often used to apply corrections or to modify the uncertainty of the factor deviation, are often not known, but are estimated. Therefore, they generate additional components through the same transformation relationships with the agents discussed above. These components can only be evaluated using the Type B assessment method.

3.5 An opaque and transparent box model for estimating uncertainty

The uncertainty of a measurement operation can be estimated using different models or with different details, or both. Two extreme examples are opaque and transparent models. In the case of an opaque model, a measurement operation whose content is unknown is modeled. The sum of the uncertainties and the components of the combined standard uncertainty describe only the total effect on the measurement operation. With this choice of the measurement model, it can be very difficult to define the functional relationship between the components of the combined standard uncertainty and the individual deviation components. In order to take full advantage of the uncertainty calculation process, it may be necessary to create a more detailed set of uncertainties. It can be based on examining the behavior of all the details of the measurement operation, i.e., assessing the uncertainty using a transparent model. The impenetrable model can also be described as a low resolution model and the transparent model as a high resolution model. In the opaque uncertainty estimation model, the units of input and output of the uncertainty pool are the same and the combined standard uncertainty components are assumed to be summed and the sum of the expected values of the uncertainty corrections is assumed to be zero. Because all opaque composite uncertainty components are converted to measurands using an opaque model, the sensitivity factors for all individual combined standard uncertainty components in this model are 1. When evaluating an uncertainty in a transparent model, the combined standard uncertainty components are not subject to these constraints. [52]

3.5.1 Adding components in combined standard uncertainty in the case of the opaque box model

The measurement result y of the combined standard uncertainty $u(y)$ components u_{xj} by using the opaque box model is added in the expression of standard uncertainty $u(y)$ partly geometrically and partly arithmetically using the relation

$$u(y) = \sqrt{u_{qj}^2 + \sum_{j=1}^p u_{pj}^2} \tag{22}$$

In relation to (22), p represents the number of independent uncertainty components and u_{qj} the sum of the significantly correlated ($r = 1$ or -1) uncertainty components calculated from the relation

$$u_{qj} = \sum_{j=1}^q u_{qj} \tag{23}$$

In equation (23), q represents the number of significantly correlated components of combined standard uncertainty. The total uncertainty component of $p + q = N$ is obtained by measuring the output quantity Y (measuring result). By the formula (22), the independent uncertainty components ($r = 0$) are added geometrically, i.e., the square root of the sum of the squares. However, the highly correlated components of uncertainty are added arithmetically. A modest approach assumes that all the components that are not known to be completely independent are highly correlated.

3.5.2 Adding components in combined standard uncertainty in the case of the transparent box model

In the uncertainty estimation transparent box model, the output quantity (measure) Y is modeled as a function f of several input variables (measure quantities) X_j of the uncertainty aggregate, whereas sizes X_j may be functions of either the transparent box model or the black box model or both

$$Y = f\left(X_1, \ X_2, \dots, X_j, \dots \ X_{p+q}\right) \tag{24}$$

In relation to (24), the index $p + q$ is equal to N according to the previous section.

The measurement result y of the combined standard uncertainty $u(y)$ is shown in this case as follows:

$$u(y) = \sqrt{u_{jq}^2 + \sum_{j=1}^{p}\left(\partial Y/\partial X_j\right)^2 \times u_{Xj}^2} \tag{25}$$

In relation (25), u_{jq} is the sum of significantly correlated components of the combined standard uncertainty, which is calculated from the relation

$$u_{jq} = \sum_{j=1}^{q}\left(\partial Y/\partial X_j\right) \times u_{Xj} \tag{26}$$

In equations (25) and (26), $\partial Y/\partial X_j$ is a partial derivative of the relation Y relative to X_j and the standard uncertainty u_{Xj} of the jth input quantity (factor). Therefore, u_{Xj} may also be the result of either the opaque box model or the transparent box model estimation method. In this case too, the independent components of combined standard uncertainty ($r = 0$) are added geometrically, i.e., the sum of the square root of the squares and the significantly correlated components q of the uncertainty are added arithmetically. In a modest approach, all the components for which it is unknown whether they are independent are considered highly correlated. Since the number of independent uncertainty components is p, the total uncertainty estimator for Y is the transparent box method $p + q = N$, which can be a combination of several uncertainty components.

3.5.3 Estimate of expanded measurement uncertainty

For all measurements, the expanded uncertainty of the measurement result y is calculated from the relation of U

$$U = u(y) \times k = u(y) \times 2 \tag{27}$$

Unless otherwise stated, then according to [53], the measurement shall be taken to take the value of the coverage factor $k = 2$.

4 Practical assessment of uncertainty using the developed method

4.1 Estimation of uncertainty

This section provides a series of steps for the simplified approximation method for the measurement of the expanded uncertainty of a measurement result in the documentation and evaluation process of each uncertainty component included in the combined standard uncertainty summary.

4.1.1 Prerequisites for compiling an uncertainty summary
The compilation of uncertainty [52], [53] is only possible if:
- the measuring task is correctly defined (the measuring object and its dimensions must be defined and presented in the measuring task, box 1 on schemes in *Figure 3.1*);
- the measurement principle is correctly defined and known or at least initially known (box 3 on schemes in Figure 3.1);
- the measurement method is well defined and known or at least initially known (box 4 on schemes in Figure 3.1);
- the measurement procedure is correctly defined and known or at least known from the outset (box 5 on schemes in Figure 3.1);
- the measurement procedure includes a measurement system or selection of measuring instruments;
- the measurement procedure provides all the details of how the measuring instrument (s) and the measuring object (the carrier of the measurand) are handled during the measurement (the uncertainty aggregate must reflect the activities and steps of the measurement procedure);
- the measurement conditions are correctly defined and known or at least initially known (box 6 on schemes in Figure 3.1).

When designing the uncertainty aggregate, it should be taken into account that each of the arbitrary measures of measurement contains the three elements shown in Figure 4.1. These elements are denoted by numbers 1, 2 and 3. The aggregation of uncertainties must therefore reflect:
- determination of the reference point for the measurement quantity (element 1 on scheme in Figure 4.1), which is often a zero value for the measurement quantity (the uncertainty is related to the setting of the reference point and the zero reading of the measuring instrument);
- determination of a measuring point for measuring quantity (element 2 on scheme in Figure 4.1), which is a specific measuring quantity and the resulting measurement (the uncertainty is related to the obtained measurement, the indication of the measuring instrument and the measuring object);
- measurement value movement (range 3 on scheme in Figure 4.1), which is the magnitude of the magnitude change from zero to a specific measurand (uncertainty related to dimensional change tolerance and instrument uncertainty, or both, hardware uncertainty usually given on the instrument calibration certificate).
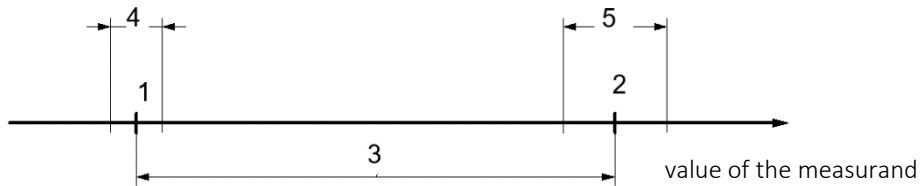
Figure 4.1 – General view for measuring the size of a model from the following five elements:
1 - reference point or dipping datum point, 2 - measuring point 3 - range of the value of variation of the measurand, 4 - uncertainty area of the reference point, 5 - uncertainty area of the measuring point.

4.1.2 Uncertainty assessment procedure

The following procedure may be useful in compiling and documenting the uncertainty pool in the first approximation cycle of the simplified approximation method. This procedure is as follows:

- Define and document the overall measurement task, i.e., the measurement quantity and the primary result for which the uncertainty aggregate will be constructed.
- The measurement principle, measurement method, measurement procedure and measurement conditions shall be documented. Where they are not fully known, the initial, or proposed design of the principle, method and procedure and proposed conditions shall be selected and documented in accordance with the principle of overestimation of the components of the combined standard uncertainty set out in section 3.1.1.
- A graphical representation of the measuring device(s) is made. Graphic material can be helpful in understanding the components of uncertainty in measurement.
- Mathematical relationships are documented or a measurement model is drawn between the measured quantity values and the quantities of the general measurement problem. As a rule, a mathematical measurement model is not required if the measurement problem can be solved according to the opaque box model. A mathematical model is required if the measurement problem is solved according to the transparent box model.
- A preliminary study is carried out and all possible components of the combined standard uncertainty of measurement are recorded. The results may be presented in tabular form, as shown in Table 4.1. The study shall be conducted in a systematic order using the three elements presented in Figure 4.1 and the data already documented in the measuring instrument at points 1 and 2. Combined standard uncertainty should be subdivided into components in a way that avoids the multiple inclusion of the same component, but in many cases, this is often not possible in practice. This principle is the most important aggregation of uncertainty for the dominant components of combined standard uncertainty.

Based on the documented information, uncertainty modeling of the respective approximation cycle is investigated and prepared. For each input uncertainty component:

- an assessment method is chosen, either type A or type B;
- the value, background information, and other aspects of the component of combined standard uncertainty are discussed;
- in the case of a Type A estimation method, the value of the input size and the number of dimensions on which the estimate is based is provided;
- for the Type B estimation method, the limit a_{xj}, a_{xj}^* (partition limit in units of input / agent), the expected distributional shape and the value of the resulting uncertainty component is reported;
- any possible correlation between the components of the non-additive uncertainty recorded is identified and documented in accordance with chapter 1;
- appropriate formulas depending on the measurement model and the correlation are selected and the combined standard uncertainty $u(y)$ is calculated;
- the expanded uncertainty U is calculated.

For the aggregate presented in Table 4.1, it is necessary to be prepared for this aggregate table to include all relevant information for the uncertainty estimation cycle if needed immediately or later. Possibilities for changes that would lead to a change in the estimation of combined standard uncertainty are further explored. [52]

Table 4.1 – An example of a generalized aggregate table that contains all of the uncertainty aggregate information

The combined standard uncertainty component name	Evalua-tion method type	Distri-bution type	Number of mea-sure-ments	Varia-tion limit a_{xj}^* in units of the agent	Dist-ribu-tion limit a_{xj}/ %	Cor-rela-tion factor r	Value of the factor b	Value of the combined standard uncertainty component u_{xj}/ %
u_{x1} x_1 title	A		10			0		1,8
u_{x2} x_2 title	B	Gauss		2,4 %	2,4	0	0,5	1,2
u_{x3} x_3 title	B	rectang-le		3,5 %	3,5	0	0,6	2,1
u_{x4} x_4 title	A		15			0		0,8
u_{x5} x_5 title	A	Gauss		2°	1,0	0	0,5	0,5
u_{x6} x_6 title	B	U		10 °C	1,6	0	0,7	1,1
u_{x7} x_7 title	B	U		15 °C	0,4	0	0,7	0,3
Combined standard uncertainty, $u(y)$ / %								3,36
Expanded uncertainty ($k = 2$), U / %								6,72

4.1.3 Connection between the measurement result and the input quantities and the expression of the combined standard uncertainty

In photometric measurements, the result of the measurement is calculated from the sum of all added values, in units of measurement which may be expressed by the following measurements of illuminance and luminance:

$$y = x + \delta x_{\text{MV}} + \delta x_{\text{MÕ}} + \delta x_{\text{KK}} + \delta x_{\text{ÜS}} + \delta x_{\text{MO}} + \delta x_{\text{MP}} + \ldots \qquad (28)$$

In equation (28), *x* denotes the arithmetic mean of the measured quantity values or a single measured quantity value, δx_{MV} is the correction value of the measuring instrument (measuring system) of which the value is obtained from the calibration certificate; the rest of the corrections, i.e., errors of measurer $\delta x_{\text{MÕ}}$, the environment δx_{KK}, the set-up $\delta x_{\text{ÜS}}$, the measuring object δx_{MO}, the measuring procedure δx_{MP} are considered to be close to zero, but they have uncertainty. Therefore, by relation (28), the combined standard uncertainty $u(y)$ is expressed by the following relation, in which the components of the combined standard uncertainty are denoted by their origin.

$$u(y) = \sqrt{u_{x\text{MV}}^2 + u_{x\text{MÕ}}^2 + u_{x\text{KK}}^2 + u_{x\text{ÜS}}^2 + u_{x\text{MO}}^2 + u_{x\text{MP}}^2 + \ldots} \qquad (29)$$

The components of the combined standard uncertainty with respect to (29) are: $u_{x\text{MV}}$ from the measuring instrument, $u_{x\text{MÕ}}$ from the measurer, $u_{x\text{KK}}$ from the measuring environment, $u_{x\text{ÜS}}$ from the measuring set-up, $u_{x\text{MO}}$ from the measuring object, $u_{x\text{MP}}$ from the measuring procedure.

Experience has shown that the various components of combined standard uncertainty do not interact with each other. This means that equation (29) can be used to estimate both the absolute and the relative effects on the combined standard uncertainty of the measurement result. The uncertainty aggregate and the change in the corresponding component of the combined standard uncertainty can be converted to economic terms and effects and thereby the uncertainty aggregate is used to assess the economic impact. [52]

4.1.4 Connection between the measurement result and the input quantities and the expression of the combined standard uncertainty

The developed method provides an opportunity to document and optimize the measurement process across multiple approximation cycles, taking into account technical, economic, or both criteria. Due to the parallel development of the measurement operation and the uncertainty pool, the approximation method described provides an opportunity to analyse the effect of each sub-procedure on the measurement uncertainty.

In many cases, the ideal measurement method and measuring instrument, such as illuminance, luminance and luminous flux, are too expensive or slow-acting, or both. An analysis of the shape and angular deviations of a measurable light object and its effect on an uncertain assembly can provide an opportunity to declare other measurement methods and tools as suitable or unsuitable and to save costs. For example, it is explored whether goniometric measurement of luminous flux with an ILMD camera, a secondary method, could be a suitable replacement for both luminous distribution and luminous flux, and is, by definition, an ideal method. [16], [55]

The specific uncertainty component $u_{x\mathrm{MV}}$ and the measurement set-up component $u_{x\ddot{\mathrm{U}}\mathrm{S}}$ of the combined standard uncertainty can be seen in the summary of uncertainty. All other components of the combined standard uncertainty can be considered as constants. If the resulting combined standard uncertainty, multiplied by the coverage factor k, meets the U_S requirements of the target uncertainty, the instrument and device are recognized as suitable for the measurement task.

Best Measuring Capability (BMC) is the minimum possible expanded uncertainty that a company or laboratory can achieve for a specific measurement task. If all the components of the combined standard uncertainty in the uncertainty pool are minimized, the value of the expanded uncertainty U_{Smin} obtained by multiplying this combined standard uncertainty by the coverage factor is the best measurement for this measurement task. [52]

4.1.5 Requirements for purchase of new measuring instruments

A simplified approximation method for estimating characteristic light measurements with defined uncertainty is used where the uncertainty component $u_{x\mathrm{MV}}$ of the instrument is a variable and all other constants result in minimal requirements, i.e., MPEs for the metrological output of the instrument. In this case, the uncertainty of a particular measurement task can be summed up by treating the uncertainty components $u_{x\mathrm{MV}}$ from the measuring instruments as unknown variables and all other uncertainty components as constants. Requirements for new measuring instruments that do not yet exist can now be derived using equation (29).

4.1.6 Connection between the measurement result and the input quantities and the expression of the combined standard uncertainty

The environmental impact of $u_{x\mathrm{KK}}$ in the combined standard uncertainty can be seen in the pool of uncertainties. If all other components of the combined standard uncertainty are treated as constants and the environmental uncertainty components are treated as variables, then the requirements for the environmental conditions can be derived by relation (29). If the resulting combined standard uncertainty $u(y)$ meets the requirements of the target uncertainty U_S, the environment is recognized as suitable for the measurement task. [52]

4.2 Road lighting illuminance uncertainty measurement

The example presented below addresses a simplified approximation of the measurement of the measurement object, the pavement between the *Akadeemia* road and the *Ehitajate* road with unidirectional light posts represented in Figure 4.2. Also, spectral luminance measurement and its uncertainty are estimated, with the acceptance of a measurement procedure and measurement conditions declared to be in accordance with the above.

Figure 4.2 – The pavement section selected for measuring illuminance and a photo of it on the right.

4.2.1 Measurement task, indeterminacy, measurement procedure and conditions

Measurement task and indeterminacy

The measurement task was to measure the illuminance of the pavement that is equipped with luminance posts on the one side between the *Akadeemia* road and the *Ehitajate* road, starting at 23:40 on 20.11.2018 in order to check the status of the existing lighting solution. Measurement uncertainty U_L = 10 % of the result of the measurement of the illuminance at the points of the light traffic raster between the posts. [52]

Measurement principle, method, procedure, conditions and the placement of measuring points

The principle of measurement is as follows: the light emitted on the surface to be measured is transmitted through a measuring sensor to a processor which devides it into different wavelengths, the intensity of which is used to record the illuminance falling on that surface. The method of measurement is the direct measurement of the illuminance at the specified measuring points in the area between the posts. The initial measurement procedure to be used is as follows: the distance between the masts of the measured road surface 34 m, depending on the raster 2 m × 3,7 m (points positions based on fixed gauge measurements) the spectrum based luxmeter BTS256-EF [56] is placed in the determined measuring points (the position diagram of the points is given in Figure 4.3). The illuminance meter transducer is positioned above the measuring point at a height of 45 mm above the measuring point so that its axis is perpendicular to the measuring surface on the measuring direction. Then, the illuminance reading at this point is fixed by using the illuminance meter (Figure 4.2).
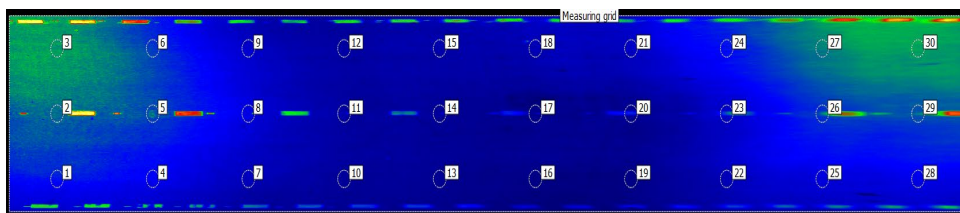

Figure 4.3 – The placement of the measuring points on the pavement surface to be measured between the posts.

The following conditions were applied to the measurement:
- the pavement is covered with new asphalt;
- spectroradiometer BTS256EF no. 17384M spectrometric illuminance meter [56] used has a measuring range (1 ... 199999), with lx at wavelengths between 360 nm to 830 nm the readings on the calibration certificate based on the manifacture's specification, MPE = ±3 % of the measurement results;
- the step number of the lux meter reading device is 0,01 lx;
- the air temperature in the vicinity of the measuring object is 2 °C ± 1 °C;
- the relative humidity of the air at the height of 1 m around the target is 80 % ± 10 %;
- the recorded temperature variation of the lux meter is less than 5 °C;
- the temperature difference between the lux meter and the measured surface of the road surface is less than 20 °C;
- the body of the lux meter is made of aluminum, covered with a plastic cover;
- the measurer is trained and competent to use the lux meter.

Measurements of the illuminance at the raster measurement points defined in the area between the pavement, see *Figure 4.3*, the resulting dimensions are given in Table 4.2.

Table 4.2 – Measuring points and resulting measurements.

Point No	1	2	3	4	5	6	7	8	9	10
Measured quantity value, x_{ji}/lx	4,76	7,92	9,32	3,80	6,56	3,80	3,04	4,24	4,09	2,11
Point No	11	12	13	14	15	16	17	18	19	20
Measured quantity value, x_{ji}/lx	2,44	2,23	1,73	1,74	1,61	1,53	1,45	1,39	1,72	1,93
Point No	21	22	23	24	25	26	27	28	29	30
Measured quantity value, x_{ji}/lx	1,78	2,69	3,74	3,62	3,54	5,93	7,42	4,34	7,32	9,50

List of uncertainty components and their discussion

Overview of the components of combined standard uncertainty in the illuminance measurement of a selected section of the surface of the pavement is shown in Table 4.2 and an explanation of these components is presented in Table 4.3 in tabular form.

4.2.2 The first approximation cycle – the measurement result and documentation and calculation of the components of the combined standard uncertainty

Measurement result   **Iterative method**

Since the measurement task is to check the current state of the lighting solution on the surface of the pavement between the lighting posts, the connection (9) is calculated using the arithmetic mean of the measurements obtained in Table 4.2, which has the value of

$$\bar{x}_j = \frac{1}{n}\sum_{i=1}^{n} x_{ji} = 3{,}91 \text{ lx}$$

The result of the measurement using the approximation method is the sum of the illuminances of which all the additions are in units of illuminance, in this case expressed as

$$y = \bar{x}_j + \delta x_{\text{MV}} + \delta x_{\text{MÕ}} + \delta x_{\text{KK}} + \delta x_{\text{ÜS}} + \delta x_{\text{MO}} = 3{,}91 \text{ lx}$$

y in $\bar{x}_j$ indicates 2 m × 3.7 m raster of the arithmetic mean of the measurements (readings) obtained in 30 points on the surface of the pavement, δx_{MV} is the measuring instrument reading correction, the rest of the equation corrections, i.e., the corrections of the measurer $\delta x_{\text{MÕ}}$, the measuring environment δx_{KK}, the setting $\delta x_{\text{ÜS}}$, the measuring object δx_{MO} are considered to be close to zero for this approximation but they have uncertainty. Thus, the combined standard uncertainty $u(y)$ of the measurement result in this case can be calculated from the relation

$$u(y) = \sqrt{u_{x\text{MV}}^2 + u_{x\text{MÕ}}^2 + u_{x\text{KK}}^2 + u_{x\text{ÜS}}^2 + u_{x\text{MO}}^2} \tag{30}$$

Using this equation, the combined standard uncertainty is calculated in *Figure 4.4*.

List of uncertainty components and discussion
An overview of the components of the combined standard uncertainty in the illuminance measurement of the luminous surface section in Figure 3.4 and the measurement points in Figure 4.3 is provided in tabular form in Table 4.3.

Table 4.3 – Basic potential components of the combined standard uncertainty in the measurement of luminous surface illuminance and their explanations

Title Low resolution	Title High resolution	Name of the combined standard uncertainty component	Explanations	
$u_{x\text{MV}}$		Measurement instrument error	The lux meter is calibrated and has a measurement deviation within the MPE value, which is 3% of the reading for a measuring range (1 ... 30) lx	
$u_{x\text{MÕ}}$	$u_{x\text{NV}}$	Taking a reading	The uncertainty of the reading is determined by the last step of the reading	The largest of these is the value of $u_{x\text{MÕ}}$
	$u_{x\text{LV}}$	Resolution	$u_{x\text{LV}} = d/2\sqrt{3}$ $= 0{,}01 \text{ lx}/2\sqrt{3} = 0{,}003 \text{ lx}$	
	$u_{x\text{KV}}$	Repetition	Based on the experimental repeatability study $a_{x\text{KV}} = 0{,}01 \times x$, where x is the measurement result	

Title Low resolution	Title High resolution	Name of the combined standard uncertainty component	Explanations	
$u_{x\text{KK}}$	$u_{x\text{EO}}$	Temperature difference between instrument and measuring object	The temperature difference between the lux meter and the road surface to be measured is expected to follow the U-shaped distribution and measurements are made so rapidly that the instrument changes little in its temperature.	The largest of these is the value of $u_{x\text{KK}}$
	$u_{x\text{ET}}$	Difference between the measuring environment and the reference temperatures	The temperature difference between the measuring medium and the reference temperature is expected to follow the U-shaped distribution.	
	$u_{x\text{EM}}$	The change in the temperature of the instrument during measurement	The temperature change of the lux meter during the measurement is assumed to follow a rectangular distribution.	
	$u_{x\text{EN}}$	Humidity of the measuring environment	It is expected that the effect of the atmospheric absorption of light and the condensation of moisture on the light transmission surfaces of the lux meter or their electrical circuits should be determined experimentally.	
$u_{x\text{ÜS}}$		Difference between instrument position and nominal position	It is assumed that the position, inclination and directional uncertainty component of the sensor light sensitive surface of the lux meter is determined experimentally.	
$u_{x\text{MO}}$		Unevenness of measurable size on a measuring object	It is assumed that the illumination irregularity of the surface of a light traffic road follows a rectangular distribution.	

Lux meter measurement error   **Type B evaluation**

The MPE estimate for the lux meter is 3% of the measurement result $y = 3,91$ lx. For certainty, a rectangular distribution with $b = 0,6$ is assumed. The result is the standard uncertainty of the measurement deviation of the lux meter according to (14)

$$u_{x\text{MV}} = \text{MPE} \times b = [(3\ \% \times 3{,}91\ \text{lx})/100\ \%] \times 0{,}6 = 0{,}07\ \text{lx}$$

Readings and resolution   **Type B evaluation**

The reading depends on the lux meter. In this case, it is a numeric indicator with a reading step
$d = 0.01$ lx. Therefore, the standard uncertainty of sampling according to relation (15) is

$$u_{x\text{NV}} = 0{,}3 \times d = 0{,}3 \times 0{,}01\ \text{lx} = 0{,}003\ \text{lx}$$

The resolution of the lux meter is given in the specification of the instrument, which reads d = 0,01 lx. Thus, the standard uncertainty due to resolution according to relation (15) is

$$u_{xLV} = 0,3 \times d = 0,3 \times 0,01 \text{ lx} = 0,003 \text{ lx}$$

Repeatability   **Type A evaluation**
Previously, a study of the repeatability of the dimensional values obtained by measuring the illuminance by meter was carried out. The resulting distribution limit a_{xKV} =1% of the arithmetic mean of the dimensions $\bar{x}_j$ = 3,91 lx. Assuming that the repetition distribution corresponds to the normal distribution, the repeatability standard uncertainty is calculated according to section 3.4.4

$$u_{xKV} = a_{xKV} \times b = [(1 \text{ \%} \times 3,91 \text{ lx})/100 \text{ \%}] \times 0,5 = 0,02 \text{ lx}$$

Of these combined standard uncertainty components, the component with the highest repetition value is the highest. Thus,

$$u_{xM\tilde{o}} = u_{xKV} = 0,02 \text{ lx}$$

Temperature of the measuring instrument and the measuring object
                                                               Type B evaluation
Based on previous tests, the difference (15-20) K between the lux meter and the pavement surface may cause a change in the reading of the measuring instrument used, which does not exceed a_{xEO} =2 % of the arithmetic mean of the measurements $\bar{x}_j$ = 3,91 lx. Assuming a U distribution such that b = 0,7, the value of this combined standard uncertainty component is given in section 3.4.4

$$u_{xEO} = a_{xEO} \times b = [(2 \text{ \%} \times 3,91 \text{ lx})/100 \text{ \%}] \times 0,7 = 0,05 \text{ lx}$$

Measuring the medium temperature and the reference temperature
                                                               Type B evaluation
The instrument specification [14] specifies the operating range of the lux in the ambient temperature range from −10 °C to + 30 °C. When measuring the luminance, the maximum difference in the ambient temperature from 20 °C is 18 °C. Assuming that a measurement of 2 °C at ambient temperature is converted to 20 °C, a measurement error of not more than a_{xET} =1 % of the measurement result y = 3,91 lx may occur. This U-distribution of the uncertainty component due to the temperature difference is given in section 3.4.4

$$u_{xET} = a_{xEO} \times b = [(1 \text{ \%} \times 3,91 \text{ lx})/100 \text{ \%}] \times 0,7 = 0,03 \text{ lx}$$

Temperature of the instrument   **Type B evaluation**
The instrument specification [14] states that a change in the temperature of the lux meter within the range of ambient temperatures between −10 °C to +30 °C will not cause a measurement error. Thus, the recorded time fluctuation of the lux meter at 5 °C gives us that

$$u_{xEM} \approx 0 \text{ lx}$$

Humidity of the measuring environment   **Type B evaluation**

Measures have been taken to measure the illuminance so that the air humidity in the measuring environment does not affect the measurement results. So, in this case,

$$u_{x\text{EN}} \approx 0 \text{ lx}$$

Of these combined standard uncertainty components, $u_{x\text{EO}}$ has the highest value. In this case,

$$u_{x\text{EO}} = u_{x\text{KK}} = 0{,}05 \text{ lx}$$

Set-up   **Type B evaluation**

The deviation of the transducer axis between the surface of the pavement, according to the lux meter specification, has a negligible influence on the reading of the gauge. The direction of the light emitted from the mast in relation to the vertical axis of the sensor has a greater influence on the reading of the measuring instrument. According to the graph of the lux meter specification, the angle of incidence of light from the light source at 70° times the vertical (in this case, the worst case) is the effect of the combined standard uncertainty component of the result due to its effect is 1% of the result. Thus,

$$u_{x\text{ÜS}} = [(1 \% \times y)/100 \%] = 0{,}01 \times 3{,}91 \text{ lx} = 0{,}04 \text{ lx}$$

Measuring object   **Type B evaluation**

The extent of the object to be measured, the length of the asphalt pavement surface, is defined by the distance between the one-sided illuminating posts, which results in a higher illuminance near the posts and the smallest at the centre of the posts. The arithmetic mean of the measurements at the specified raster measurement points is significantly affected by the illumination irregularity of the surface of the intersection between the posts, which results in a compound uncertainty component with rectangular distribution that can be calculated from the connections given in Table 4.2 (excluding those obtained at measuring points 3 and 30 directly below the lighting posts)

$$u_{x\text{MO}} = \left(x_{j2} - x_{j18}\right)/2\sqrt{3} = (7{,}92 \text{ lx} - 1{,}39 \text{ lx})/2\sqrt{3} = 1{,}88 \text{ lx}$$

Assembly of uncertainty budget

The uncertainty is summarized in section 4.2.3 in a simplified form, using a low distinction, for the first approximation cycle in the form of the table given in Table 4.4.

Table 4.4 – The first uncertainty summary approximation cycle

The name of the component	Indications of the standard uncertainty	Evaluation type	Distribution type	Number of measurements	Variation limit in units of the agent a^*_{xj}	Variation limit a_{xj}/ lx	Correlation factor	Distribution factor b	Value of the combined standard uncertainty component u_{xj}/ lx
Measuring instrument	$u_{x\text{MV}}$	B	rectangular		3 %	0,12	0	0,6	0,07
Measurer	$u_{x\text{Mõ}}$	B	Gauss	30	1 %	0,04	0	0,5	0,02
Environment	$u_{x\text{KK}}$	B	U		18 °C	0,07	0	0,7	0,05
Set-up	$u_{x\text{ÜS}}$	B	experiment		70°	0,04	0		0,04
Measured object	$u_{x\text{MO}}$	B	rectangular		3,26 lx	3,26	0	0,6	1,88
Combined standard uncertainty, $u(y)_{\text{E1}}$ / lx									1,90
Expanded measurement uncertainty, U_{E1}/ lx									3,80

Combined standard uncertainty and expanded measurement uncertainty
It is assumed that the components of combined standard uncertainty do not correlate with each other. In this case, the combined standard uncertainty can be found from the relation given by the equation in *Table 4.4* according to formula (29)

$$u(y)_{\text{E1}} = \sqrt{u^2_{x\text{MV}} + u^2_{x\text{Mõ}} + u^2_{x\text{KK}} + u^2_{x\text{ÜS}} + u^2_{x\text{MO}}} =$$

$$= \sqrt{(0{,}07^2 + 0{,}02^2 + 0{,}05^2 + 0{,}04^2 + 1{,}88^2)\text{lx}^2} = 1{,}90 \text{ lx}$$

The connection of expanded measurement uncertainty according to formula (27) is

$$U_{\text{E1}} = u(y)_{\text{E1}} \times k = 1{,}90 \text{ lx} \times 2 = 3{,}80 \text{ lx}$$

or

$$U_{\text{E1}\%} = U_{\text{E1}}/\bar{x}_j = 3{,}80 \text{ lx}/3{,}91 \text{ lx} \times 100 \% = 97 \% \gg 10 \%$$

Discussion of the uncertainty summary
The condition $U_{\text{E1}} \leq U_{\text{L}}$ for the first approximation cycle uncertainty summary is not met. In this assembly, a component $u_{x\text{MO}}$ of the excess is the combined standard uncertainty caused by the uneven illumination of the measurable section of the light traffic path equipped with unilateral masts. Based on the information available, it is not

possible to obtain a lower estimate for $u_{x\text{MO}}$. The only option is to redesign and rebuild the pavement lighting facility. Temperature convergence should also be better, allowing the $u_{x\text{KK}}$ component to be reduced. This should be done by allowing more time for acclimatization or by selecting a more suitable measurement time to keep the ambient temperature as close to 20 °C as possible. It should also be possible to provide more effective protection from the heat of the body parts of the meter and the humidity level of the surrounding measuring environment during handling and measurement of the measuring instrument. Modifying (reducing) any of the other components of non-uniformity of illuminance and non-ambient uncertainty has no effect on the combined standard uncertainty in this case. [52]

Conclusion from the first approximation cycle

On the basis of the first approximation cycle, the measurement operation described above, based on which the arithmetic mean and its expanded uncertainty were calculated using the measurements obtained at the various measuring points of the illuminance between the masts, cannot not be validated because the condition $U_{\text{E}1} \leq U_{\text{L}}$ is not followed.

A second approximation cycle of measuring the luminance at a particular raster measurement point must be performed to verify the accuracy of the selected measurement operation. For this measuring point, the least-lit point on the road surface where the uncertainty in the illuminance measurement is likely to have the greatest value shall be selected. In this case, this point is the midpoint of the distance between the posts, which, according to the data in *Table 4.2*, is the measuring point No 18.

4.2.3 The second approximation cycle – documentation and calculation of the measurement result and the combined standard uncertainty

Measurement result and its combined standard uncertainty   Approximation method

According to the results of the first approximation cycle, the expanded uncertainty of the mean value obtained from measuring the illuminance of the section of the pavement between the posts does not satisfy the condition $U_{\text{E}1} \leq U_{\text{L}}$, therefore, the suitability of the measurement procedure for measuring the illuminance of the surface of the pavement by means of a second approximation cycle shall be checked.

As a precondition for this approximation cycle, the illuminance inequality must be eliminated and the measurement procedure is to be performed for the measurement of the illuminance intensity at the point of measurement of the illuminance surface raster, at which the illuminance measurement is likely to have the greatest uncertainty. In this case, the most unfavorable raster measurement point in terms of uncertainty is the point 18 measurement in *Table 4.2*, the value of

$$x_{j18} = 1{,}39 \text{ lx}$$

The measurement result at measuring point 18 using the approximation method shall be calculated from the sum of all additions in units of illuminance, in this case expressed as

$$y = x_{j18} + \delta x_{\text{MV}} + \delta x_{\text{MÕ}} + \delta x_{\text{KK}} + \delta x_{\text{ÜS}} = 1{,}39 \text{ lx}$$

The measurement result *y* from x_{j18} represents the 2 m × 3,7 m raster measured at the measuring point 18 of the pavement surface, δx_{MV} is the correction of the lux meter; in this case, the calibration certificate declares that the measurement of the lux meter is

within the range (1 ... 30) lx of the specifications within the MPE, the rest of the equation corrections, i.e., the corrections for the measurer, the environment and the set-up, are considered to be close to zero for the purpose of this approximation method, but they have uncertainty. Thus, the combined standard uncertainty $u(y)$ of the measurement result in this case can be calculated from the relation

$$u(y) = \sqrt{u_{x\text{MV}}^2 + u_{x\text{M\~O}}^2 + u_{x\text{KK}}^2 + u_{x\text{\"US}}^2} \qquad (31)$$

Using this relationship, the combined and expanded uncertainties in *Table 4.5* have been calculated.

Measuring instrument   **Type B evaluation**
The MPE value for a lux meter is 3 % of the measurement result, y = 1,39 lx. For certainty, a rectangular distribution with b = 0,6 is assumed. The result calculated using formula (16) gives the standard uncertainty of the reading of the lux meter

$$u_{x\text{MV}} = \text{MPE} \times b = [(3\ \% \times 1,39\ \text{lx})/100\ \%] \times 0,6 = 0,03\ \text{lx}$$

Measurer-induced component   **Type B evaluation**
The metric uncertainty component is the combined standard uncertainty component of repeatability described above, which has the value of

$$u_{x\text{M\~O}} = 0,02\ \text{lx}$$

Measuring environment induced component   **Type B evaluation**
Based on previous tests, the difference in temperature between the lux meter and the pavement (15...20) K between the ambient temperature in the range of −10 °C to +30 °C and measuring at the ambient temperature of 2 °C can result in $a_{x\text{KK}}$ = 2% change in the reading of the lux meter used from the measurement result y = 1,39 lx. Assuming a U distribution, in which case b = 0,7, the value of this combined standard uncertainty component is given in 3.4.3

$$u_{x\text{KK}} = a_{x\text{EO}} \times b = [(2\ \% \times 1,39\ \text{lx})/100\ \%] \times 0,7 = 0,02\ \text{lx}$$

Set-up induced component   **Type B evaluation**
The direction of the light from the light meter transducer axis to the transducer at the measuring point No 18 may be up to 70°. The value of the component uncertainty that influences the measurement result for this direction angle is 1% of the dimension, as plotted in the lux meter specification. So

$$u_{x\text{\"US}} = [(1\ \% \times x_{j18})/100\ \%] = 0,01 \times 1,39\ \text{lx} = 0,01\ \text{lx}$$

Measuring object   **Type B evaluation**
Based on the conclusions of the first approximation cycle, the illuminance irregularity of the surface of the pavement between the light posts is excluded.

Combined standard and expanded uncertainty

It is assumed that the components of combined standard uncertainty do not correlate with each other. In this case, the combined standard uncertainty can be found from the values given in formula (25) above, using the connection

$$u(y)_{E2} = \sqrt{u_{xMV}^2 + u_{xM\tilde{O}}^2 + u_{xKK}^2 + u_{x\ddot{U}S}^2} =$$

$$= \sqrt{(0{,}03^2 + 0{,}02^2 + 0{,}02^2 + 0{,}01^2)\ \text{lx}^2} = 0{,}04\ \text{lx}$$

The expanded uncertainty is

$$U_{E2} = u(y)_{E2} \times k = 0{,}04\ \text{lx} \times 2 = 0{,}08\ \text{lx}$$

or

$$U_{E2\%} = U_{E2}/x_{j18} = 0{,}08\ \text{lx}/1{,}39\ \text{lx} \times 100\ \% = 6\ \% < 10\ \%$$

Summary of uncertainty

The uncertainty aggregation for the second approximation cycle using low distinction is summarized in Table 4.5.

Table 4.5 – Summary of uncertainties in the second approximation cycle

The name of the component	Indication of the standard uncertainty	Evaluation method	Distribution type	Number of measurements	Variation limit In units of the agent a_{xj}^*	Variation limit a_{xj} / lx	Correlation factor	Distribution factor b	Value of the combined standard uncertainty component u_{xj} / lx
Measuring instrument	$u_{x\text{MV}}$	B	rectangular		3 %	0,042	0	0,6	0,03
Measurer	$u_{x\text{MÕ}}$	B	Gauss	1	1 %	0,040	0	0,5	0,02
Environment	$u_{x\text{KK}}$	B	U		18 K	0,028	0	0,7	0,02
Set up	$u_{x\text{ÜS}}$	B	experiment		70°	0,010	0		0,01
Combined standard uncertainty, $u(y)_{\text{E2}}$ / lx									0,04
Expanded measurement uncertainty, U_{E2}/ lx									0,08

Discussion of the uncertainty summary

Based on the second approximation cycle uncertainty summation, the condition $U_{\text{E2}} \leq U_{\text{L}}$ is satisfied. The uncertainty aggregate is the component $u_{x\text{MV}}$ of the combined standard uncertainty due to the predominant illuminance, the value of which is approximately one third of the combined standard uncertainty. The combined uncertainty in the measurement of one third of the component uncertainty due to a measuring instrument is typically present in all measurements. [52]

Conclusion from the second approximation cycle

There is reason to believe that the uncertainty summary for the second approximation cycle adequately estimates the uneven illuminance of the one-sided pavement section. Thus, the uncertainty criterion is met by initial assumptions and measurement instruments. This fact qualifies the measurement procedure used to be suitable for measuring the illuminance of the surface of a pavement at a single defined raster measurement point.

4.2.4 Conclusion

The example presented demonstrates that by using the simplified approximation method described above, the measurement method and the measurement conditions can be accepted as suitable for the uncertainty condition in order to ensure the condition

$$U_{\text{E}m} \leq U_{\text{L}} \tag{32}$$

In this case, after the first approximation cycle, it is quite obvious what should be done if the uncertainty conditions are not met. Only one component of uncertainty in the pool of uncertainties in Table 4.4 is dominant. In this case, in order to satisfy the uncertainty conditions of the agreement, the measuring task must be redefined and the illuminance measurement must be performed at a given or selected point on the measuring surface. The example illustrates very clearly how one component of uncertainty (in this case, the unevenness of the illuminance on the pavement) affects the combined standard uncertainty of the average illuminance after the first approximation cycle. Depending on the relative values of the uncertainty components in Table 4.4, a further strategy to reduce uncertainty was established, leading to a second approximation cycle. It should be taken into account that the example given is merely an illustration of a simplified approximation method for estimating uncertainty. The example contains the components of uncertainty that are relevant only in this particular example. For other applications, other components of uncertainty may be relevant. [52]

4.3 Information on using the interative method approach

The simplified approximation method for estimating and expressing the uncertainty described is based on GUM and uses its general concept. If more detailed procedures are described in GUM (e.g., the maximum uncertainty may include up to 33 components) for a more accurate estimation of uncertainty, such as in a flux photometric sphere, then the approximation described is based on an upper limit strategy. This slight overestimation of the uncertainty at all levels where convergence cycles determine the overestimation rate, allows the low-impact components to be dispensed with and the combined standard uncertainty to form a low distinction of 4 to 6 by the applied overestimated component. Deliberate overestimation is necessary to avoid misjudgments based on the measurement results. In most cases, the proposed approximation method requires very small resources (a small number of overestimated low-resolution components) to estimate the uncertainty, which may result in a slight overestimation of the uncertainty. If a more accurate measurement uncertainty assessment for photometric measurements is required, should still be used the more detailed procedures described and presented in GUM [57].

The approximation method described above can be used as a practical method for estimating measurement uncertainty in photometric measurements, which allows minimizing costs and maximizing the benefits of the expanded measurement uncertainty calculation process. The developed iterative method is economically independent. This approximation method has been used in the measurement processes of Tallinn University of Technology Lighting Laboratory, in the development and qualification of new measurement applications to ensure that the obtained experimental expanded uncertainty $U_{\mathrm{E}m}$ exceeds the given agreement uncertainty U_{L} as well as the target uncertainty U_{S} requirements, such that $U_{\mathrm{E}m} \leq U_{\mathrm{L}}$ and $U_{\mathrm{E}m} \leq U_{\mathrm{S}}$.

The described approximation method illustrated by the example of illuminance measurement is fully applicable to other types of technical illumination measurements, such as uncertainty in the measurement and documentation of measurements of light luminance, color temperature, spectral composition, glare, flicker, etc. [51], [58]

5 Development of a measuring instrument and measurement methodology for measuring the values characterizing the reflection of light from surfaces

5.1 Main measurement method, essential features and shortcomings

The properties of current roadway and walkway surfaces and the road materials used to produce them (additives, fillers and binders) have gradually changed. Therefore, the measurements obtained based on the measurement operations used for road surface luminance have a measurement uncertainty of up to 30 % of the measurement result and sometimes even 50 % of the measurement result [20], [34]. Luminous intensity distribution of the new type of light sources, especially the SSL-type light sources, is very sharp, which increases the impact of light characteristics reflected from the surface. Even the current LED technology supports smart road surface lighting and the opportunity to adapt the luminous flux at any time in terms of intensity and direction according to the characteristics of the road surfaces and the luminance requirements. These circumstances require development of new modern measurement methods and mobile measurement instruments in order to design more efficient, more economic and safer road surfaces and road lighting installations. There is a significant need to simplify and improve the measurement methods currently used to measure values characteristic of light reflection. With mobile measuring instruments, it is necessary to measure in situ the luminance of the coating surface directly surrounding the measuring point of the measuring grid defined on the coating surface and other light characteristics reflected from this surface and the diversity of these values. [VII]

The standard method and equipment for measuring the surface luminance of road pavements is mainly used [10], [11]. According to the method given in the standard, the luminance of the pavement is measured at predetermined points in the measuring field (calculation field) defined by the pavement standard (Figure 5.1) [11]. According to this standard, the measuring points of the measuring field defined for measuring the luminance of the pavement of a road section are evenly distributed, forming a raster of measuring points. The raster of the measuring points must be the same as for measuring the illuminance of the pavement of the same road section, which takes place before the measurement luminance of the pavement. When measuring the luminance of light reflected from the pavement surface, a measuring instrument, such as a luminance meter, is usually placed on a tripod 1,5 m above the pavement surface and 60 m above the closest measuring points of the road surface pavement field (calculation field). Measurements may also be made at each measuring point at a shorter distance from the measuring point, but in this case, the extent of the surface of the pavement touched by the luminance meter and the height of the measuring instrument above the surface of the pavement must be proportionally smaller. The angle of reference of the luminaire itself (angle of observation) in relation to the normal surface of the pavement shall be kept within 89° ± 0,5°. In the transverse direction, the luminance meter shall be located in the center line of the selected measurement field on the pavement of each lane of the road. When measuring the luminance of the pavement surface of a road section, the average luminance of the pavement surface, the overall uniformity of luminance and the elevation factor of the luminance threshold are calculated on the basis of the measurements obtained at the given measuring points. In this case, the longitudinal

uniformity of the luminance of the pavement surface is calculated on the basis of the measurements obtained for the measurement of luminance for a multi-lane pavement for the center line of all lanes. [11], [VII]
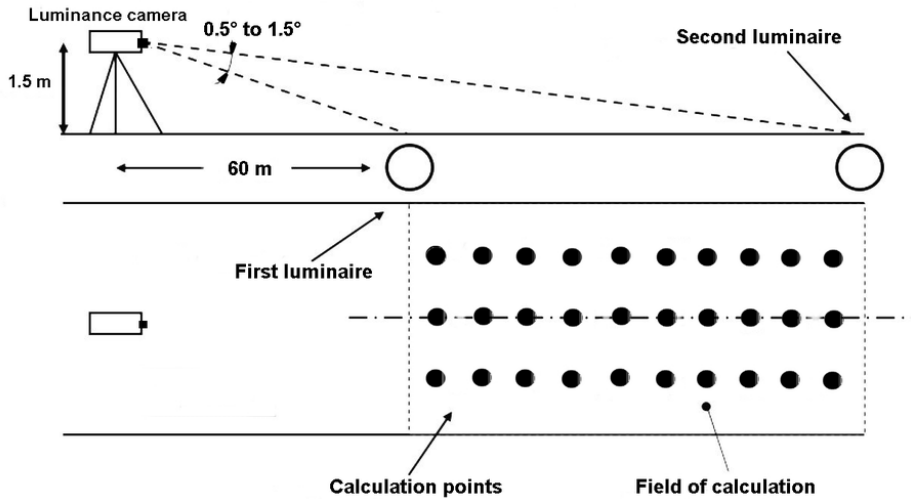

Figure 5.1 – Field of calculation and measurement for luminance.

The disadvantage of the measurement method used is that it is very measurement-intensive, expensive and has a relatively low level of accuracy. When implementing the method for all possible types of illuminance and luminance meters used, the location of the measuring points outside the given pavement surface and the light sources adjacent to the grid and the effect of the light generated by them on the luminance of the pavement surface must be taken into account. Also, for all luminance meters used, the grip angle of the pavement surface to be measured when measuring the luminance of any point on the grid of the measuring points shall not exceed 2 angular minutes in the vertical position and not more than 20 angular minutes in the horizontal position. However, this angle must not be less than 1 minute, which is the normal angle of human visual acuity. In order to obtain results for measuring the luminance, luminance factor, reduced luminance factor, color temperature and chromaticity coordinates of the pavement surface, the luminance of the pavement surface must be measured in advance at each of these measuring points, usually between 1 lx and 50 lx for all types of pavements. Luminance is measured by placing a measuring instrument, such as an illuminance meter, above the raster measurement point on the surface of the pavement. Thus, with this measurement method, the measurement of illuminance and luminance obtained at any point in the raster of the measuring points of the measuring field is affected by the instantaneous characteristics of the road lighting installations, weather and ambient conditions, and extraneous and disturbing light. Also, the road surface to be measured may be newly built, due to which the reflective properties of the surface of this road surface have not been stabilized. The reflective surface properties of this pavement may not stabilize for a few months. [VII], [8]-[12]

Low accuracy of the method used has been demonstrated in the present research. Using the uncertainty estimation method developed in Section 3, the estimation of the

uncertainty components of the measurement results obtained in the measurements is presented in Section 4. The standard data methodologies analyzed in publications I, III and IV are used as a basis.

During the research (as a result of the analysis of published publications I to VII), a structure with a new measurement method was developed, which allowed us to increase the universality of measurement, reduce measurement volume and ensure measurement accuracy, eliminating the effects of road lighting equipment, weather and ambient conditions and disturbing light.

5.2 Development of the new measurement method

In order to develop a method and a device for measuring the reflectance properties of surface light, various close patent solutions were developed and compared, which are reflected in the description of the patent application. [VII]

An example is Cidaut Technologies Llc road sign luminance measurement method and the luminance meters [59]. According to this measurement method, road sign surface luminance is measured indirectly based on the difference between two values characteristic of the level of reflection of light. Luminance meters are fixed to the front side of the vehicle between the lights. The values characteristic of one level of reflection of a road sign surface are fixed based on road surface lighting installations by one luminance meter and the values characteristic of the other level of reflection are determined based on the luminous flux coming from the vehicle's lights by the other luminance meter. The difference between the obtained values characteristic of the light reflection levels is fixed by an indicating device attached to the vehicle, which has a system for recording the reflection of light, positioning and synchronisation, which displays the final data from the measurement of road sign luminance.

A disadvantage of this method and the used luminance meters is their relatively high cost. The method and devices are applicable by using a respective moving vehicle. Thus, the method and the luminance meters used for its implementation only enable measuring the luminance of road signs. [59]

Another device developed by IWASAKI ELECTRIC Co., Ltd. for measuring the luminance of the road surface [60] allows one to measure the luminance of a road section at the measuring points specified in the measuring field and then evaluated by image processing. The luminance of the road surface is measured by a large number (e.g. 100) of measuring points under spotlight, which are used to estimate the average luminance. To shorten the measurement time, the image of the target area is taken with an imaging device, such as a semiconductor sensor, and processed with image processing equipment. When measuring the luminance of the road section surface, the average luminance of the target area and the luminance uniformity are calculated on the given grid on the basis of the measured values obtained at the given measuring points. The meter has a monitor for capturing the image, and it displays the mask of the metering area on top of the image taken in the imaging device. [VII], [60], [61]

A disadvantage of the described measurement device is its high price and relatively low accuracy. For calculating the luminance values, the measurement instrument uses grayscale, and due to its light reflecting characteristics (according to spectral distribution), it cannot be calibrated. The measurement device uses imaging software, which increases the measurement capacity and the inaccuracy of measuring. In addition, this measurement device enables measuring the luminance of the surface of road surface illuminated by only certain determined lighting installations and also does that relatively

inaccurately, i.e., with an approximately 30 % measurement uncertainty from the measurement result. [VII], [61]

A third example for comparison is the device and measuring method patented by Schreder [62], a bundle of light rays is directed in an open environment from the light source to the surface of the studied measurement object with a diameter of 113 mm gradually fixed at 0-, 30-, 50- or 70-degree angles from the surface normal of the measurement object. The measured luminance values of the light reflected from this 113 mm diameter surface of the measurement object are fixed by respective sensitive elements based on the horizontal of the surface in the direction of 5, 10, 20, 30, 40, 50, 60, 70 or 80 angular degrees. The measured values fixed by the sensitive elements are the basis for calculating the luminance coefficient and the reduced luminance coefficient. As a result, values of light reflected from the surface of the measurement object are obtained, which is a basis for calculating the luminance coefficient and reduced luminance coefficient of the surface of liquids as well as the surface of objects of fibrous material (road surface samples) depending on the angle of incidence of light and the direction of the luminance fixing element in relation to the surface of the measurement object. According to the method, the illuminance of the light directed to the measurement object is in the range of 5000 lx to 15000 lx, wherein illuminance is not measured. The mobile device used for the method is placed above the measurement object, and consists of a curved housing open from below and from the sides. Light source assemblies and sensitive elements fixing luminance have been attached to the surface of the curved housing positioned at an angle. At that, the light source assemblies are fixed at a 0-, 30-, 50- and 70-degree angle from the vertical direction. The luminance fixing sensitive elements used for measuring the reflective characteristics of the 113 mm diameter surface of the illuminated measurement object in an open environment have been fixed in place and are directed to the surface of the measurement object at a 5-, 10-, 20-, 30-, 40-, 50-, 60-, 70- and 80-degree angle from the horizontal. [62], [VII]

The described technical solution is the closest solution to the present invention and has thus been taken as a prototype.

Based on the measurement methodology [VII] developed in the course of this PhD dissertation, the basic scheme of the developed new measurement solution is presented in *Figure 5.2*. When using the measurement method in the diagram in the figure, the object of measurement is pavement 1, and when using the method, if necessary, the adaptation of the method to the measurement conditions of the pavement lighting quantities shall be checked first. To this end, the beam of free light from the calibrated light source 6 is directed at an angle to the surface of the illuminance sensor 5 placed above the pavement measuring point, the position of the center of the sensor surface 9 coincides with the pavement measuring point 2 and the illuminance and light spectrum are measured. If the measurements show that the measurement conditions are not in accordance with the illumination measurement method, the luminous flux of the light source, the angle of incidence (beam angle with respect to the pavement surface) and the distance l of the light source should be adjusted until the measurement conditions are met, i.e., the values of illuminance, spectral distribution of light and color temperature of the sensor surface 9 as reference values. These reference values are necessary because it is not possible to determine the values of the light reflected from the pavement without them, except for the values of the luminance factor and the reduced luminance factor at a relatively low level of accuracy, which considerably increases the universality of the measurement method and reduces the measurement

intensity. Sensor 5 is then removed from the grid measuring surface raster measuring point 2 and a beam of light is directed to the measuring point of the pavement surface to be measured under adapted lighting conditions (see Figure 5.2 pos 6, 7, 8) and from this surface, the light beam is exposed to the light beam. In *Figure 5.2* (pos 11, 12, 13, 14), the dimensions of light quantities reflected from the surface surrounding this measuring point of the road surface, such as luminance, luminance factor, reduced luminance factor, color temperature, color coordinates and other dimensions, are fixed. These dimensions shall be fixed under adapted measuring conditions for the measurement of the quantities of light reflected from the pavement. If the measuring conditions of these light quantities do not correspond to the adaptive measuring conditions, the observation angle β of the luminance meter and the distance l1 of the luminance measuring element from the center of the measuring surface (measuring point) shall be adjusted to ensure this. After adjusting the measurement conditions, the measurement data / measurements obtained are transferred to a program-based calculation model and the measurement results of the light quantities reflected from the pavement surface are obtained from the calculation model with the uncertainty of these results and displayed on a display or computer screen. [VII], [61]
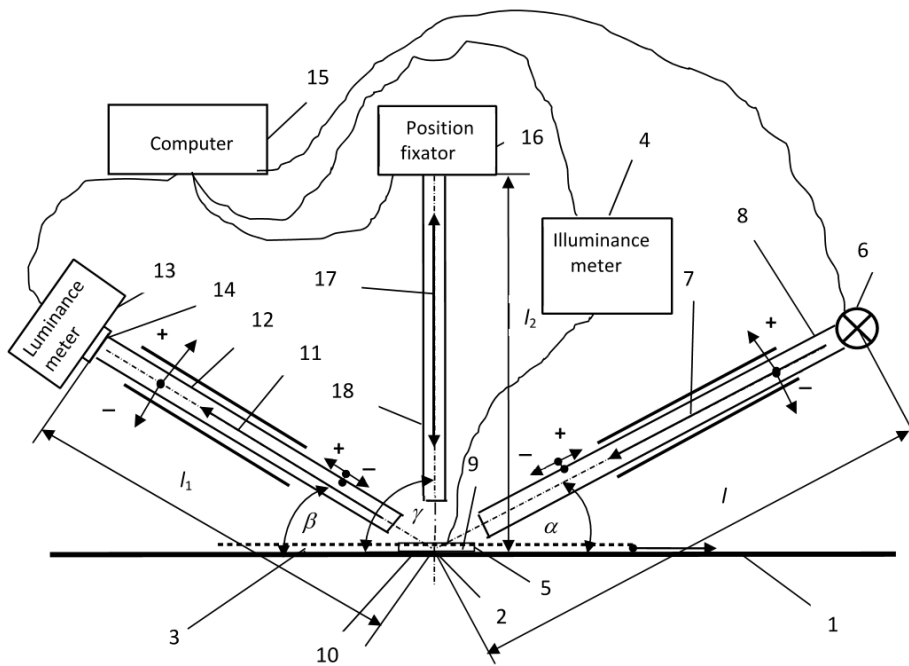
Figure 5.2 – Schematic diagram of the measurement method:
1 - road surface, 2 - measuring point, 3 - holder, 4 - illuminance meter, 5 - sensor, 6 - light source, 7 - light beam, 8 - tubular protection element, 9 - surface of the sensor, 10 - surface surrounding the measuring point, 11 - around the measuring point, beam reflected from the surface, 12 - tubular protection element, 13 - luminance meter, 14 - sensing element, 15 - computer, 16 - position fixator, 17 - tactile beam, and 18 - tubular protection element. [VII]

Since the method eliminates the effect of the location of light sources adjacent to the grid of measuring points on the pavement surface and the light generated by them on the measurement of pavement surface luminance, it significantly increases the measurement accuracy of all light reflected from the pavement surface.

The method also makes it possible to measure the quantities of light reflected from the surface of the pavement in a situation when the beam of light directed from the light source is perpendicular to the surface of the object to be measured. In this case, the position of the center of surface 9 of sensor 5 coincides with the measuring point of the pavement at an oblique angle α, interchanging the positions of light source 6 assembly and the measuring point positioner 16, which in turn increases the universality of the method. [VII]

5.3 Device developed for realizing the measurement method

To realize the method, a corresponding measuring device has been developed in the course of the research. The basic components of this measuring device are given in Figures 5.3 and Figure 5.4 in accordance with the item numbers given in the explanatory scheme of the developed method [VII].
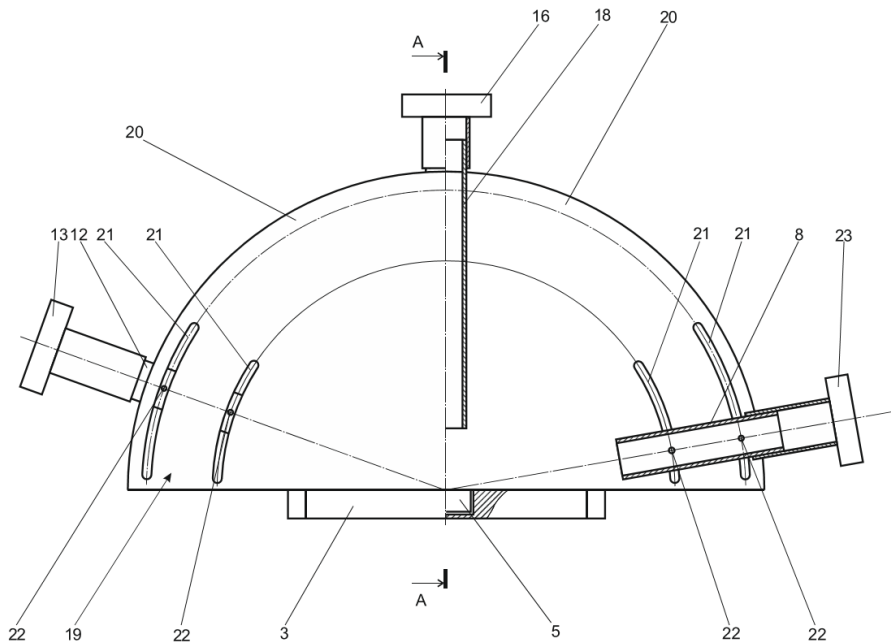
Figure 5.3 – Front view of a measuring device for measurement of the characteristics of the reflection of surface light in the ready-to-adjust condition (basic diagram):
3 - holder, 5 - sensor, 8, 12 and 18 - protection elements, 13 - luminance meter, 16 - position indicator, 19 - housing, 20 - segment-shaped parallel side panels, 21 - grooves through side panels, 22 - mounting parts, 23 - light source assembly with power supply, regulation and control components. [VII]
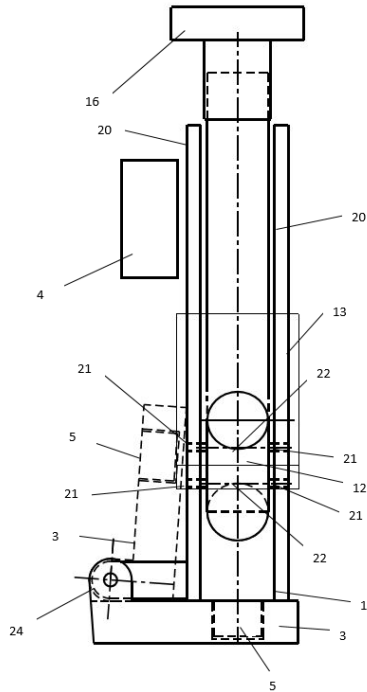
Figure 5.4– Enlarged end view of the same device in accordance with the schematic diagram of the measuring device shown in Figure 5.3 (luminance meter 13 removed, as a result of which the outlines of the luminance meter are shown in a thinner line in the figure): 3 - holder, 4 - illuminance meter, 5 - sensor, 12 - tubular protection element, 13 - luminance meter, 16 - position fixator, 19 - housing, 20 - side panels, 21 - grooves through the panel panels, 22 - mounting parts, 24 - swivel joints. [VII]

The developed measuring device consists of a bottom open curved housing (19) and a light source assembly (23) at an angle fixed to its curved upper part and a luminance-fixing sensitive element (13). A curved segmental side panel (20) and length-adjustable tubular external protectors (8) and (12) and a tubular protector (18) rigidly fixed in the plane of symmetry of the housing towards the interior of the housing, the axis of which is perpendicular to the support surface of the housing. The two tubular guards (8) and (12) can be adjusted longitudinally and at an angle by circular grooves (21) through the panels formed in the side panels (22) with fastening elements (22). As a luminance-sensitive sensitive element A light source assembly (23) with power, adjustment and control components and a positioner (16) and two pivot joints (24) are attached to the outer surface of the rear side panel, the pivots of which are attached to a rotatable holder (3), carrying the illuminance sensor (5). In addition, the light source assembly, measuring point positioner, luminance meter, luminance meter attached to the side panel of the instrument housing, and the luminance meter sensor in the holder are wired or wirelessly connected to a computer (see Figure 5.2). [VII]

By providing longitudinal and angular adjustment of the two tubular protection elements, the necessary adjustment of both the illuminance values directed at the surface of the pavement and the illuminance values reflected from this surface is

achieved, which increases the versatility of the measuring device, reduces measurement intensity and allows more accurate measurement. [VII]

By attaching a rotatable holder (3) carrying the luminance sensor to the side panel (20) of the meter housing, control over the adjustment of the luminance and related measurement conditions is achieved at all times, increasing the accuracy of the fixed reference values and thus the accuracy of the light reflected from the pavement. [VII]

Connecting a light source assembly, measuring point position indicator, luminance meter, luminance meter attached to the side panel of the meter housing, and a luminance meter sensor to a computer significantly reduces the measurement time, simplifies the measurement time, and simplifies universality.

The measuring device makes it possible to precisely fix and also adjust the position of the center of the surface (9) of the illuminance sensor (5) when adjusting the device (adjusting the lighting conditions) before measuring. The surface (10) between the tactile beam (17) and pavement 1 (perpendicular to the lower end faces of the side panels (20) of the measuring device housing (19)) at the right angle of the tubular protection element (18). When the reflected light quantities have been measured at the first measuring point 2 of the pavement 1, the measuring device is raised above the arbitrary measuring point 2 of the raster of the next pavement 1. A rotatable holder (3) with an illuminance meter (4) sensor (5) is attached to the side panel (20) of the device housing by means of rotating joints (24) to ensure that at adjusting the device (adjusting the measurement conditions), the surface (9) of the sensor (5) coincides with the surface surrounding in the same plane as the surface (9) of the sensor (5) adapted to the previous method (see Figure 5.1). It is easy to match the position of the center of the sensor (5) when setting the measuring device with the position of the arbitrary measuring point 2 of the pavement 1 when measuring with this device. [VII]

At each subsequent arbitrary measuring point 2 of the pavement 1, the measurement of the surface reflectance is performed with a measuring device already set (adapted to the measuring conditions) without further adjustment or adjustment operations analogous to the one described above at all measuring points of the pavement 1 raster 2. [VII]

If there is a need to measure the reflection values of the surface light in a situation where the light is directed only perpendicular to the pavement 1 to be measured, this situation can be solved by changing the positions of the assembly (23) and the positioner (16) (see Figure 5.3). Further, the measuring device is adjusted analogous to the above (measurement conditions apply) by means of the illuminance meter (4) sensor (5), directing light from the light source (6) perpendicular to the surface (9) of the sensor (5) and measuring the illuminance transversely to the surface (9) of the sensor (5) by adjusting the distance and luminous flux. After setting the measuring instrument (application of measuring conditions), in this case, the reflectance of the pavement 1 is measured analogous to the above, except that the position of the center (9) of the sensor (5) is fixed when adjusting the measuring instrument (applying the measuring conditions) and the measuring surface (2). [VII]

Attached to the lower part of the measuring device housing (19) is a deflectable holder (3) with a luminance meter (4) sensor so that when adjusting the measuring surface (9) coincides with the measuring surface 2 of the pavement 1 when measuring the measuring instrument, and then the lower part of the device housing (19) rests on the surface (10) of the pavement 1 and the previous setting of the device (application of measuring conditions) remains valid. [VII]

5.4 Validation of the developed measurement method and device

The developed measuring device and the measurement methodology created for the values characteristic of light reflection can also be applied for new purposes. In addition, the developed invention makes it possible to obtain new reliable values for the luminance of modern road surfaces and the relationships between the correlated color temperature of light, and for other purposes [VII].

Use of the method and equipment, for example, in the modern road asphalt pavements with traditional gas-fired lighting or lighting solutions already based on modern LED technology enables quick assessment of the changes in light reflection values. The reason is that the surface and environmental wear provides safer and more efficient solutions depending on the changes in the traffic environment, the weather environment, visual conditions, etc.

The benefit of the measuring method and the device invented is also in the fact that their application takes into account the scotopic and mesopic human vision in dark and dim environments, which have not been used so far. In LED lighting solutions and modern asphalt and concrete surfaces and in the case of the various additives used in them, it is possible to assess the values characteristics of the light reflection of the road surface. The method takes into account the spectral composition of the visible light or the effect of color temperature on the assessment of surface light reflection, thus providing safer and more efficient solutions for the traffic environment. [VII]

According to the experiment carried out in the present study, using the developed method and device for measuring the reflectance of surface light (device test specimen), the light reflected from the surface at different light color temperatures at different surface values is different, as shown in Figure 5.5.
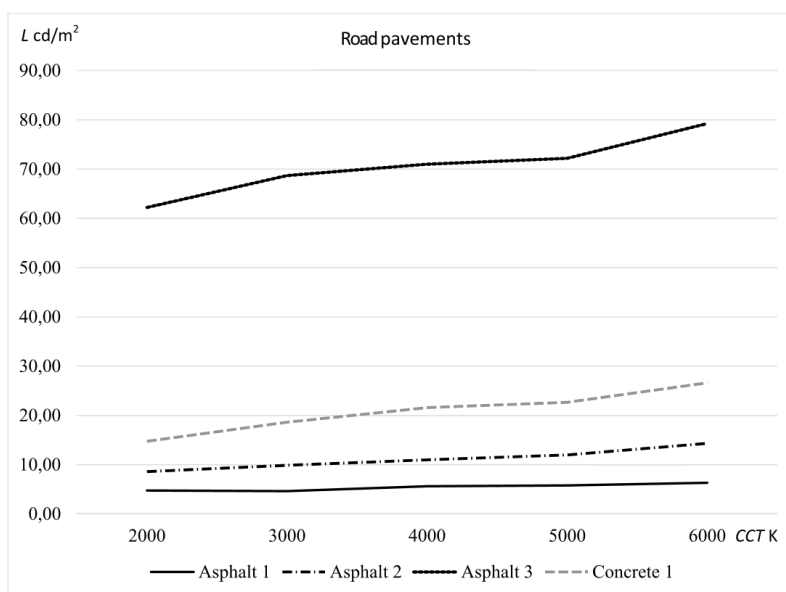

Figure 5.5 – Graphical representation of the dependence of the surface luminance values of different pavements on the color temperature obtained by measuring the surface luminance of different pavements using a test specimen of the developed device. [VII]

Since the developed method for measuring surface light reflection quantities is simple and the portable device used to perform it can measure the light quantities reflected from the surface of the pavement surrounding the point, the diversity of these quantities can be reduced and increased. This is also supported by the benchmark analysis of some of the characteristics of pavements reflected in the standard pavement measurement method used so far and in the commonly used measuring instruments and the developed measurement method described in section 5.2 and the device described in section 5.3 (device test specimen). [VII]

Table 5.1 – Benchmark analysis of light reflection quantities using commonly used measurement methods and instruments and the developed measurement method and device (device test specimen) [VII]

Applied measurement method	Measurement and calculation possibilities for values characteristic of light reflection in road surfaces				
	Illuminance	Luminance	Luminance coefficients	Colour temperature	Chromaticity coordinates
EN 13201-3 and EN 13201-4 measurement methods	Method realizable with $V(\lambda)$ correction by means of a luxmeter	Method realizable with a luminance meter placed on a tripod	Calculable by applying readings of luminance meter and lux meter and using data presented in the standard	Method realizable with colour temperature meter	It is not possible to measure chromaticity coordinates
The measument method described in the invention description	All values characteristic of reflection of light from road surfaces are measurable and calculable.				
Measurement devices applied	The time used for measuring and calculating values characteristic of reflection of light from road surfaces depends on the time for executing the measurement procedure described in the instruction for the measurement device.				
	Illuminance	Luminance	Luminance coefficients	Colour temperature	Chromaticity coordinates
Measurement devices in ordinary use	Spectral lux meter BTS256 EF	Spectro-radiometer JETI specbos 1211UV	Calculable using luminance meter, lux meter and data presented in the standard	Spectro-radiometer JETI specbos 1211UV	Spectro-radiometer JETI specbos 1211UV

Measurement devices in ordinary use	Spectral lux meter BTS256 EF	Spectro-radiometer JETI specbos 1211UV	Calculable using luminance meter, lux meter and data presented in the standard	Spectro-radio-meter JETI specbos 1211UV	Spectro-radiometer JETI specbos 1211UV
The measurement method described in the invention description	All values characteristic of reflection of light from road surfaces are measurable and calculable during 2 hours.				
Applied measure-ment method	The obtainable average value of expanded uncertainty in percent of the measurement and calculation results of values characteristic of light reflection on road surfaces is on the level of 95% probability. (The obtainable values of expanded uncertainty of color temperature and chromaticity coordinates are expressed in units of measure)				
	Illumi-nance	Lumi-nance	Lumi-nance coefficient	Reduced Luminance coefficient	Color tempe-rature	Color coordi-nates
EN 13201-3 and EN 13201-4 measure-ment method	10 lx	15 cd/m²	18	20		
The measurement method described in the invention description	5 lx	10 cd/m²	12	12	100 K	0,001

As seen from the data presented in Table 5.1, the developed method and device allow for an increase in the measurement accuracy [VII]. For the standard measurement method, the data are given for the mean value of the expanded uncertainty of the measurement result obtained at the measuring point of the pavement as a percentage of the measurement result. It turns out that the expanded uncertainty value of the measurement result given using the standard measurement method is about 1/3 of the components of the uncertainty due to the factors. As the new measurement method described makes it possible to minimize the proportion of agents, it makes it possible to significantly reduce the expanded uncertainty of the measurement results of the lighting technical quantities (reflection quantities) of the pavement surface. The possible average values of the expanded uncertainties of the measurement results obtained using the new measurement method presented in Figure 5.2 were confirmed as a result of testing a prototype of the device used to implement the measurement method. [VII]

6 Conclusions and future work

The present doctoral thesis offers an innovative measurement technical solution and a measurement methodology developed for this purpose, which makes it possible to assess human perceived lighting in scotopic and mesopic environments.

The work has been compiled based on several pilot projects. The pilot projects analysed the design of outdoor lighting in settlements from design to lighting measurements. The technical solution and measurement methodology created by the doctoral thesis allow us to enter more precise lighting technical input data into modern software solutions to characterize real environments.

In the course of the dissertation, modern street lighting measurement methods and measuring instruments were analysed and classified. When analysing lighting measurement methods, the analysis and classification of measurement uncertainty components was performed. Based on theoretical and practical knowledge, the upper limit of the known uncertainty components of lighting measurements was determined.

The measurement methodology and measuring device presented in Estonian Patent Application No. P2019000291 allow the measurement of the light reflection values of any externally lit roads. The measuring device is designed to measure the illumination and reflection of the surface of illuminated objects on a spectral basis. This solution can be used to measure and analyse all kinds of characteristics of road surface light reflection, such as road surface luminance, luminance factor, light color temperature. As a result of the application of the established measurement methodology and the device, the conditions for measuring the amounts of ambient light are adjusted and the values of the amounts of light obtained under these conditions are taken as reference values. Based on these values, the light reflectance values of the coatings for full-spectrum visible lighting solutions (including LED technology) and modern asphalt and concrete coatings used in modern road lighting can be realistically estimated with the invented solution. The application of the present invention takes into account the effect of the spectral composition of visible light in the evaluation of light reflected from the surfaces in a mesopic environment.

As a result, it is possible to offer safer and more energy-efficient solutions based on the environment, to reduce the measurement intensity and to increase the measurement accuracy. The innovative solution described and analysed in the dissertation enables greater measurement accuracy compared to the measurement method and measuring instruments that have been used so far for measurements according to the road surface standard.

The new invented measurement method described in the work allows one to minimize the proportion of influencers and thus allows a significant reduction of the expanded uncertainty of the measurement results of the lighting quantities (reflective quantities) of the pavement surface.

In the analysis of the uncertainty of the input variables of the lighting measurements and the measurement results performed in the framework of the thesis, the worst case contributed to the upper limit of each known component of uncertainty and thus the certainty of the evaluation results was ensured.

An examination of the measurement methods used so far has shown the need to improve the measurement methodology. Based on the conducted research and experiments, a novel measurement algorithm was developed. The dissertation describes

and analyses the effect of light color temperature and relationships on the reflective properties of coatings as an example of a new measurement method.

The analysis of the developed solution reached the following conclusions:

- The dissertation offers an innovative technical solution and methodology for measuring the values characterizing the light reflection of surfaces.

- The developed measuring device and measurement methodology allow one to measure the values of light reflection on roads with any external light.

- The implementation of the measurement methodology allows significant time savings.

- The application of the present invention takes into account the effect of the spectral composition of visible light in the evaluation of light reflected from surfaces in a mesopic environment.

- The innovative solution described and analysed in the dissertation enables higher measurement accuracy compared to the measurement method and measuring instruments according to the used pavement standard, and the measurement uncertainty of the measurements decreases to about 10 %, which was previously 40-50 %.

- Based on the methodology developed during the research and applying an innovative measuring instrument, we can use the equipment in accredited laboratories for real measurements.

6.1 Future research

Future challenges are to expand the studies to achieve energy savings in road lighting through the targeted application of lighting technologies in response to changes in environmental conditions and pavement properties.

The following directions have been proposed by the author:

- Research and development of reflective properties of pavements on the basis of the measurement methodology and the developed measuring instrument.

- Continuous research to identify previously undetected factors and components of measurement uncertainty and to evaluate them more accurately in photometric measurements.

- Planned in-depth research on real objects and in different real mesopic environments to further develop this topic.

- Further research and application possibilities of a patented technical solution in the Nordic countries.

References

[1] E. Petritoli, F. Leccese, S. Pizzuti, F. Pieroni, "Smart lighting as basic building block of smart city: An energy performance comparative case study," *Measurement,* vol. 136, pp. 466–477, 2019.

[2] K. Brocka, E. Ouden, K. Klauw, K. Podoynitsyna, F. Langerak, "Light the way for smart cities: Lessons from Philips Lighting," *Technological Forecasting and Social Change,* vol. 142, pp. 194–209, 2019.

[3] Strategic Roadmap 2025 of the European Lighting Industry, Lighting Europe Secretariat, 2016.

[4] S. P. Lau, G. V. Merrett, A. S. Weddell, N. M. White, "A traffic-aware street lighting scheme for Smart Cities using autonomous networked sensors," *Computers and Electrical Engineering,* vol. 45, p. 192–207, 2015.

[5] "Energy Efficiency Market Report 2014," OECD/IEA, 2014.

[6] G. I. Crabb, R. Beaumont and D. Webster, "Review of the class and quality of street lighing," 2009. [Online]. Available: https://courtneystrong.com/wp-content/uploads/2017/07/css-sl1-class-and-quality-of-street-lighting.pdf. [Accessed 06 04 2021].

[7] F. Valpreda, P. Iacomussi, G. Rossi, "Innovative design and metrological approaches to smart lighting," in *Proceedings of the 29th Quadrennial Session of the CIE*, Washington D.C., 2019.

[8] "Road lighting - Part 1: Guidelines on selection of lighting classes," CEN/TR 13201-1:2014.

[9] "Road lighting - Part 2: Performance requirements," EN 13201-2:2015.

[10] "Road lighting - Part 3: Calculation of performance," EN 13201-3:2015.

[11] "Road lighting - Part 4: Methods of measuring lighting performance," EN 13201-4:2015.

[12] "Road lighting - Part 5: Energy performance indicators," EN 13201-5:2015.

[13] CIE 081-1989, *Mesopic photometry: history, special problems and practical solutions,* http://cie.co.at/publications/mesopic-photometry-history-special-problems-and-practical-solutions.

[14] CIE TN 007:2017, *Interim recommendation practical application CIE system mesopic photometry outdoor lighting,* http://cie.co.at/publications/interim-recommendation-practical-application-cie-system-mesopic-photometry-outdoor.

[15] R. Dronneau, F. Fournela, V. Boucher, V. Muzet, F. Greffier, "Use Of An Imaging Luminance Measuring Device To Evaluate Road Lighting Performance At Different Angles Of Observation," in *International Commission on Illumination, CIE*, 2019.

[16] U. Krüger, I. Rotscholl and A. Fong, "Critical Considerations for Characterizing and Standardizing ILMDs," *Journal of the Society for Information Display,* pp. 25–29, 2020.

[17] "Road Surfaces and Lighting (Joint Technical Report CIE/PIARC)," Commission Internationale de l'Eclairage, Vienna, 1984.

[18] "Calculation and Measurement of Illuminance and Luminance in Road Lighting," Commission Internationale de l'Eclairage, Vienna, 1984.

[19] G. Rossi, P. Iacomussi and M. Zinzi, "Lighting Implications of Urban Mitigation Strategies through Cool Pavements: Energy Savings and Visual Comfort," *Climate journal,* vol. 6, no. 2, 04 2018.

[20] H. Gidlund, M. Lindgren, V. Muzet , G. Rossi and P. Iacomussi, "Road Surface Photometric Characterisation and Its Impact on Energy Savings," *Coatings,* p. 286–286, 2019.

[21] Interreg Baltic Sea Region, "LUCIA project 2021," [Online]. Available: https://lucia-project.eu/wp-content/uploads/2020/03/LUCIA-factsheet-TFS-6-20-03-25.pdf. [Accessed 28 09 2020].

[22] G. Zissis, R. Karlicek, C. C. Sun and R. Ma, "Energy Consumption and Environmental and Economic Impact of Lighting: The Current Situation," in *Handbook of Advanced Lighting Technology*, Cham, Switzerland, Springer, 2016, pp. 1–13.

[23] P. Jaskowski and P. Tomczuk, "Measurement systems used in measuring the illuminance of the road," in *2019 Second Balkan Junior Conference on Lighting*, Plovdiv, Bulgaria, 2019.

[24] "Estonia's 2030 National Energy and Climate Plan (NECP 2030)," European Commission, 2019.

[25] European Union Road Federation, "ERF Road Statistics Yearbook 2017," 2017. [Online]. Available: http://www.erf.be/wp-content/uploads/2018/01/Road_statistics_2017.pdf. [Accessed 28 09 2020].

[26] European Parliament, Council of the European Union, "Directive 2009/125/EC of the European Parliament and of the Council of 21 October 2009 establishing a framework for the setting of ecodesign requirements for energy-related products," 21 10 2009. [Online]. Available: https://eur-lex.europa.eu/legal-content/EN/ALL/?uri=celex%3A32009L0125. [Accessed 28 09 2020].

[27] Commission Internationale de l'Éclairage., "Calculation and Measurement of Luminance and Illuminance in Road Lighting," CIE 030:1976., Vienna, 1976.

[28] Commission Internationale de l'Éclairage, "Calculation and Measurement of Luminance and Illuminance in Road Lighting," CIE 030.2:1982., Vienna, 1982.

[29] Commission Internationale de l'Éclairage, "Road surface and road marking reflection characteristics," CIE 144:2001., Vienna, 2001.

[30] A. V. Rusu, C. D. Galatanu, G. Livint and D. D. Lucache, "Measuring Average Luminance for Road Lighting from Outside the Carriageway with Imaging Sensor," *Sustainability,* vol. 13, no. 16, 2021.

[31] V. Muzet, J. Bernasconi, P. Iacomussi, S. Liandrat, F. Greffier, P. Blattner, J. Reber and J. Lindgren, "Review of road surface photometry methods and devices – Proposal for new measurement geometries," *Lighting Research & Technology,* vol. 53, pp. 213–223, 2020.

[32] H. W. Bodmann and H. J. Schmidt, "Road surface reflection and road lighting: Field investigations," *Lighting Research and Technology,* vol. 21, no. 4, pp. 159–170, 1989.

[33] W. v. Bommel, Road Lighting, London: Springer International Publishing, 2015, p. 334.

[34] P. J.-L. Dumont E, "Are standard tables r still representative of the properties of road surfaces in France?," in *Proceedings of the CIE 26th Session*, Beijing, China, June 4 to 11: 2007.

[35] M. Casol, P. Fiorentin and A. Scroccaro, "On road measurements of the luminance coefficient of paving," in *16th IMEKO TC4 Symposium Exploring New Frontiers of Instrumentation and Methods for Electrical and Electronic Measurements*, Florence, Italy, 2008.

[36] V. Muzet, F. Greffier, A. Nicolaï, A. Taron and P. Verny, "Evaluation of the performance of an optimized road surface/lighting combination," *Lighting Research and Technology,* 2018.

[37] V. Muzet, M. Colomb, M. Toinette, P. Gandon-Leger and J. P. Christory, "Towards an optimization of urban lighting throug a combined approach of lighting and road building activities," in *Proceedings of the 29th CIE SESSION*, Washington D.C., USA, 2019.

[38] A.-M. Ylinen, L. Tähkämö, M. Puolakka and L. Halonen, "Road Lighting Quality, Energy Efficiency, and Mesopic Design – LED Street Lighting Case Study," *Leukos,* vol. 8, no. 1, pp. 9–24, 2011.

[39] CIE, "Spectral luminous efficiency (of a monochromatic radiation of wavelength λ) [V(λ) for photopic vision; V'(λ) for scotopic vision]," CIE e-International Lighting Vocabulary, [Online]. Available: https://cie.co.at/eilv/1222. [Accessed 15 08 2021].

[40] M. Maksimainen, M. Kurkela, P. Bhusal and H. Hyyppä, "Calculation of Mesopic Luminance Using per Pixel S/P Ratios Measured with Digital Imaging," *Leukos,* vol. 15, no. 4, pp. 309–317, 2019.

[41] A. Ylinen, M. Puolakka and L. Halonen, "Road surface reflection properties and applicability of the r-tables for today´s pavement materials in Finland," *Light and Engineering,* vol. 18, no. 1, pp. 78–90, 2010.

[42] V. Muzet and J. Abdo, "On site photometric characterisation of cement concrete pavements with Coluroute device," *Light Engineering,* 2018.

[43] 1. Petrinska, D. Ivanov, D. Pavlov and K. Nikolova, "Road Surface Reflection Properties of Typical for Bulgaria Pavement Materials," in *In Proceedings of the Lux Junior*, Dörnfeld, Germany, 25–27 September 2015.

[44] G. I. Crabb, M. H. Burtwell and R. J. Beaumont, "Reflectance Measurements on three pavement surfaces using CMH and HPS Lamps," in *Light Sources 2004 Proceedings of the 10th International Symposium on the Science and Technology of Light Sources*, Toulouse, France, 2004.

[45] S. Fotios, P. Boyce and C. Ellis, "The Effect of Pavement Material on Road Lighting Performance," Report, Sheffield, 2005.

[46] A. Ekrias, A. Ylinen, M. Eloholma and L. Halonen, "Effects of pavement lightness and colour on road lighting performance," in *CIE Expert Symposium on road surface photometric characteristics*, Torino, Italy, 2008.

[47] A. Ylinen, T. Pellinen, J. Valtonen, M. Puolakka and L. Halonen, "Investigation of pavement light reflection characteristics," *Road Materials and Pavement Design,* vol. 12, no. 3, p. 587–614, 2011.

[48] A. M. Ylinen, Development and analysis of road lighting – Road surfaces and mesopic dimensioning, Helsinki: School of Electrical Engineering, 2011, p. 170.

[49] P. Fiorentin and A. Scroccaro, "Analysis of the Performance of a Goniometer for Studying Surface Reflection," *IEEE Transactions on Instrumentation and Measurement 57,* vol. 57, no. 11, pp. 2522–2527, 2008.

[50] X. Chen, X. Zheng and C. Wu, "Portable instrument to measure the average luminance coefficient of a road surface," *Measurement Science and Technology,* vol. 46, no. 27, 2014.

[51] "Guide to the Expression of Uncertainty of Measurement," ISO, First edition 1993, Geneva, Correlated and reprinted 1995.

[52] T. Varjas, R. Laaneots, T. Möller and R. Teemets, "Mõõtetulemuse määramatuse hindamise lähendmeetod valgustehnilistel mõõtmistel," 2021 [forthcoming]. [Online]. Available: www.ester.ee/record=b5304909*est.

[53] R. Laaneots, O. Mathiesen and J. Riim, Õpik kõrgkoolidele (Metrology — Textbook for Higher Education Institutions), Tallinn: Tallinn University of Technology, 2012.

[54] "EN ISO 1:2016. Geometrical product specifications (GPS) — Standard reference temperature for the specification of geometrical and dimensional properties (ISO 1:2016)," CEN, Brussels, 2016.

[55] D. Gall, U. Krüger, F. Schmidt and S. Wolf, "Moderne Möglichkeiten zur Messung und Bewertung von Beleuchtungsparametern. Herbstkonferenz 2002 der GfA e.V.," in *Modern possibilities to measure and assess lighting parameters. Fall Conference, 2002. GfA, e.V.*, Ilmenau, Technical University, 2002.

[56] BTS256-EF. Spectral light meter with flicker measurement function., Munich: Gigahertz-Optik GmbH, 2019.

[57] R. Laaneots, Mõõtmine (Measurement), Tallinn: Tallinn University of Technology, 1998.

[58] K. Godo, "A new traceability chain for luminance scale with LED-based transfer standard," *Measurement Science and Technology,* vol. 32, no. 1, 2020.

[59] F. J. B. Roman, J. A. G. Mendez, A. M. Gallo, D. O. d. Lejarazu Machin and A. S. Perales Garcia, "Method for determining the luminance of traffic signs and device for implementing same". US Patent US9171360B2, 27 10 2015.

[60] L. IWASAKI ELECTRIC Co., "Luminance measuring apparatus". US Patent WO/2013/133033, 12 09 2013.

[61] Q. Li-jun, S. Zi-zheng and J. Feng, "Intelligent streetlight energy-saving system based on LonWorks power line communication technology," *Electric Utility Deregulation and Restructuring and Power Technologies (DRPT), 2011 4th International Conference,* pp. 663-667, 06 07 2011.

[62] M. Frankinet and S. SA, "Method and apparatus for establishing reflection properties of a surface". US Patent US7872753B2, 18 01 2011.

[63] "https://eur-lex.europa.eu/," EUR-Lex, 21 10 2009. [Online]. Available: https://eur-lex.europa.eu/legal-content/EN/ALL/?uri=CELEX%3A32009L0125. [Accessed 12 02 2021].

[64] C. Chain, F. Lopez and P. Verny, "Impact of real road photometry on public lighting design," in *Proceedings of the CIE 26th Session*, Beijing, China, June 4–11: 2007.

[65] P. Iacomussi, G. Rossi, P. Blattner, C. Chain, V. Muzet, J. Dubard, C. Van Trang, A. Jouanin, T. Kübarsepp, M. Lindgren, F. Manoocheri and P. Zehntner, "Metrology of Road Surface for Smart Lighting," in *Proceedings of LUX Europa 2017*, Ljubljana, Slovenia, September 18–20: 2017.

[66] T. Uchida and Y. Ohno, "Defining the visual adaptation field for mesopic photometry: Does surrounding luminance affect peripheral adaptation?," *Lighting Research & Technology,* p. 46, 2013.

[67] J. Hovila, New measurement standards and methods for photometry and radiometry — Doctoral Dissertation, Helsinki: Helsinki University of Technology, 2005.

[68] T. Uchida, M. Ayama, Y. Akashi, N. Hara, T. Kitano, Y. Kodaira and K. Sakai, "Adaptation luminance simulation for CIE mesopic photometry system implementation," *Lighting Research and Technology,* vol. 48, pp. 14–25, 2016.

[69] K. Painter, "The Influence of Street Lighting Improvements on Crime, Fear and Pedestrian Street Use, after Dark," *Landscape and Urban Planning,* vol. 35, pp. 193–201, 1996.

[70] S. P. Lau, G. V. Merrett and N. M. White, "Energy-efficient street lighting through embedded adaptive intelligence," in *2013 International Conference on Advanced Logistics and Transport*, Sousse, Tunisia, 29-31 May 2013.

[71] European Commission, "https://ec.europa.eu/transport/road_safety/," 19 06 2019. [Online]. Available: https://ec.europa.eu/transport/road_safety/sites/default/files/move-2019-01178-01-00-en-tra-00_3.pdf. [Accessed 17 10 2020].

Acknowledgements

Abstract
Research and development of measurement solution and methodology for assessment of light reflection from surfaces

The level of traffic safety and safety of the environment in the dim or dark conditions is to a large degree dependent on the quality of road ligthing. Along with their rapid development, the new LED light sources in use in today's road ligthing and the characteristics of road surfaces have created a situation, where the measurement methods and means have become obsolete with respect to their possibilities and exactness. Unfortunately, the same applies to the corresponding normative documents. Therefore, a need was experienced in the scientific research to develop a new measurement method, which would increase the universality of measurement, decrease substantially the measurement operations and ensure a significantly higher accuracy of measurement by excluding weather and environmental conditions as well as the disturbing effect of sidelight.

Within the frame of the doctoral thesis, an innovative measurement solution and the relevant implementation method have been developed. In real life, it enables us to estimate the perceived light for humans in scotopic and mesopic environments, which differs considerably from seeing conditions in daylight. The innovative measuring equipment can be used for spectrographical measurement and estimation of the different values characterizing light, such as luminance of the road surface, luminance coefficient, reduced luminance coefficient, color temperature, and chromaticity coordinates. The innovative measurement method described and analysed in the thesis enables higher accuracy than the existing measurement methods.

As a result of the measurement method and the relevant measurement equipment implemented, the characteristic values of illuminance emitted by the luminaires are imitated and these values are taken as base values. These base values allow for the estimation of the light reflecting characteristics in asphalt and concrete pavements even when different additives are used in them. In the implementation of the device, the effect of the spectral composition of visible light is taken into account when estimating the light reflected from the surface; thus, more safe and efficient solutions can be recommended for the traffic environment.

Existing measuring methods have been analysed and classified for the components of measurement uncertainty. Based on theoretical knowledge and practical experiences, an innovative method for estimating measurement uncertainty was developed for the measurement of light. The new measurement method makes it possible to minimize the share of side effects and therefore substantially decrease the overall uncertainty of measurement results when measuring (reflecting values) road surface lighting. The innovative solution described and analysed in the thesis enables a greater measurement certainty. As a result, the measurement uncertainty decreases from 40-50 percent to 10 percent.

Thanks to its simplicity in use and greater measurement precision, the practical value of the developed measurement method and the device is to use it first and foremost in light measurements in accredited measurement laboratories that conform to higher requirements imposed on the measurement procedures, including the measurement uncertainty.

Lühikokkuvõte
Mõõtmislahenduse ja metoodika uurimine ja arendamine pindadelt peegeldumise hindamiseks

Tänavavalgustuse kvaliteedist oleneb suurel määral liiklusohutuse tase ja elukeskkonna turvalisus hämara ja pimeda ajal. Nüüdisaja tänavavalgustuses kasutatavate uudsete leedvalgusallikate ja teekatendite omadused on oma kiire arenguga tekitanud olukorra, kus valgustuse mõõtemeetodid ja -vahendid on oma võimaluste ja täpsuse osas ajale jalgu jäänud. Kahjuks kehtib sama ka vastavate normdokumentide kohta. Seega tekkis teadusuuringute käigus vajadus välja töötada uus mõõtemeetod, mis suurendaks mõõtmise universaalsust, vähendaks oluliselt mõõtetööde mahtu ja tagaks oluliselt suurema mõõtetäpsuse, välistades ilma- ja keskkonnaolude ning kõrvalise häiriva valguse mõju.

Doktoritöö raames on loodud uuenduslik mõõtetehniline lahendus ja selle kasutamiseks välja töötatud mõõtemetoodika, mis võimaldab praktikas täpsemalt ning tunduvalt lihtsamini (seega ka kiiremini) hinnata inimesele tajutavat valgustust skotoopilises ja mesopilises keskkonnas, mis erineb oluliselt päevasest nägemise oludest. Leiutisena väljatöötatud mõõteseadet saab kasutada erinevate teekatendite pinnalt valguse peegeldust iseloomustavate suuruste, nagu sõidutee katendi pinna heleduse, heledusteguri, taandatud heledusteguri, värvsustemperatuuri, värvsuskoordinaatide, spektripõhiseks mõõtmiseks ja hindamiseks. Väitekirjas kirjeldatud ja analüüsitud uuenduslik mõõtemetoodika ja mõõtevahend võimaldab võrreldes olemasolevate mõõtelahendustega suuremat mõõtetäpsust.

Mõõtemeetodi ja selleks kasutatava mõõtevahendi rakendamise tulemusena imiteeritakse valgustuspaigaldiste poolt esile kutsutud valgustustihedust iseloomustavaid suurusi ja need väärtused võetakse tugiväärtusteks. Tugiväärtustest lähtuvalt saab hinnata teekatendite valguse peegeldust iseloomustavate suuruste väärtusi asfalt- ja betoonkatendite ning nendes kasutatud erinevate lisandite puhul. Seadme rakendamine võtab arvesse nähtava valguse spektraalse koostise mõju pinnalt peegeldunud valguse hindamisel ning võimaldab välja pakkuda liikluskeskkonnale ohutumaid ning efektiivsemaid lahendusi.

Olemasolevate mõõtemeetodite puhul on läbi viidud mõõtemääramatuse komponentide analüüs ja klassifikatsioon. Teoreetilistele teadmistele ja praktilistele kogemustele tuginedes töötati välja valgustehniliste mõõtmiste jaoks uudne mõõtemääramatuse hindamise metoodika. Uus mõõtemetoodika võimaldab minimeerida mõõtetulemuste kõrvalmõjude osakaalu ja seega oluliselt vähendada teepinna valgustuse (peegeldavate suuruste) mõõtmistulemuste laiendmääramatust. Väitekirjas kirjeldatud ja analüüsitud uuenduslik lahendus võimaldab suuremat mõõtetäpsust, mille tulemusena langeb mõõtemääramatus seniselt 40-50 protsendilt kuni 10 protsendini.

Tänu oma kasutamise lihtsusele ja suuremale mõõtetäpsusele seisneb väljatöötatud mõõtemeetodi ja seadme praktiline väärtus võimaluses kasutada neid eelkõige valgustehnilistel mõõtmistel akrediteeritud mõõtelaborites, millede mõõtetoimingute kohta sh mõõtemääramatusele kehtivad kõrgendatud nõuded.

Appendix

Case Study of Smart City Lighting System with Motion Detector and Remote Control

Marko Kuusik
Toivo Varjas
Argo Rosin
Department of Electrical Engineering
Tallinn University of Technology
Tallinn, Estonia
markokuusik83@gmail.com

Marko Kuusik
Toivo Varjas
Argo Rosin
Department of Electrical Engineering
Tallinn University of Technology
Tallinn, Estonia
markokuusik83@gmail.com

Abstract— **Public lighting is an important factor in ensuring safety in public areas. However, its costs to be covered by local municipality are heavy. Focus in this paper on the use of motion detection devices on the street. The aim is to help increase the sense of safety in an urban environment and at the same time to reduce the costs on urban lighting. According to the study, motion detection devices may help to save up to 40% of energy per month, still ensuring 100% of the required lighting norms for all road users.**

Index Terms—**lighting control, radar detection, remote monitoring, smart grid.**

I. INTRODUCTION

Electricity consumed by lighting accounts for approximately 20% of the world electricity consumption [1], out of which 5% is used in public lighting, such as street lighting, parking lots lighting, pedestrian area lighting, and park lighting. Continual rise in electric energy prices has urged municipalities to find opportunities for saving in street lighting. Commonly, after peak hours, some luminaires are switched off, which result in a considerable reduction of electric energy consumption. However, it also creates inferior lighting conditions and significantly diminishes traffic safety in urban areas.

Road and street lighting plays a very important role and its expenses are huge, accounting for almost 40% of the total energy consumption in a city. As a result, heavy pressure is placed on electric energy supply and environmental protection [2].

Results of different studies also provide convincing evidence that sensitively deployed street lighting can lead to reductions in crime and fear of crime, and increase pedestrian street use after dark [3]-[5]. According to British studies, crimes decreased by 38% in experimental areas compared to control areas [6]. Street lights also help to promote and extend socioeconomic activities, for example by allowing extended business hours, and by giving people the freedom to go out during the night [7]. Part-night lighting schemes aim to reduce the energy consumption of conventional street lights (those without the ability to dim) by turning them off at specific times and locations [8]. Time-based dimming schemes such as Philips Chronosense and Dynadimmer [9] reduce the brightness of a street light to 25-50% at strategic geographic locations and at specific times where traffic flow is expected to be low [10][11].

This paper introduces a study focused on a possibility to save on street lighting while ensuring the safety of traffic. The studied street lighting control system consists of motion detectors, a gateway, and a central management system software. Communication between every motion detector is based on wireless communication. Commissioning and control can be done locally or remotely over web services [12]-[15].

Studies were carried out in 2015 over the period of three months. The study was conducted in Väike-Turu Street, Tartu, Estonia. Motion detectors were installed in 14 luminaries. The aim of the study was to monitor how smart city lighting solutions and applications perform in the street lighting control. Additional savings in electricity costs were evaluated in situations where luminance was kept within the limits of standards and demands for various traffic situations. Thus, traffic safety was not compromised. The studied system lowered luminance up to 10% and restored the normal level when any traffic in the form of a pedestrian, a cyclist or a car was detected.

II. SMART CITY LIGHTING SYSTEM

A. Lighting Norms

Norms for road lighting are determined by users, traffic density, particularities of the road, and environmental conditions [16]. Lighting is designed and built according to the maximum lighting requirements of a road. Since roads are

Authorized licensed use limited to: Tallinn University of Technology. Downloaded on July 29,2021 at 20:41:11 UTC from IEEE Xplore. Restrictions apply.

not used in the same way round the clock, it is possible to use lower lighting requirements after peak hours. For example, if a peak hours, the traffic frequency of 7 000 vehicles in twenty-four hours implies the illumination class ME4b (average illuminance is $L \geq 0.75$ cd/m^2; overall uniformity is $U_0 \geq 0.40$; longitudinal uniformity is $U_1 \geq 0.60$), then after the peak hours, when the traffic frequency is less than 7 000 vehicles in twenty-four hours, the illumination class is ME5 (average illuminance is $L \geq 0.5$ cd/m^2; overall uniformity is $U_0 \geq 0.35$; longitudinal uniformity is $U_1 \geq 0.40$) [16]. During the night, when the number of moving vehicles on city streets is very low, in theory, lighting could be switched off.

During the period when the lighting level is reduced or lighting is switched off, unfortunately, safety on the road is not guaranteed. If a vehicle uses a road during this period, lighting conditions are below the required norms. The only way to guarantee right lighting conditions in the case of a moving vehicle or pedestrian, at the same time maximizing a possibility to reduce power consumption through reduced lighting level, is to use motion detection devices.

Not using motion detection devices enables the reduction of lighting level approximately up to 50%. Using motion detection devices enables higher reduction of the lighting level, because when a motion detection device detects a fast moving object on a road, then lighting will be immediately restored.

B. Study Location

The street surveyed in this study is located in Tartu near the city center. This street is a connection between the main street and the bus station. Locations of the lighting points on the street are shown in Figure 1.

Figure 1.   Location of Lighting Points

All of the old high pressure sodium lamp luminaires have been recently replaced with new LED luminaries. In the new LED luminaries, Siteco streetlight 10 midi LED luminaries with a power of 149 W are used. Each lighting point has been equipped with a motion detection device.

C. Motion Detection Devices

In this case, Comlight motion detection devices were been used. Devices will detect objects moving from 2 km/h to 200 km/h. Detection algorithms divide object detection into two separate data channels for slow and fast moving objects. This gives the possibility to set different lighting levels

depending on whether the detected object is a slow or a fast moving object. For example, when a slow moving object such as a pedestrian is detected, the lighting level increases to 80%, whereas if a fast moving object is detected, the lighting level increases to 100%, and if no movement is detected, all the luminaries work at a lighting level of 20%. If a device has detected motion, a signal will be sent to the next device via radio frequency communication. The number of devices that are activated upon receiving the signal can be set. For example, if this number is four, the lighting level of the next four luminaries' is increased to 100% after the first detector has detected a fast moving object. As the object arrives to the next detector's detection area, the command to increase the lighting level to 100% will be sent also to the following four devices [12]-[15]. This is illustrated in Figure 2. .
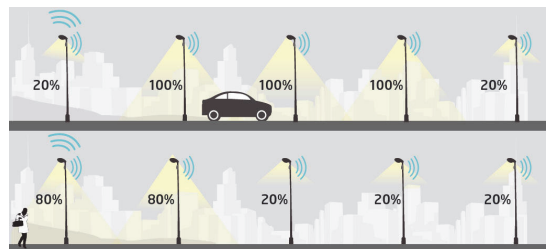

Figure 2.   Different Settings for Different Objects [15]

In the present study, lighting levels are the same. If the motion detector devices sense any vehicles or pedestrians, the lighting level will be increased to 100%, otherwise the luminaries work at the 10% lighting level.

D. Lighting Levels

The studied street section connects one of the main streets of Tartu with the bus station. Keeping the lighting on a lower level (at 10%) is only justified when there is no traffic. Also, the lighting level on the given section was surveyed to evaluate its concordance to the required lighting class in urban areas. The required lighting class of the given section is ME4b.

Figure 3. illustrates the lighting at level of 100%, and Figure 4. the lighting at a dimmed level of 10%.

Figure 3.   Lighting at level of 100%

In case of traffic, the lighting level has to be raised to a required level of class ME4b according to the standard EVS-EN 13201-2:2007 [17]. Lighting illuminance was measured with a luminance measuring imaging photometer LMK Mobile. Measured illuminance values for the lighting level of 10% and 100% and illumination classes required for illuminance values are shown on TABLE I.
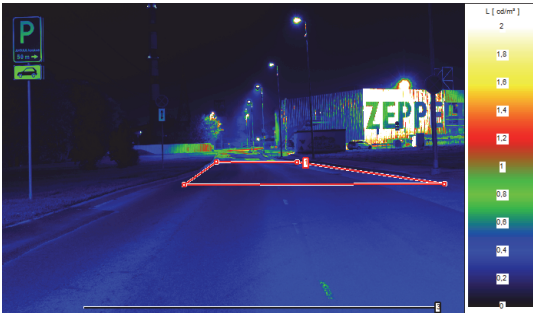

Figure 4.   Lighting at a dimmed level of 10%

TABLE I.   MEASURED AND REQUIRED ILLUMINANCE VALUES [17]

Lighting Level/ Illumination Class	Average Illuminance (cd/m2)	Overall Uniformity	Longitudinal Uniformity
10% level	0.2	0.5	0.4
100% level	1.7	0.5	0.8
ME4b	0.75	0.4	0.6
ME5	0.5	0.4	0.4

According to the measurement results, the required lighting norm was guaranteed in case of traffic.

III.   MEASUREMENTS (RESULT)

A. Working Time

The first calculation was made from 1st to 29th of September. In September, an average length of darkness in Tartu is 10.37 hours. If the street lighting is switched on at sunset and switched off at sunrise, then working time of the street lighting from 1st to 29th of September should theoretically be 300.73 hours. The actual working time was lightly shorter – 294 hours.

Figure 5.   shows separate working times when the luminaries worked at 10% and at 100% lighting. Also, actual dark time from sunset to sunrise on each day is illustrated.

Working time of the luminaries is generally related to the length of dark time. Actually, switch-on of luminaries is not conducted exactly at sunset, neither is switch-off conducted at sunrise. Switch-on and switch-off time depends on the weather conditions – cloudiness, rain, fog, etc.
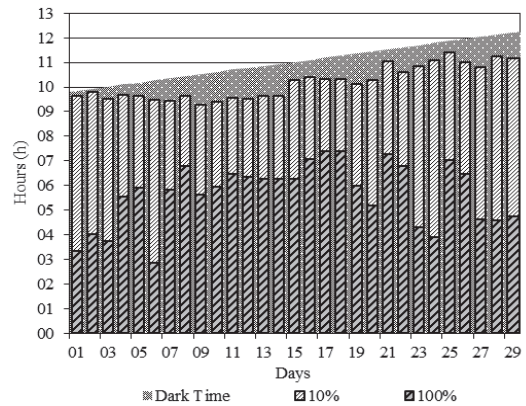

Figure 5.   Working Time

B. Detected Motions

During the study from 1st to 29th of September, all the motion detection devices detected 1.05 million moving objects. Maximum, minimum and average detected moving object numbers are presented in Figure 6.
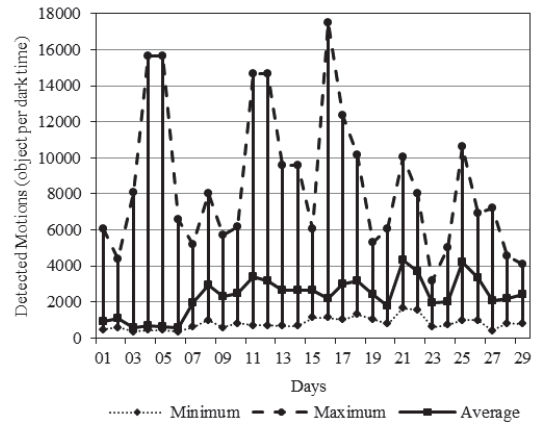

Figure 6.   Number of Detected Motions from 1st to 29th of September

Average number of detected moving objects ranged from 612 to 4 293 during dark time from 1st to 29th of September. At the same time, the maximum number of detected moving objects during dark time ranged from 1 260 to 17 506, and the minimum number of those detected ranged from 355 to 1 656.

Since it can be assumed that most of the moving objects were detected by several motion detectors, an average number of detected moving objects was used for the analysis.

C. Energy Consumption

The power of a lighting point is 150.5 W including luminaries power (149 W) and motion detection device

power (1.5 W). The total power of the measured section is 2.1 kW.

Total energy consumption and average detected motions for each day are presented in Figure 7.
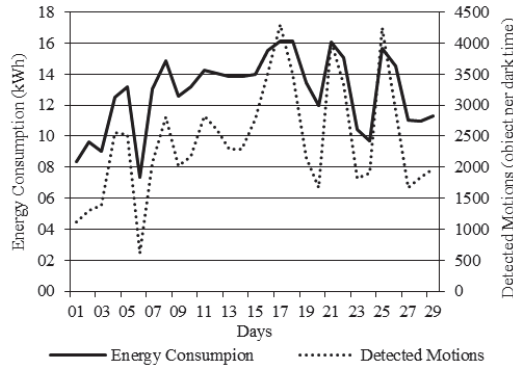

Figure 7. Energy Consumpion and Number of Average Detected Motions

As seen in Figure 7. , although mean working hours are similar, actual power consumption can vary two times between the days. Power consumption has a clear correlation to the traffic frequency.

D. Energy Saving and Alternative Solutions

In order to assess the suitability of motion detector devices, assessment of alternative solutions is necessary. The first alternative solution is that the dimming possibility is not used. In this case, luminaries work during the dark period all the time at a power level of 100%.

The second solution is that the luminaries are preconfigured. In this case, luminaries work on a power level of 100% from sunset to 11.00 PM and from 05.00 AM to sunrise. In the meantime, luminaries work on a power level of 50%.

Three different solutions (w/o – without dimming possibilities; SR – with self-sufficient power reduction; MDD – with motion detection devices) for energy consumption and differences in consumption are shown in TABLE II.

From 1st to 29th of September, energy consumption in one day decreased up to 63%. The overall energy saving during the study period was 40%. Figure 8. shows the energy saving for a different number of detected objects. It is obvious that with an infrequent use of the road during some dark time, greater energy saving was achieved.

Based on the results of the measurements carried out between 1st and 29th of September, it is possible to calculate an estimated energy saving (ΔE) from (1), when the motion detection devices detect a given number of objects (N) during the dark time:

$$\Delta E = (- 0.0099N) + 63.847. \qquad (1)$$

If all 14 luminaries had been working during that time period with setting SR, then the energy saving for the entire study period would have been only 9%. Also, as shown in TABLE II. , if motion detection devices had detected more moving objects, then the luminaries' working time would have been longer. Therefore, the given SR setting saves even more energy.
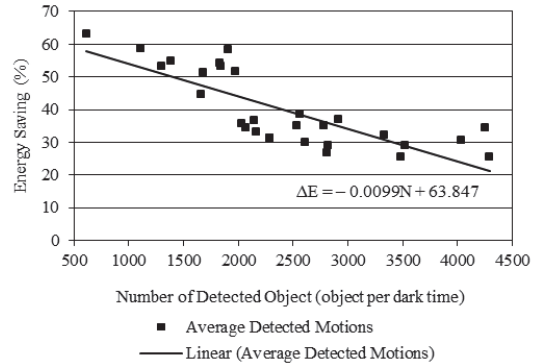

Figure 8. Energy Saving

TABLE II. THREE DIFFERENT SOLUTIONS FOR ENERGY CONSUMPTION

Date	Energy Consumption (kWh)			Difference in Consumption (%)	
	w/o	SR	MDD	w/o - SR	w/o - MDD
01.09	20.19	12.92	8.34	36	59
02.09	20.58	13.30	9.62	35	53
03.09	19.96	12.69	9.03	36	55
04.09	20.30	13.03	12.49	36	39
05.09	20.23	12.96	13.17	36	35
06.09	19.90	12.63	7.36	37	63
07.09	19.81	12.54	13.02	37	34
08.09	20.23	12.95	14.83	36	27
09.09	19.50	12.23	12.55	37	36
10.09	19.72	12.45	13.17	37	33
11.09	20.07	12.80	14.22	36	29
12.09	19.98	12.71	14.02	36	30
13.09	20.19	12.91	13.87	36	31
14.09	20.19	12.91	13.87	36	31
15.09	21.61	14.32	14.01	34	35
16.09	21.81	14.52	15.51	33	29
17.09	21.66	14,38	16,16	34	25
18.09	21.62	14.34	16.12	34	25
19.09	21.26	13.98	13.46	34	37
20.09	21.58	14.30	11.97	34	45
21.09	23.19	15.89	16.07	31	31
22.09	22.26	14.94	15.06	33	32
23.09	22.79	15.50	10.41	32	54
24.09	23.27	15.98	9.69	31	58
25.09	23.90	16.60	15.66	31	34
26.09	23.05	15.76	14.52	32	37
27.09	22.69	15.40	11.02	32	51
28.09	23.58	16.28	10.99	31	53
29.09	23.39	16.09	11.30	31	52
Total	618.50	407.28	371.48	34	40

The standard deviation of the total difference in consumption for w/o-SR and w/o-MDD is 2.12 and 11.33 accordingly; standard error is 0.39 and 2.1 accordingly; and coefficient of variation is 6.2% and 28.5% accordingly.

IV. Conclusions

Use of motion detection devices enables lighting to be ensured on a road from the moment it is needed. Energy saving obtained by using motion detection devices depends on the traffic frequency. The more traffic during the night, the smaller is the obtained energy saving. Nevertheless, if some other dimming solution is used and higher energy saving is achieved, it does not outweigh the fact that using motion detection devices helps to ensure safety for all the night-time road users.

According to the first part of the study carried out from September 1st until September 29th, the energy saving achieved using motion detection devices was up to 40%, maximum energy saving per day up to 63%, and at the same time, the 100% lighting level was ensured when a user was on the road. With alternative solutions, such as preprogrammed luminaires, the energy saving of up to 34% would be achieved at the same time period and maximum energy saving per day up to 37%.

The difference in energy saving between the preprogrammed lighting time and using object recognition depends heavily on object frequency. For example, if the frequency is so high that the lighting must be 100% during night-time, then the use of motion detection gives no energy saving. According to the study result, using motion detection devises achieve higher energy saving then preprogrammed settings, if object frequency is less then 3 000 during a night-time.

To achieve better and more trustworthy results, more studies should be carried out during a period of one year at least to compare the relation between the traffic frequency and energy savings on different months. Also, settings of the devices need to be revised overviewed as there were disruptions in transmiting the data to the central data server. Also, it is required to examine whether the difference between the maximum and minimum values of the identified objects was the normal behavior of road users, or were objects falsely detected during some period.

Acknowledgment

References

[1] "Energy Efficiency Market Report 2014," OECD/IEA, 2014.

[2] Qin Li-jun; Shen Zi-zheng; Jiao Feng, "Intelligent streetlight energy-saving system based on LonWorks power line communication technology," in *Electric Utility Deregulation and Restructuring and Power Technologies (DRPT), 2011 4th International Conference on*, vol., no., pp.663-667, 6-9 July 2011 doi: 10.1109/DRPT.2011.5993976.

[3] Kate Painter, The influence of street lighting improvements on crime, fear and pedestrian street use, after dark, Landscape and Urban Planning, Volume 35, Issues 2–3, August 1996, Pages 193-201, ISSN 0169-2046, http://dx.doi.org/10.1016/0169-2046(96)00311-8.

[4] R. A. Hargroves, "Road lighting," Physical Science, Measurement and Instrumentation, Management and Education - Reviews, IEE Proceedings A, vol. 130, no. 8, pp. 420 -441, Nov. 1983.

[5] D. Herbert and N. Davidson, "Modifying the built environment: the impact of improved street lighting," Geoforum, vol. 25, no. 3, pp. 339 - 350, 1994.

[6] B. C. Welsh and D. P. Farrington, "Effects of improved street lighting on crime," Campbell Systematic Reviews. 2008,

[7] Hiranvarodom, S., "A comparative analysis of photovoltaic street lighting systems installed in Thailand," in *Photovoltaic Energy Conversion, 2003. Proceedings of 3rd World Conference on*, vol.3, no., pp.2478-2481 Vol.3, 18-18 May 2003.

[8] Sei Ping Lau; Merrett, G.V.; White, N.M., "Energy-efficient street lighting through embedded adaptive intelligence," in *Advanced Logistics and Transport (ICALT), 2013 International Conference on*, vol., no., pp.53-58, 29-31 May 2013 doi: 10.1109/ICAdLT.2013.6568434.

[9] Koninklijke Philips Electronics N. V., "Different ways: The Dynadimmer and the Chronosense," 2010. [Online]. Available: http://www.lighting.philips.co.uk/subsites/oem/product_pages/dynadimmer_overview.wpd. [Accessed 21 05 2012].

[10] A. Matheson, "Reducing Energy Consumption - Street Lighting," 2008.

[11] Somerset County Council, "Somerset County Council: Reduction of street lighting in Somerset," 2011. [Online]. Available: http://www.somerset.gov.uk/irj/public/council/initiatives/initiative?rid=/guid/30afb148-555c-2e10-10be-ae0d39444537. [Accessed 19 Mar. 2012].

[12] "Eagle Eye – stand alone system," Comlight AS.

[13] "Comlight Streetlighting Control Solution," Comlight AS.

[14] "LUMINIZER (CMS) – your streetlight organizer!" Comlight AS.

[15] "Motion Sensing Street lighting," Comlight AS.

[16] CEN/TR 13201-1:2004 Road lighting/ Part 1: Selection of lighting classes. Tallinn: Estonian Centre for Standardisation, 2004.

[17] EVS-EN 13201-2:2007 Road lighting/ Part 2: Performance requirements. Tallinn: Estonian Centre for Standardisation, 2007.

Publication II

Armas, J.; Ivanov A.; Varjas T. (2017). Short-Circuit Currents Calculations in Street Lighting Networks. 58th International Scientific Conference on Power and Electrical Engineering of Riga Technical University, RTUCON 2017, Riga, Latvia, 2017-November. IEEE, 1–9, doi: 10.1109/RTUCON.2017. 8124758

Short-Circuit Currents Calculations in Street Lighting Networks.

Jelena Armas
Elektrilevi OÜ
Estonia

Aleksandr Ivanov
MeteorOwl OÜ
Estonia

Toivo Varjas
TTÜ
Estonia

Abstract – **The main feature of street lighting networks is that street lighting feeders usually have a considerable length (up to 1000m). That is the reason why the accurate calculations of short-circuit currents at endpoints of feeders are very important for selection of the feeder protection devices. The protection of people against indirect contact in the event of a fault is considered the most important in outdoor lighting installations.**

The purpose of the present publication is to introduce a practical method to be used in the MeteorCalc SL software when calculating short-circuit currents in street lighting installations (in three-phase low-voltage radial TN-systems), considering the specific characteristics of these networks. The described procedure fully complies with the IEC 60909 (last edition 2016). The numerical example illustrates all the steps of short-circuit currents calculations in a street lighting network.

Keywords – **Fault currents; Grounding; Street lighting installations, Calculation of short-circuit currents, Cable impedance, Method of symmetrical components;**

I.   INTRODUCTION

The protective device of a street lighting feeder must provide two basic protections: the protection of people against indirect contact and the protection of cables and other equipment against an overcurrent and against thermal effects, followed by the overcurrent.

The protection of people against indirect contact in the event of a fault should be considered as the most important in outdoor street lighting installations. This protection provides by specified disconnection time of an overcurrent cut-out device combined with an earthing. According to the IEC 60364-4-41, the maximum disconnection time t_b (sec) for TN and IT systems with the nominal voltage 230/400V is 0,2 sec (if a nominal current not exceeding 32A).

The calculated minimum short-circuit current allows to choose the setting of thresholds for overcurrent protective devices and fuses and allows to verify disconnection time of protective devices.

Thus, the calculations of minimum short-circuit current at the end points of street lighting feeders are the most important, but at the same time the most time-consuming calculation. Additional difficulties in the calculations arise because street lighting feeders usually consist of a number of cable sections of different cross-sections and different cable types.

There are various software tools to perform calculations of short-circuit currents and voltage losses in the low voltage networks. In this publication is used the calculation software known as MeteorCalc SL that allows to make accurate models of street lighting networks and to perform calculations of short-circuit currents at endpoints of feeders. This program was chosen because it allows receive detailed reports on the calculation process with all the intermediate and auxiliary results of calculations.

II.   PRINCIPLE OF SHORT-CIRCUIT CURRENTS CALCULATION

According to the IEC 60909 for balanced and unbalanced short circuits it is useful to calculate short-circuit currents by application of symmetrical components. The symmetrical components method allows to calculate all types of short-circuit currents at any point in a street lighting feeder with a high degree of accuracy.

The method used for calculation is based on the introduction of an equivalent voltage source at the short-circuit location. The equivalent voltage source is the only active voltage of the system [1].

To choose the protective device of a street lighting feeder the following calculations must be performed:

A. The calculation of the maximum short-circuit current

The estimated short-circuit point is located at the end terminals of the protective device at a distribution panel board. The calculated maximum short-circuit current (rms and peak values) determines the breaking capacity and the making capacity of circuit breakers and the breaking capacity of fuses, as well as the electrodynamic withstand of switchgears.

B. The calculation of the minimum short-circuit current

The estimated short-circuit point is located at the end terminals of the feeder cable. The calculated minimum short-circuit current (rms value) allows to choose the setting of thresholds for overcurrent protective devices and allows to verify disconnection time of protective devices.

III. CALCULATION ASSUMPTIONS AND CONDITIONS

According to the IEC 60909-0 Clause 5.2 the calculation of maximum and minimum short-circuit currents is based on the following simplifications:

a) For the duration of the short circuit there is no change in the type of short circuit involved, that is, a three-phase short circuit remains three-phase and a line-to-earth short circuit remains line-to-earth during the time of short circuit [1];

b) For the duration of the short circuit, there is no change in the network involved [1];

c) The impedance of the transformers is referred to the tap-changer in main position. This is admissible, because the impedance corrector K_T for network transformers is introduced [1];

d) Arc resistances are not taken into account [1];

e) All line capacitances and shunt admittances and non-rotating loads, except those of the zero-sequence system, are neglected [1].

According to the IEC 60909-0 Clause 7.1.2 when calculating maximum short-circuit currents, it is necessary to introduce the following conditions:

- Voltage factor c_{max} according to table I shall be applied for the calculation of maximum short-circuit currents in the absence of a national standard [1];

- Choose the system configuration and the maximum contribution from power plants and network feeders which lead to the maximum value of short-circuit current at the short-circuit location, or for accepted sectioning of the network to control the short-circuit current [1];

- Impedance correction factors shall be introduced in the positive-, the negative- and the zero-sequence system with exception of the impedances between neutral point and earth [1];

- When equivalent impedances Z_Q are used to represent external networks, the minimum equivalent short-circuit impedance shall be used which corresponds to the maximum short-circuit current contribution from the network feeders [1];

- Resistance R_L of lines (overhead lines and cables) are to be introduced at a temperature of 20 °C [1].

According to the IEC 60909-0 Clause 7.1.2 when calculating minimum short-circuit currents, it is necessary to introduce the following conditions:

- Voltage factor c_{min} for the calculation of minimum short-circuit currents shall be applied according to table 1 [1];

- Choose the system configuration and the minimum contribution from power stations and network feeders which lead to a minimum value of short-circuit current at the short-circuit location [1];

- The impedance correction factors are equal to 1 [1];

- Resistances R_L of lines (overhead lines and cables, line conductors, and neutral conductors) shall be introduced at a higher temperature [1].

IV. MAIN FACTORS AFFECTING THE RESULTS OF CALCULATIONS

There are factors that most significantly affect the results of calculations and they must be necessarily taken into account as the main parameters of calculations.

A. Voltage tolerance in street lighting networks

The voltage tolerance in street lighting networks (in low-voltage up to 1kV systems) defines the voltage factors used in short-circuit calculations. The voltage tolerance is defined by regional standards.

A voltage factor (as the part of an equivalent voltage source) directly affects the results of calculations. The values of a voltage factor in low-voltage networks are shown in the table I.

TABLE I

VOLTAGE FACTOR C ACCORDING TO THE IEC 60909-0 (2016)

Nominal voltage U_n	c_{max}	c_{min}
Low-voltage systems (up to 1kV) with a tolerance of ±6 %	1,05	0,95
Low-voltage systems (up to 1kV) with a tolerance of ±10 %	1,10	0,90

B. Conductors temperature for SCC calculations

The temperature of cable conductors directly affects the results of short-circuit current calculations.

According to the IEC 60909-0, a conductor temperature of 20 °C is assumed for the calculation of the maximum short-circuit current.

According to the IEC 60909-0, when calculating minimum short-circuit currents, the value of the cable resistance has to be introduced at a higher temperature. This temperature usually is defined by regional standards. The maximum permissible temperature of power cable at a short circuit may be used in the absence of such a standard.

C. Transformer winding circuit scheme

The transformer winding connection scheme can significantly affect the current of the single phase fault. The zero-sequence short-circuit impedance of transformers with D/Y and Y/Y winding scheme can differ by 10 or more times.

The zero-sequence short-circuit impedances of two-winding transformers at the low voltage side are determined from the

manufacturer. If data of the transformer are not available, the zero-sequence short-circuit impedances can be obtained using typical values of the ratios $R_{(0)T}/R_{TLV}$ and $X_{(0)T}/X_{TLV}$.

V. CALCULATION MODEL

The model of a street lighting network for performing the calculations where a street lighting feeder is presented as one cable section is shown in Fig. 1.
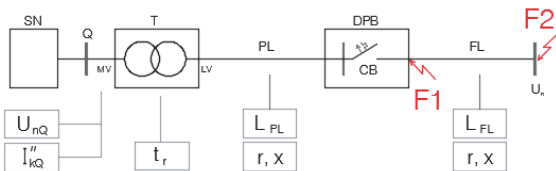

Fig. 1. System diagram for the calculation of short circuit currents in a street lighting feeder.

where:

SN   is the medium voltage supply network;

Q   is the MV feeder connection point on the primary side of a transformer;

T   is the network transformer;

PL   is the power line from the transformer to the distribution panel board;

DPB   is the street lighting distribution panel board;

CB   is the protective device of a street lighting feeder (circuit breaker or fuse);

FL   is the street lighting feeder line as the sum of all cable sections from the distribution panel board to the short-circuit point;

F1   is the short-circuit point for calculation of the maximum short-circuit current;

F2   is the short-circuit point for calculation of the minimum short-circuit current;

The simplified model of a street lighting network was created to verify the calculations of short-circuit currents performed by the calculation software MeteorCalc SL.

To simplify the verification calculations the model consists of a single feeder cable section, but this model has all the necessary elements of the calculation. The original street lighting model in a dwg-file is available on the meteorcalc.com/resources webpage. In practical applications, the MeteorCalc SL can work with models of any complexity.

VI. CALCULATION PROCEDURE

The short-circuit currents calculation procedure fully complies with the IEC 60909 (last edition 2016). All the steps of short-circuit currents verification calculations are summarized in the tables II-VI. The numbers of formulas in the tables are given in accordance with the numbering of formulas in the relevant standard.

Table II includes the steps and results of determination of the impedances for calculation of maximum short-circuit currents.

Table III includes the steps and results of calculation of maximum short-circuit currents at the point F1.

Table IV includes the steps and results of determination of the impedances for calculation of minimum short-circuit currents.

Table V includes the steps and results of calculation of minimum short-circuit currents at the point F1.

Table VI includes the steps and results of calculation of minimum short-circuit currents at the point F2.

The "Calculation of short circuit currents" columns contain the steps of verification calculations. The "MeteorCalc SL report" columns contain fragments from the detailed report generated by the MeteorCalc SL software.
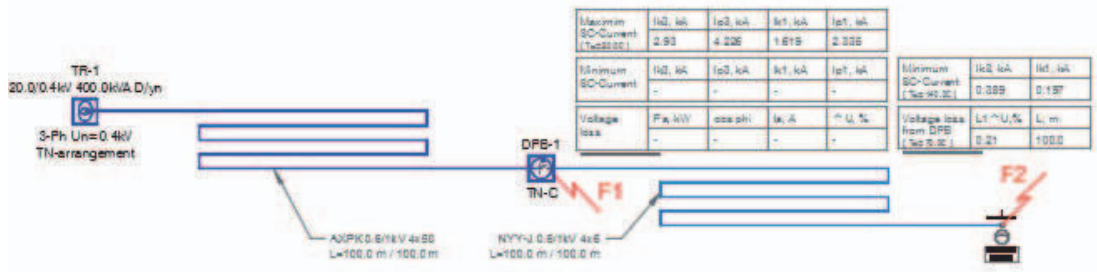

Fig. 2. The simplified model of a street lighting network for the calculation of short circuit currents in a street lighting feeder.

TABLE II

THE NUMERICAL RESULTS OF DETERMINATION OF THE IMPEDANCES FOR CALCULATION OF MAXIMUM SHORT CIRCUIT CURRENTS

Electrical equipment	Calculation of maximum short circuit currents	MeteorCalc SL report
Network feeder 3-Phase 50 Hz, $U_n = 20,0$ kV $I_{kq\ max} = 10,0$ kA, $R_q/X_{q\ max} = 0,1$	IEC60909-0 [6] $$Z_{Qt} = \frac{1,1 \times 20kV}{\sqrt{3} \times 10kA} \times \left(\frac{0,41}{20}\right)^2 = 0,534 \text{ m}\Omega$$ Max. voltage factor for supply network c=1,1 $X_{Qt} = 0,995 \times 0,534 = 0,531$ mΩ $R_{Qt} = 0,1 \times 0,531 = 0,0531$ mΩ	Positive-sequence short-circuit impedance (HV side): IEC60909-0 [4][5] Z(1) [HV] = 126.3868 + j1263.8676 = 1270.1712 mOhm Positive-sequence short-circuit impedance (LV side): IEC60909-0 [6] Z(1) [LV] = 0.0531 + j0.5311 = 0.5338 mOhm Rated transformation ratio t = 48.78
Transformer 20,0/0,41kV $S_n = 400$kVA D/yn $u_k = 4,0\%$, $u_r = 1,15\%$, $P_k = 4,6$ kW, $I_n = 563,3$ A, $R_{(0)}/R_{(1)} = 1,0$, $X_{(0)}/X_{(1)} = 0,95$	Positive-sequence short-circuit impedance IEC60909-0 [7] $$Z_T = \frac{4\%}{100\%} \times \frac{(410V)^2}{400kVA} = 16,81 \text{ m}\Omega$$ IEC60909-0 [8] $$R_T = \frac{4,6kW \times (410V)^2}{(400kVA)^2} = 4,833 \text{ m}\Omega$$ IEC60909-0 [9] $$X_T = \sqrt{16,81^2 - 4,833^2} = 16,1 \text{ m}\Omega$$ Relative reactance and impedance correction factor IEC60909-0 [12a] $x_t = 16,1/((410V)^2/400kVA) = 0,03831$ $k_T = 0,95 \times \frac{1,05}{1+0,6\times0,03831} = 0,975$ Max. voltage factor for secondary network: c=1,05 Corrected positive-sequence short-circuit impedance $R_{TK} = 0,975 \times 4,833 = 4,712$ mΩ $X_{TK} = 0,975 \times 16,1 = 15,698$ mΩ Corrected zero-sequence short-circuit impedance $R_{(0)TK} = 1,0 \times 4,712 = 4,712$ mΩ $X_{(0)TK} = 0,95 \times 15,698 = 14,913$ mΩ	Transformer Positive-sequence short-circuit impedance: IEC60909-0 [7][8][9] Z(1) = 4.8329 + j16.1003 = 16.81 mOhm Relative reactance: xt = 0.038311 EC60909-0 [12a] Impedance correction factor: kt = 0.975 EC60909-0 [12a] Corrected positive-sequence short-circuit impedance: Z(1) = 4.7125 + j15.6992 = 16.3912 mOhm Zero-sequence short-circuit impedance: IEC60909-4 Z(0) = 4.8329 + j15.2953 = 16.0406 mOhm Impedance correction factor: Kt = 0.975 EC60909-0 [12a] Corrected zero-sequence short-circuit impedance: IEC60909-4 Z(0) = 4.7125 + j14.9142 = 15.641 mOhm
Cable PL **AXPK 0,6/1kV 4x50** L = 100,0 m Phase = Al 50 mm2 $r_{(1)} = 0,641$ mOhm/m [20ºC] $x_{(1)} = 0,079$ mOhm/m, [50Hz] Return by fourth conductor = Al 50 mm² $R_{(0)}/R_{(1)} = 4,0$ $X_{(0)}/X_{(1)} = 3,75$	Temperature of conductors = 20ºC Temperature factor of phase conductor metal Al = 0,00403 [1/K] Cable positive-sequence impedance at 20ºC and 50Hz $R_{(1)PL} = 100,0 \times 0,641 = 64,1$ mΩ $X_{(1)PL} = 100,0 \times 0,079 = 7,9$ mΩ Cable zero-sequence impedance at 20ºC and 50Hz $R_{(0)PL} = 100,0 \times 0,641 \times 4,0 = 256,4$ mΩ $X_{(0)PL} = 100,0 \times 0,079 \times 3,75 = 29,625$ mΩ	Resistance per unit length of phase conductor = 0.641 mOhm/m, [20C], IEC60909-0 [32] Positive-sequence resistance of cable R(1) = 64.1 mOhm, [20C] Positive-sequence reactance per unit length = 0.079 mOhm/m, [50Hz] Positive-sequence reactance of cable X(1) = 7.9 mOhm, [50Hz] Z(1) = 64.1 + j7.9 = 64.585 mOhm, [20C][50Hz] Zero-sequence resistance of cable R(0) = 256.4 mOhm, [20C] Zero-sequence reactance of cable X(0) = 29.625 mOhm, [50Hz] Z(0) = 256.4 + j29.625 = 258.1058 mOhm, [20C][50Hz]
Distribution Panel Board	$Z_{(1)DPB} = 10,0 + j1,0 = 10,05$ mΩ $Z_{(0)DPB} = 20,0 + j2,0 = 20,1$ mΩ	Positive-sequence short-circuit impedance: Z(1) = 10.0 + j1.0 = 10.0499 mOhm Zero-sequence short-circuit impedance: Z(0) = 20.0 + j2.0 = 20.0998 mOhm

TABLE III

THE NUMERICAL RESULTS OF CALCULATION OF THE MAXIMUM SHORT CIRCUIT CURRENTS AT THE POINT F1

Short circuit	Calculation of maximum short circuit currents	MeteorCalc SL report
Three-phase maximum short-circuit current Conditions: 3-Phase 50 Hz $U_n = 0,4$ kV Max. voltage factor for supply network $c=1,1$ Max. voltage factor for secondary network: $c=1,05$	$R_{(1)K} = 0,0531 + 4,712 + 64,1 + 10,0 = 78,865$ mΩ $X_{(1)K} = 0,531 + 15,698 + 7,9 + 1,0 = 25,13$ mΩ Initial three-phase short-circuit current IEC60909-0 7.2.1.[33] $I_K'' = \dfrac{1,05 \times 400V}{\sqrt{3} \times \sqrt{78,865^2 + 25,13^2}} = 2,93$ kA Peak factor IEC60909-0 8.1.1.[57] $\dfrac{R_{(1)K}}{X_{(1)K}} = \dfrac{78,865}{25,13} = 3,138k = 1,02 + 0,98 \times \exp^{-9.414} = 1,02$ Peak three-phase short-circuit current IEC60909-0 8.1.1.[56] $i_p = 1,02 \times \sqrt{2} \times 2.93kA = 4,226$ kA	3-PHASE SHORT-CIRCUIT CURRENT (MAX) Sum of positive-sequence short-circuit impedance $Zk = 78.8656 + j25.1303 = 82.7727$ mOhm Initial three-phase short-circuit current $Ik3 = 2.93$ kA, IEC60909-0 7.2.1.[33] Positive-sequence short-circuit R/X ratio = 3.1383 Peak factor $k = 1.0201$ IEC60909-0 8.1.1.[57] Peak three-phase short-circuit current ip3 = 4.226 kA IEC60909-0 8.1.1.[56]
Line-to-earth maximum short-circuit current Conditions: 3-Phase 50 Hz $U_n = 0,4$ kV Max. voltage factor for supply network $c=1,1$ Max. voltage factor for secondary network: $c=1,05$	$R_{(0)K} = 4,712 + 256,4 + 20,0 = 281,112$ mΩ $X_{(0)K} = 14,913 + 29,625 + 2,0 = 46,538$ mΩ $R_K = 2 \times 78,865 + 281,112 = 438,842$ mΩ $X_K = 2 \times 25,13 + 46,538 = 96,798$ mΩ Initial line-to-earth short-circuit current IEC60909-0 7.5.[54] $I_{K1}'' = \dfrac{\sqrt{3} \times 1,05 \times 400V}{\sqrt{438,842^2 + 96,798^2}} = 1,6187$ kA Peak factor IEC60909-0 8.1.1.[57] $\dfrac{R_{(0)K}}{X_{(0)K}} = \dfrac{438.84}{96.8} = 4,533$ $k = 1,02 + 0,98 \times \exp^{-13.5} = 1,02$ Peak line-to-earth short-circuit current $i_p = 1,02 \times \sqrt{2} \times 1,6187kA = 2,335$ kA	1-PHASE SHORT-CIRCUIT CURRENT (MAX) Sum of zero-sequence short-circuit resistance R(0) = 281.1125 mOhm Sum of zero-sequence short-circuit reactance X(0) = 46.5392 mOhm Sum of 1-phase short-circuit impedance IEC60909-0 7.5.[54] $Zk = 438.8436 + j96.7998 = 449.3929$ mOhm Initial 1-phase short-circuit current Ik1 = 1.619 kA, IEC60909-0 7.5.[54] 1-phase short-circuit R/X ratio = 4.5335 Peak factor k = 1.02 IEC60909-0 8.1.1.[57] Peak 1-phase short-circuit current ip1 = 2.335 kA

TABLE IV

THE NUMERICAL RESULTS OF DETERMINATION OF THE IMPEDANCES FOR CALCULATION OF MINIMUM SHORT CIRCUIT CURRENTS

Electrical equipment	Calculation of minimum short circuit currents	MeteorCalc SL report
Network feeder 3-Phase 50 Hz, $U_n = 20,0$ kV $I_{kq\,max} = 10,0$ kA, R_q/X_q max = 0,1	IEC60909-0 [6] $Z_{Qt} = \dfrac{1,0 \times 20kV}{\sqrt{3} \times 10kA} \times \left(\dfrac{0,41}{20}\right)^2 = 0,485$ mΩ Min. voltage factor for supply network $c=1,0$ $R_{Qt} = 0,1 \times 0,4828 = 0,0483$ mΩ $X_{Qt} = 0,995 \times 0,485 = 0,4828$ mΩ	Positive-sequence short-circuit impedance (HV side): IEC60909-0 [4][5] $Z(1)$ [HV] = 114.8971 + j1148.9705 = 1154.7011 mOhm Positive-sequence short-circuit impedance (LV side): IEC60909-0 [6] $Z(1)$ [LV] = 0.0483 + j0.4829 = 0.4853 mOhm Rated transformation ratio t = 48.78
Transformer 20,0/0,41kV $S_n = 400$kVA	Positive-sequence short-circuit impedance IEC60909-0 [7] $Z_T = \dfrac{4\%}{100\%} \times \dfrac{(410V)^2}{400kVA} = 16,81$ mΩ	Positive-sequence short-circuit impedance: IEC60909-0 [7][8][9] $Z(1) = 4.8329 + j16.1003 = 16.81$ mOhm Impedance correction factor: Kt = 1.0 IEC60909-0

D/yn $u_k = 4,0\%$, $u_r = 1,15\%$, $P_k = 4,6$ kW, $I_n = 563,3$ A, $R_{(0)}/R_{(1)} = 1,0$, $X_{(0)}/X_{(1)} = 0,95$	IEC60909-0 [8] $R_T = \frac{4,6\text{kW}\times(410\text{V})^2}{(400\text{kVA})^2} = 4,833$ mΩ IEC60909-0 [9] $X_T = \sqrt{16,81^2 - 4,833^2} = 16,1$ mΩ Zero-sequence short-circuit impedance $R_{(0)TK} = 1,0 \times 4,833 = 4,833$ mΩ $X_{(0)TK} = 0,95 \times 16,1 = 15,295$ mΩ	7.1.2 R(0)/R(1) = 1.0, X(0)/X(1) = 0.95 Zero-sequence short-circuit impedance: IEC60909-4 Z(0) = 4.8329 + j15.2953 = 16.0406 mOhm
Cable PL **AXPK 0,6/1kV 4x50** L = 100,0 m Phase = Al 50 mm^2 $r_{(1)} = 0,641$ mOhm/m [20°C] $x_{(1)} = 0,079$ mOhm/m, [50Hz] Return by fourth conductor = Al 50 mm^2 $R_{(0)}/R_{(1)} = 4,0$ $X_{(0)}/X_{(1)} = 3,75$	Temperature of conductors = 140°C Temperature factor of phase conductor metal Al = 0,00403 [1/K] Cable positive-sequence impedance at 140°C $R_{(1)PL} = [1 + 0,00403\,(140 - 20)] \times 0,641 \times 100 =$ $= 95,099$mΩ Cable positive-sequence reactance at 50Hz $X_{(1)PL} = 100,0 \times 0,079 = 7,9$ mΩ Cable zero-sequence impedance at 140°C and 50Hz $R_{(0)PL} = 95,099 \times 4,0 = 380,396$ mΩ $X_{(0)PL} = 7,9 \times 3,75 = 29,625$ mΩ	Resistance per unit length of phase conductor = 0.641 mOhm/m [20C] Temperature factor of phase conductor metal = 0.00403 [1/.K] Temperature of conductors = 140.0 C Resistance per unit length of phase conductor = 0.951 mOhm/m, [140C], IEC60909-0 [32] Positive-sequence resistance of cable R(1) = 95.0988 mOhm, [140C] Positive-sequence reactance per unit length = 0.079 mOhm/m, [50Hz] Positive-sequence reactance of cable X(1) = 7.9 mOhm, [50Hz] Z(1) = 95.0988 + j7.9 = 95.4263 mOhm, [140C][50Hz] Zero-sequence resistance of cable R(0) = 380.395 mOhm, [140C] Zero-sequence reactance of cable X(0) = 29.625 mOhm, [50Hz] Z(0) = 380.395 + j29.625 = 381.5469 mOhm, [140C][50Hz]

Distribution Panel Board	$Z_{(1)DPB} = 10,0 + j1,0 = 10,05$ mΩ
	$Z_{(0)DPB} = 20,0 + j2,0 = 20,1$ mΩ
		Positive-sequence short-circuit impedance:
		  Z(1) = 10.0 + j1.0 = 10.0499 mOhm
		
		Zero-sequence short-circuit impedance:
		  Z(0) = 20.0 + j2.0 = 20.0998 mOhm

Cable FL **NYY-J 0.6/1kV 4x6** L = 100,0 m Phase = Cu 6,0 mm^2 $r_{(1)} = 3,08$ mOhm/m [20°C] $x_{(1)} = 0,1005$ mOhm/m, [50Hz] Return by fourth conductor = Cu 6,0 mm^2 $R_{(0)}/R_{(1)} = 4,0$ $X_{(0)}/X_{(1)} = 3.95$	Temperature of conductors = 140°C Temperature factor of phase conductor metal Cu = 0.00393 [1/K] Cable positive-sequence impedance at 140°C R(1)FL = $[1 + 0,00393\,(140 - 20)] \times 3.08 \times 100 =$ $= 453,253$mΩ Cable positive-sequence reactance at 50Hz $X_{(1)FL} = 100,0 \times 0.1005 = 10,05$ mΩ Cable zero-sequence impedance at 140°C and 50Hz $R_{(0)FL} = 453,253 \times 4,0 = 1813,012$ mΩ $X_{(0)FL} = 10,05 \times 3,95 = 39,697$ mΩ	Resistance per unit length of phase conductor = 3.08 mOhm/m [20C] Temperature factor of phase conductor metal = 0.00393 [1/.K] Temperature of conductors = 140.0 C Resistance per unit length of phase conductor = 4.5325 mOhm/m, [140C], IEC60909-0 [32] Positive-sequence resistance of cable R(1) = 453.2528 mOhm, [140C] Positive-sequence reactance per unit length = 0.1005 mOhm/m, [50Hz] Positive-sequence reactance of cable X(1) = 10.05 mOhm, [50Hz] Z(1) = 453.2528 + j10.05 = 453.3642 mOhm,

		[140C][50Hz]
		Zero-sequence resistance of cable R(0) = 1813.0112 mOhm, [140C]
		Zero-sequence reactance of cable X(0) = 39.6975 mOhm, [50Hz]
		Z(0) = 1813.0112 + j39.6975 = 1813.4458 mOhm, [140C][50Hz]

TABLE V

THE NUMERICAL RESULTS OF CALCULATION OF THE MINIMUM SHORT CIRCUIT CURRENT AT THE POINT F1

Short circuit	Calculation of minimum short circuit currents	MeteorCalc SL report
Three-phase minimum short-circuit current Conditions: 3-Phase 50 Hz $U_n = 0{,}4$ kV Min. voltage factor for supply network c=1,0 Min. voltage factor for secondary network: c=0,95	$R_{(1)K} = 0{,}0483 + 4{,}833 + 95{,}099 + 10{,}0 = 109{,}98$ mΩ $X_{(1)K} = 0{,}04828 + 16{,}1 + 7{,}9 + 1{,}0 = 25{,}48$ mΩ Initial three-phase short-circuit current IEC60909-0 7.2.1.[33] $I_K'' = \dfrac{0{,}95 \times 400V}{\sqrt{3} \times \sqrt{109{,}98^2 + 25{,}48^{\,2}}} = 1{,}943$ kA	3-PHASE SHORT-CIRCUIT CURRENT (MIN) Sum of positive-sequence short-circuit impedance IEC60909-0 4.2.1.[30][31] Zk = 109.9799 + j25.4831 = 112.8936 mOhm Positive-sequence short-circuit R/X ratio = 4.3158 Initial three-phase short-circuit current Ik3 = 1.943 kA, IEC60909-0 7.2.1.[33]
Line-to-earth minimum short-circuit current Conditions: 3-Phase 50 Hz $U_n = 0{,}4$ kV Min. voltage factor for supply network c=1,0 Min. voltage factor for secondary network: c=0,95	$R_{(0)K} = 4{,}833 + 380{,}396 + 20{,}0 = 405{,}228$ mΩ $X_{(0)K} = 15{,}295 + 29{,}625 + 2{,}0 = 46{,}92$ mΩ $R_K = 2 \times 109{,}98 + 405{,}228 = 625{,}19$ mΩ $X_K = 2 \times 25{,}48 + 46{,}92 = 97{,}887$ mΩ Initial line-to-earth short-circuit current IEC60909-0 7.5 [54] $I_{K1}'' = \dfrac{\sqrt{3} \times 0{,}95 \times 400V}{\sqrt{625{,}19^{\,2} + 97{,}887^{\,2}}} = 1{,}04$ kA	1-PHASE SHORT-CIRCUIT CURRENT (MIN) Sum of zero-sequence short-circuit impedance Z(0) = 405.2279 + j46.9203 = 407.9353 mOhm Sum of 1-phase short-circuit impedance IEC60909-0 7.5.[54] Zk = 625.1878 + j97.8866 = 632.8045 mOhm 1-phase short-circuit R/X ratio = 6.3869 Initial 1-phase short-circuit current Ik1 = 1.04 kA, IEC60909-0 7.5.[54]

TABLE VI

THE NUMERICAL RESULTS OF CALCULATION OF THE MINIMUM SHORT CIRCUIT CURRENT AT THE POINT F2

Short circuit	Calculation of minimum short circuit currents	MeteorCalc SL report
Three-phase minimum short-circuit current Conditions: 3-Phase 50 Hz $U_n = 0{,}4$ kV Min. voltage factor for supply network c=1,0 Min. voltage factor for secondary network: c=0,95	$R_{(1)K} = 0{,}0483 + 4{,}833 + 95{,}099 + 10{,}0 + 453{,}253 = 563{,}233$ mΩ $X_{(1)K} = 0{,}04828 + 16{,}1 + 7{,}9 + 1{,}0 + 10{,}05 = 35{,}533$ mΩ Initial three-phase short-circuit current IEC60909-0 7.2.1.[33] $I_K'' = \dfrac{0{,}95 \times 400V}{\sqrt{3} \times \sqrt{563{,}233^2 + 35{,}533^2}} = 0{,}389$ kA	3-PHASE SHORT-CIRCUIT CURRENT (MIN) Sum of positive-sequence short-circuit impedance Zk = 563.2327 + j35.5331 = 564.3525 mOhm Positive-sequence short-circuit R/X ratio = 15.8509 Initial three-phase short-circuit current Ik3 = 0.389 kA, IEC60909-0 7.2.1.[33]
Line-to-earth minimum short-circuit current Conditions: 3-Phase 50 Hz	$R_{(0)K} = 4{,}833 + 380{,}396 + 20{,}0 + 1813{,}012 = 2218{,}24$ mΩ $X_{(0)K} = 15{,}295 + 29{,}625 + 2{,}0 + 39{,}697 = 86{,}62$ mΩ	1-PHASE SHORT-CIRCUIT CURRENT (MIN) Sum of zero-sequence short-circuit impedance Z(0) = 2218.2391 + j86.6178 = 2219.9296 mOhm Sum of 1-phase short-circuit impedance IEC60909-0 7.5.[54]

$U_n = 0,4$ kV	$R_K = 2 \times 563,233 + 2218,24 = 3344.7$ mΩ	$Z_k = 3344.7046 + j157.6841 = 3348.4195$ mOhm
Min. voltage factor for supply network c=1,0	$X_K = 2 \times 35,533 + 86,62 = 157,684$ mΩ	1-phase short-circuit R/X ratio = 21.2114
Min. voltage factor for secondary network: c=0,95	Initial line-to-earth short-circuit current IEC60909-0 7.5.[54] $$I''_{K1} = \frac{\sqrt{3} \times 0,95 \times 400V}{\sqrt{3344,7^2 + 157,684^2}} = 0,197 \text{ kA}$$	Initial 1-phase short-circuit current Ik1 = 0.197 kA, IEC60909-0 7.5.[54]

VII. ANALYSIS OF THE RESULTS

All the results of short-circuit currents calculations are summarized in the table VII. The results obtained by the MeteorCalc SL are fully consistent with the results of the verification calculations.

TABLE VII

THE COMPARISON OF CALCULATION RESULTS

Calculation mode	SC-point	SC-current	Verification calculations	MeteorCalc calculations
Maximum short-circuit current	F1	Initial three-phase short-circuit current	2.93 kA	2.93 kA
		Peak three-phase short-circuit current	4.226 kA	4.226 kA
		Initial line-to-earth short-circuit current	1.6187 kA	1.619 kA
		Peak line-to-earth short-circuit current	2.335 kA	2.335 kA
Minimum short-circuit current	F1	Initial three-phase short-circuit current	1.943 kA	1.943 kA
		Initial line-to-earth short-circuit current	1.04 kA	1.04 kA
	F2	Initial three-phase short-circuit current	0.389 kA	0.389 kA
		Initial line-to-earth short-circuit current	0.197 kA	0.197 kA

The short-circuit current is significantly reduced at the end of the 0,4 kV feeder line. The designer of street lighting networks must pay special attention to the careful selection of the cable cross-sections and must constantly to check the compliance of the protection disconnection time to the standard.

Verification calculations can also be performed using another similar program. For a correct comparison of short-circuit currents calculated in MeteorCalc SL with calculation results made in other programs, it is necessary to introduce the following conditions:

- Network model has to be identical;

- Methods of setting the source data must be the same;

- The source data for the calculation of impedance of the transformers should be the same (it is necessary to pay attention to the equality of „total losses" value P_{krT} and to the equality of relations $R_{(0)T} / R_{TLV}$ and $X_{(0)T} / X_{TLV}$ used to find the zero-sequence impedance of the transformers);

- Initial impedances of conductors and temperature coefficients of metals must be the same;

- Impedances of electrical switchgears should be the same;

The method of the calculation must exactly match with the IEC 60909. It is necessary to pay special attention to the mandatory fulfilment of the standard IEC 60909-0 requirements:

- The condition of clause 2.2 (when calculating values from MV to the LV side transformation ratio U_{rTMV} / U_{rTLV} must be used instead of U_{nTMV} / U_{nTLV});

- The condition of clause 3.3.3 (using the impedance correction factor KT for transformers).

In case of mismatch of short circuit currents resulting from the calculations, the comparison of the results is recommended to be carried out step by step, separately for each element of the calculation circuit. To do this, both programs should be switched to the interim results show mode on each calculation step. In MeteorCalc SL this mode is called „Detailed report of short-circuit currents calculations"

VIII. CONCLUSION

The MeteorCalc SL software allows to calculate short-circuit currents in street lighting networks according to last version of IEC60909 (2016) with high level of accuracy.

Only software computation is possible for calculations of short-circuit currents in street lighting feeders. Manual calculations is very time-consuming, therefore very simplified algorithms usually are used in manual calculations. With manual calculation it is impossible to take into account all the requirements of IEC60909.

For calculations, it is desirable to use programs that allow to receive detailed reports on the calculation process with all the

intermediate results, which allows to control the calculation process at each step.

REFERENCES

[1] IEC 60909-0 (2016): Calculation of short-circuit currents.
[2] IEC/TR 60909-2 (2008): Data of electrical equipment for short-circuit current calculations.
[3] IEC 60909-4 (2000): Examples for the calculation of short-circuit currents.
[4] IEC 60228 Conductors of insulated cables.
[5] IEC 60287-1-1 (2014): Electric cables - Calculation of the current rating - Part 1-1: Current rating equations (100 % load factor) and calculation of losses - General.
[6] IEC 60364-4-41 (2007) Low-voltage electrical installations - Part 4-41: Protection for safety - Protection against electric shock.
[7] IEC 60076-1 (2012) Power transformers - Part 1: General.
[8] IEC 60947-2 (2006) Low-voltage switchgear and controlgear - Part 2: Circuit-breakers.
[9] IEC 60038 IEC standard voltages.
[10] IEC 60076 – Power transformers.

Publication III

Varjas, T.; Kuusik, M.; Armas, J.; Rosin, A. (2018). Assessment of pedestrian crossings measuring parameters and implementation of new measuring methods in Estonia. 59th International Scientific Conference on Power and Electrical Engineering of Riga Technical University: 2018 IEEE 59th International Scientific Conference on Power and Electrical Engineering of Riga Technical University (RTUCON), Riga, Latvia, 12-13 November 2018. IEEE, 1–4, doi: 10.1109/RTUCON.2018.8659822

Assessment of pedestrian crossings measuring parameters and implementation of new measuring methods in Estonia

Toivo Varjas, Marko Kuusik, Jelena Armas, Argo Rosin
Electrical Power Engineering and Mechatronics
School of Engineering, Tallinn University of Technology
Tallinn, Estonia

Abstract—Focus is on the assessment of measuring parameters of pedestrian crossings with additional lighting in Estonia and on the implementation of recommendatory measuring methods. Current coverage of normative documents is insufficient in the context of lighting unregulated pedestrian crossings; also, measurement and evaluation of the lighting parameters on crossings have been poorly covered. This paper focuses on the measurement and analysis of light parameters. Lighting was surveyed with a contemporary photographic measuring method, which enables us to define light technical parameters more effectively, to evaluate modern LED lighting and to apply safer solutions. Surveys were made on the crossroads with new LED-based lighting solutions; light-technical parameters are recommended and new solutions for safer lighting solutions on pedestrian crossings were developed.

Keywords—*pedestrian crossings, normative document, additional luminaire, simulations with software, safer lighting solutions, vertical illuminance, measuring method, image luminance measuring.*

I. Introduction

Over the years, the traffic has become increasingly car-centred. Crossings are rated as the most dangerous conflict areas in traffic. Safety of the crossings has become a crucial problem in urbanizing environments. Crossings have been the safest areas for pedestrians and bicyclists to cross the road, but sacrificing the safety of the pedestrians to the smoothness of the traffic flux is expanding.

Due to the emerging new lighting solutions, it is reasonable to re-evaluate existing lighting solutions and notification systems on pedestrian crossings. While creating new smart crossings, it is important to ensure the conditions for the drivers to notice the crossings for the pedestrians and bicyclists in a distance that allows them to react on time if the dangerous situation occurs. Crucial factors here are complementing crossing with an additional lighting, which ensures higher level of lighting that is drawing attention, the difference of the lighting temperature, and notification via change in lighting conditions, all forming better traffic safety. At the same time, new notification solutions aimed to pedestrians are also available on unregulated crossings.

Most important and general lighting parameters are presented in the new standards CEN/TR 13201-1:2014 and EVS-EN 13201, translated into Estonian and are effective from 2014 and 2015, respectively [1]. Unfortunately, the guidelines and normative regulatory documents that the projects are based on are too vague. On April 2017, a new Estonian two-part standard was taken into use EVS 935:2017 - Lighting of pedestrian crossings with additional lighting [2], which is supplementing the pre-existing standard series EN 13201. The conflict areas for which the requirements of EN 13201-2 apply can include the carriageway only, when applying separate requirements for the adequate lighting of other road areas for pedestrian and cyclists, or it can include also other road areas, lighting classes based on road surface illuminance. According to the standard EN 13201, if the normal lighting is sufficient, there is no need for additional lighting. If additional lighting is required, parts 1 and 2 of the standard EVS 935:2017 give specific guidance. Contemporary measuring technologies, including image luminance measuring device ILMD, calibrated for measuring the luminance distributions of the framed scene, create new opportunities for surveys and present elaborate light-technical parameters, including photographing measuring of luminance. ILMD every pixel is calibrated to determine the luminance values of the space imaged on its surface by the lens system [4].

Measuring the luminance, covered in the new standards EN13201-1 through EN13201-5, gives new opportunities for measurements and defines more precise lighting parameters. Standard EVS 935:2107 provides means to compare different lighting solutions for illuminance performance and evenness of light density. Measurements performed according to those norm documents on typical crossings this year gave a general view of existing lighting conditions. In an area of intense traffic, the crossings are not easily spotted, marking lights are drawing drivers attention away from the conflict area and contrast ratio does not support noticing pedestrians. Although standards have been updated, coverage of the measurements of new smart led lighting on pedestrian crossing is still insufficient. To ensure safety, existing quality indicators and guiding values must be supplemented via road surface luminance and contrast ratio measuring. Software simulations (e.g., in DIALux) and measurements based on normative document values fail to give an overview of pedestrian crossings light conditions that would be comprehensive enough [7].
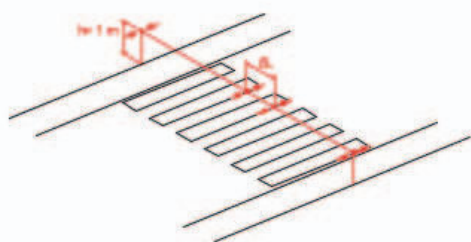
II. Lighting of a Crossing

Normative document for lighting of pedestrian crossings EVS 935:2017 describes the general quality of characteristics and guide values and calculation and measuring of these values. Unfortunately, in the standards, the LED-lighting remains almost untouched. However, the new light installations of the crossings are most often using contemporary LED-luminaires.

LED allows guided lighting levels, changed according to traffic density and dimming according to lighting class.

The standard states how the quantitatively interpreted light-technical quality factors must be calculated and measured. The necessary parameters are defined, so the calculations can be compared and the unified measurements can be conducted.

For situations where the lighting class of a conflict area is insufficient and it is a necessary to support the safety of a pedestrian crossing solutions with light-technical methods, the installations of the additional luminaires are described. In the evaluation of the additional lighting of a pedestrian crossing, the crucial criterion of quality is the vertical illuminance Ev (Fig. 1). This parameter is essential when defining the contrast that accentuates the pedestrian's luminance on a relatively dark background (Figs. 2 and 3). Simulations were created with DIALux evo software. When calculating and measuring the additional lighting, only the luminosity given by the additional luminaire was considered. By measuring the vertical illuminance of a pedestrian crossing in specific points defined by the standard, the functioning state of the additional luminaire of the crossing can be inspected. For unified measuring of an additional luminaire, it is agreed to use the quadrangular horizontal evaluation field (Fig. 1).

where

$\Delta L = 1$ m, distance between the measuring points

h = 1 m, height from the road surface

Fig. 1. Measuring field of lighting at a pedestrian crossing.

The safety of a crossing is influenced by the speed of a vehicle chosen by the driver, traffic flow, traffic composition, the overall lighting of the area, complexity of traffic and the resulting lighting class of the road. For the driver to notice the pedestrian on a waiting area or on a crossing, the illuminance of a crossing on a vertical plane, 1 m from the ground, on a centre line of a crossing must be 1.5 times higher than the horizontal illuminance produced by road lighting on the carriageway of the road. The current standards in Europe establish the requirements of conflict areas, which can also be the areas used by pedestrians and bicyclists, such as crossings with lighting class C. According to the requirements, the entire crossing must be lighted uniformly. Uniformity is described by the general uniformity of light density U_0 that is measured in some measuring point as a quotient of the least and the average light density $U_0=0.4$. The average light density $\bar{E}$ and total overall uniformity of light density U_0 is calculated and measured according to the standards EVS-EN 13201-3 and EVS-EN 13201-4 [1].

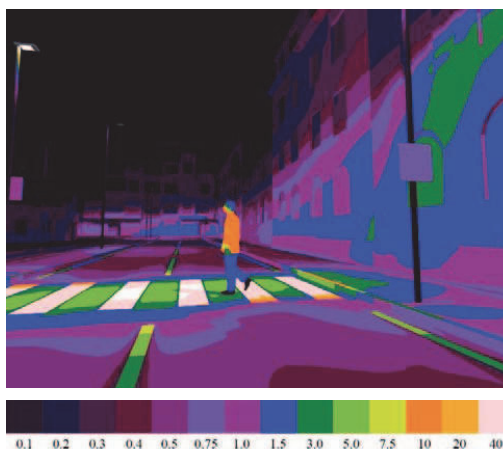Fig. 2. Simulation of the lighting of a crossing – view from a driver.

Fig. 3. Pseudocolors simulation of the lighting of a crossing (values of pseudocolors are cd/m^2).

On the streets with bidirectional traffic, two luminaires must be installed on each crossing for the pedestrian crossing; the street must be enlightened from a side from both directions of traffic. The additional luminaires must be installed prior to the pedestrian crossing. If the street lighting on a road surface is lower than the prescribed maintained level of average road surface luminance of 0.3cd/m^2, the luminance level in the area of 100 m before and 100 m after the crossing has to correspond at least to the lighting class M6 in EVS-EN13201-2:2015 to prevent the adaption difficulties when driving through the crossings with additional lighting. In addition, the light colour of the additional lighting, if it is clearly different from the surrounding traffic lighting, can increase the attention and safety.

III. MEASURING

A. General requirements for measuring

Resulting from the articles of the standard EVS-EN 13201-4 and EVS 935:2017, it is essential to follow the adequate methodology of the measurements [1, 2]. When measuring, the effects of other light sources must be eliminated, discharge lamps must be aged and the measured installation should show the established state.

In this study, based on our surveys, our purpose was to find the best practical solutions for applying the recommended light-technical parameters and defining safer installations. We have used innovative measuring devices, including a video luminance measuring device. All the devices used in the surveys were calibrated and metrologically traceable. The following devices were used: Gigahertz-Optik BTS256-EF spectral-luxmeter and ILMD LMK Mobile Air [5, 6, 7].

B. Results of the measurements

Based on the survey results, installation of a crossing was evaluated. In the survey, we used the standard EVS 935:2017 for measuring the crossings with additional lighting, and lighting classes C recommended for the conflict areas in the standard EVS-EN13201:2-2015 that are based on the definition of the illumination of the road surface.
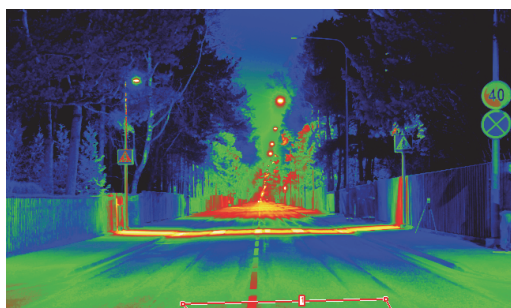
Fig. 4.   Pseudocolors picture taken with a luminance measuring camera.

Luminance was measured between the road surface and the surrounding background.

B. Results of the survey
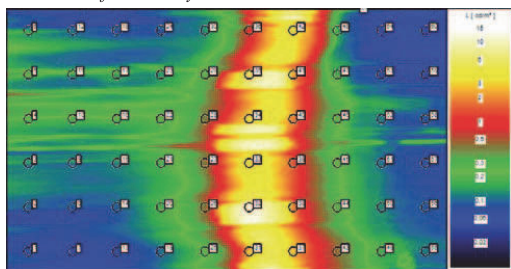
Fig. 5.   Luminance measurement results taken with a ILMD measuring camera.
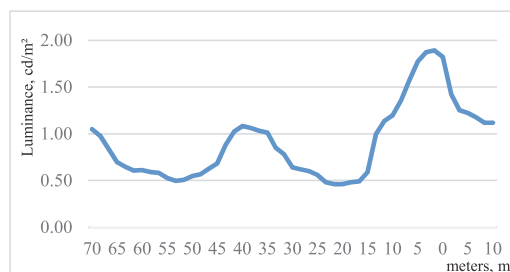
Fig. 6.   Luminance values on the axis of the driveway and pedestrian crossing

IV.   CONCLUCION

In the new series of the standard EN13201, the measuring of outdoor lighting and the analysis with contemporary measuring methods have been thoroughly covered. At the same time, the measuring methods, comparative analysis and recommendations for applications on pedestrian crossings are missing. EVS 935:2017 gives opportunity to measure and analyse lighting of pedestrian crossings with additional light instalments; however, luminance contrast definitions need updating as well. Luminaires and means of lighting have been considerably changed and the photometric method has made its way to the new normative regulatory documents EVS-EN13201 1-5: 2015 about the outdoor lighting. Measuring devices and measuring technologies allow more effective solutions based on light-technical measurements. Focus in this article is on the measurement and evaluation of the standard solutions of the crossings in Estonia with new LED-lighting, using innovative light-technical instruments and elaborating on the recommended light-technical parameters for safer crossing on the roads. This study also advances developments of new smart solutions for light instalments on crossings.

When lighting the crossing with modern smart solutions, the following aspects are crucial:

• A positive contrast and highlighting pedestrian on the road must be created;

• The flow of the additional light must be in the direction of the traffic, so it would not blind the driver;

• Additional light-instalment automation and dimming need to be clearly defined;

• Waiting areas must have the same illuminance as the pedestrian crossings;

• Vertical lighting (lighting of a vertical plane) of the crossing must be higher than that of the road;

• Luminance regularity to guarantee traffic smoothness and safety is required.

The results of the surveys showed that implementation of the basics of the new standards enables the evaluation of the light installations, taking into consideration also the specification of the contrast ratio and general uniformity of the installation. In the further studies in 2018, several new light installations will be evaluated, including streets with controlled LED-lighting, using these measuring methods. Our surveys help to make the light installations safer, identify the most economical level of lighting and ensure the uniform lighting level on the road and street surfaces, creating bases for smart solutions for pedestrian crossing lightings and eventually guaranteeing the safest conditions of traffic.

REFERENCES

[1]   Estonian National Standard EVS-EN 13201:2015, Road Lighting.

[2]   Estonian National Standard EVS-935:2017, Lighting of pedestrian crossings with additional lighting.

[3]   Road safety in the European Union. http://ec.europa.eu/roadsafety European Commission, Mobility and Transport DG, BE-1049 Brussels, 2015.

[4]   Gall, D.; Krüger, U.; Schmidt, F. & Wolf, S. (2002). Moderne Möglichkeiten zur Messung und Bewertung von Beleuchtungsparametern. Herbstkonferenz 2002 der GfA e.V. (Modern possibilities to measure and assess lighting parameters. Fall Conference, 2002. GfA, e.V.). Ilmenau, Technical University, 2002.

[5]   Image-resolving luminance measurement using luminance measuring camera type LMK Mobile, TechnoTeam Bildverarbeitung GmbH, www.technoteam.de, Germany.

[6]   Gigahertz-Optik GmbH, https://www.gigahertz-optik.de, Germany.

[7]   Kuusik, M.; Varjas, T.; Rosin, A. (2016). Case Study of Smart City Lighting System with Motion Detector and Remote Control. IEEE International Energy Conference (ENERGYCON), Leuven, Belgium, 4-8 April 2016. Leuven, Belgium: IEEE, 1−5.10.1109/ENERGYCON.2016.7513906.

Toivo Varjas received his engineering degree in Instrument Engineering from Tallinn University of Technology, Estonia, in 1994. From 2014 he has been studying for his PhD at Tallinn University of Technology. From 2014 he works in the Lighting Laboratory as a measurement specialist. His reseach intrests are in the analysis of quality in the street lighting.

Publication IV

Korõtko, T.; Rosin, A.; Varjas, T.; Ahmadiahangar, R. (2020). Awareness of BSR Municipalities about Sustainable Urban Lighting and Green Public Procurements. 2020 IEEE International Conference on Environment and Electrical Engineering and 2020 IEEE Industrial and Commercial Power Systems Europe (EEEIC / I&CPS Europe). Madrid, Spain: IEEE, 1−6. doi: 10.1109/EEEIC/ICPSEurope49358.2020.9160761.

Awareness of BSR Municipalities about Sustainable Urban Lighting and Green Public Procurements

Tarmo Korõtko, Argo Rosin, Toivo Varjas, Roya Ahmadiahangar
Smart City Center of Excellence (Finest Twins) &
Department of Electrical Power Engineering and Mechatronics
Tallinn University of Technology
Tallinn, Estonia
tarmo.korotko@taltech.ee

Abstract—**Sustainable urban lighting and advances in light emitting diode (LED) technology promise significant cost savings and environmental benefits. For municipalities to tap into benefits of modern technologies, their awareness towards state of the art lighting technology needs to be high. The European Union (EU) has implemented the concept of green public procurements (GPP), which guide public authorities in procurements for reducing environmental impact. This paper describes the development of a questionnaire for assessing awareness about sustainable urban lighting technologies and GPPs. The paper presents results of a survey, carried out using the developed questionnaire, conducted in the scope of the project LUCIA, which is supported by the Interreg Baltic Sea Region (BSR) program. Based on a survey carried out among five municipalities of the BSR, their awareness towards state of the art lighting and control technologies and GPP criteria for streetlights and lighting of recreational areas is assessed. It is concluded that awareness about dimming, control systems, reparability, labelling, ingress protection rating, expected lifetime and warranty is high, while knowledge about supporting technologies, reduction of maintenance costs and energy consumption indicators is poor. Another finding is that public authorities have greater knowledge about street lighting technologies than they do about recreational lighting technologies.**

Keywords— Urban lighting, GPP, lighting control, LED.

I. INTRODUCTION

The project titled "Lighting the Baltic Sea Region - Cities accelerate the deployment of sustainable and smart urban lighting solutions" (acronym: LUCIA), which is supported from the Interreg Baltic Sea Region (BSR) Program 2014 – 2020, aims to increase energy efficiency based on enhanced capacity of public and private actors involved in energy planning. Project LUCIA helps municipalities to unlock savings from urban lighting by providing public authorities with profound and up-to-date knowledge of state of the art energy efficient urban lighting, covering aspects of environment, technology, economy and social acceptance. As a result, decision makers will be more aware of energy efficient lighting solutions and should prefer such investments. To tackle the root cause, energy efficient technologies need to be considered already in the planning and procurement processes; hence, project LUCIA will also provide up-to-date information to public authorities on urban planning and procurement issues. The aim of the project is to improve planning and procurement procedures in municipalities. Project LUCIA will demonstrate the potential of innovative energy efficient lighting solutions in 6 pilot sites: Hamburg, Tallinn, Porvoo, Jurmala, St. Petersburg and in the DOLL living lab in Albertslund, Denmark. The pilot

cases will serve as beacon projects in the BSR, which can be visited and replicated in other cities of the BSR, thereby contributing to climate mitigation efforts in the region. The duration of project LUCIA is 2,5 years with a project budget of 3,12 M€, from which 2,17 M€ is funded by the European Regional Development Fund.

Urban lighting is required to have a central role in the design of future "smart" cities. The term urban lighting refers to both, street and other lighting installations (e.g. recreational areas, infrastructure etc.). A great part of energy consumption in Europe originates from urban areas that produce notable emissions of greenhouse gasses. Over 90 million lighting poles worldwide count for more than 50 % of public energy consumption and about 60 % of relative costs [1]. By 2050, nearly 70 % of the world's population will live in urban areas, creating challenges and opportunities for municipalities and industries, where digital technology will function as a catalyst for urban transformation towards more efficient and livable cities [2]. In future cities, street lighting will play an essential role in security and life quality. Modern lighting control systems are capable of adapting lighting conditions to suit the user, thus improving personal wellbeing and perceived quality of life [3]. Modern luminaires and control systems provide effective street lighting, which can reduce crime and traffic collisions, but also encourage socio-economic activities at night and improve the perception of personal safety and security [4]. Innovations in lighting, such as solid-state light emitting diodes (LED), promise energy savings of about one half and a notable reduction of maintenance costs [1]. Supporting technologies like photovoltaic (PV) panels and battery storage are able to transform street lighting from passive consumers to active prosumers [5], [6]. Although the technology is available, it will have limited impact if municipal workers responsible for urban lighting lack knowledge and confidence in procuring it. The EU has implemented the concept of green public procurements (GPP), which aim to guide public authorities in procuring goods, services and works with reduced environmental impact throughout their entire life cycle. For the implementation of sustainable and smart urban lighting in the EU, municipalities need to be aware of state of the art lighting and control technologies and procurement criteria suggested by GPPs.

The aim of this paper is to describe the development of a questionnaire for assessing the awareness of public authorities in the BSR towards state of the art lighting and control technologies and green public procurement criteria regarding the lighting of streets and recreational areas. The paper also disseminates the results of a survey, performed using the developed questionnaire, among five municipalities in the BSR and carried out in the scope of project LUCIA.

The remainder of this paper is structured into four paragraphs. Section II provides insight into the state of the art of lighting technologies and describes the development of

questions for assessing awareness regarding lighting technologies. An overview about green public procurements in the EU is presented in section III, along with a general description about the development of questions for evaluating knowledge about GPPs. Section IV describes the survey carried out in the scope of project LUCIA. Lastly, section V includes the discussion and future work.

II. STATE OF THE ART OF LIGHTING TECHNOLOGIES

Most potential technologies concerned with sustainable urban lighting are LED lighting and advanced control, management and communication systems.

A. LED Lighting

LED lighting is considered highly potential for increasing energy efficiency of urban lighting and thereby help reduce CO_2 emissions [7]. LEDs offer unique characteristics: they are compact, have long life, are resistant to mechanical impacts and vibration, offer better performance in colder environments, provide light instantly when energized and are dimmable (applies to selected models). LEDs emit nearly monochromatic light and can be adjusted to provide different colored light with high efficiency, which makes them especially useful for applications like traffic signals and public information signs [8]. The most important physical influencing factors on the reliability and lifetime of LED light sources include humidity, temperature, current and voltage, mechanical forces, chemicals and light radiation. These can even lead, in a worst-case situation, to a total failure or influence the aging characteristics in the long term (e.g. brightness), and thus produce a change in the reliability and lifetime [9]. A detailed overview of different characteristics of modern LED lamps and luminaires is provided in TABLE I.

LED technology provides more than double the energy performance of a compact fluorescent lamp (CFL) and over 10 times higher efficiency than an incandescent lamp [8]. In addition, the lifetime of LED lighting (the time when light output of half the product population has fallen below 70% of average initial light output for any reason [10]) is up to 20 times longer than for other lighting options [11]. It has also been found that the manufacturing of LED lighting solutions produces less CO_2 emissions than the manufacturing process of other technologies [11]. Additionally, LEDs offer better service reliability and lower maintenance costs [12]. A downside to LED technology is the rapid growth of innovation and volume, which hinders the maturing of this technology. Manufacturers are still forming their strategies for the serviceability, modularity and recyclability of LED lighting, which is considered as risk when planning long-term investments. A summary of the advantages and disadvantages of LED lighting is presented in TABLE II. To assess how aware municipalities are about the potential energy savings and reduction in CO_2 emissions of LED lighting technology,

TABLE I. LED LIGHTING TYPICAL PERFORMANCE SPECIFICATION [8]

Characteristic	Typical Quantities	
	LED Lamp	LED Luminaire
Luminous Efficacy Range(initial)	60-130 lm/W	80-150 lm/W
Lamp Lifetime	15000-30000 h	20000-60000 h
Color Rendering Index (RI)	70-95	80-95
Correlated color	2700-6500 K	2700-6500 K
Dimmable?	If dimmable driver	If dimmable driver

TABLE II. ADVANTAGES AND DISADVANTAGES OF LED LIGHTING [13]

LED Lighting	
Advantages	Disadvantages
Highest efficacy light	Control gear (driver) required for operation
Lowest running costs	Higher relative first costs (but competition is driving prices down)
long operating life–typically more than 20,000 hours	Needs good thermal design because waste heat is conducted, not projected
High flux in a small package, good for optical control	
offering excellent color rendering	
Instant on, instant re-strike, dimmable	
Contains no mercury	

a question regarding the savings potential was included in the developed questionnaire. Questions regarding the reliability and lifetime of LED lighting were also included into the developed questionnaire.

B. Control and communication in public lighting systems

Luminaires can be controlled either by bang-bang control (on or off) or by dimming. The dimming of luminaires refers to the intentional decrease of light intensity through dedicated equipment (dimmers). The decrease in light intensity introduces lower energy consumption, which is why dimming is considered relevant in sophisticated efficient lighting systems. The dimming of LED luminaires is carried out using specific drivers. A LED driver is a solid-state device used to control the current to LEDs in reference to the desired dimming level and provide several protection functions (e.g. overcurrent protection) [14].

The main objective of a lighting control system is to enable the switching and dimming of luminaires. Three types of lighting control systems can be distinguished: autonomous, centralized and dynamic control. In autonomous control of street lighting, the luminaires are pre-programmed and do not require additional networks and management systems. Such systems provide limited flexibility and functionality, but they might be equipped with sensors for improved functionality, which also increases their cost. In centralized control of street lighting, a central system controls all luminaires within a group. Such a setup is relatively simple and allows for some flexibility, but it also requires the implementation of ICT solutions. In dynamic control of street lighting, the luminaires can be controlled and monitored, which is done either in groups or on an individual basis. The monitoring of luminaires provides advanced diagnostic functions (e.g. failures, energy consumption, operating and ambient temperature etc.), which allows for improved efficiency of maintenance. The added flexibility comes with increased complexity and thus additional costs and risks. Dynamic management systems require highly trained operators and maintenance providers, dedicated control software development, support and maintenance, expertise in control networks etc., all of which increase the total cost of implementation and operation of such systems. [15]

State of the art control systems for public lighting are commonly dynamic control systems, which reside in a central command center in the local authority or their service

provider. Such systems depend on communication technologies. A common communication solution for public lighting systems is a two-layer communication setup. At a higher hierarchy level, the control center communicates with data concentrators. At the lower communication layer, the data concentrators handle the communication between individual luminaires and other supporting devices (e.g. sensors). They can either transmit information via cable or as wireless signals. Common communication interfaces used for public lighting systems include power line communication (PLC), DALI bus, Ethernet etc. More common wireless communication interfaces used in public lighting systems include ZigBee, GPRS, LTE and Wi-Fi. Common communication protocols for public lighting systems include the DALI protocol, the ZigBee protocol and IPv6 over Low power Wireless Personal Area Networks protocol. [15]

Lighting management systems reside on top of the lighting control and communications systems and are used to execute control strategies. More common control strategies include astronomical timers, daylight harvesting and adaptive control. Astronomical timers rely on precise information about sunrise and sunset times for a given geographical position and control lighting based on that. Daylight harvesting strategies use sensors to detect ambient light intensity and adjust artificial lighting accordingly. Adaptive control strategies commonly make use of sensory information and change luminaire output accordingly. An example is the control of streetlight illumination (in compliance with requirements stipulated in EN 13201) based on traffic intensity. Traffic detection systems rely on motion sensors. Common types of motion sensors include ultrasonic and microwave motion detectors, infrared sensors and video surveillance systems. For improved performance, motion detection systems can be combined where one compensates the disadvantages of the other. Motion detector based systems commonly require integration into larger ICT systems, which might benefit traffic controllers, urban planners, emergency services etc., by enabling the collection of traffic data [15].

Modern control systems provide large contributions into the overall energy efficiency of lighting systems. By combining astronomical timers, daylight harvesting, and traffic detection schemes with dimming, energy savings of up to 85 % can be attained, while reducing discomfort glare for nearby residents by gradually increasing and decreasing illumination [15]. An adaptive lighting scheme proposed in [16], which is based on traffic sensing, demonstrated a decrease in energy consumption by an average of 32 % compared to the zoning lighting scheme proposed in [17]. The dynamic control of LED streetlights with an adaptive control strategy using sensors and cameras is presented in [1], which reported a reduction of energy consumption by nearly 60 %. There have been several studies regarding the effect of adaptive lighting in the BSR. In [18], an intelligent LED lighting pilot was carried out along a light traffic route in a housing area in Helsinki, Finland. It was found that strong winds and cold ambient temperatures caused a significant amount of false readings from sensors. The relative energy savings, when compared to the previous control solution, ranged from 60 % to 77 %, depending on the control scenario and calendar time. According to a study carried out on experimental results from Tartu, Estonia, average energy savings reach 40 % when using motion detection sensors and 34 % when using preprogrammed luminaires [19]. It was also concluded in [19] that the energy usage of systems that utilize

object recognition depends heavily on object frequency and such systems achieve higher energy savings than preprogrammed settings when a maximum of 3 000 motions are detected during a night.

To evaluate the level of knowledge public authorities have in regard to dimming, control and communication systems used for urban lighting, different questions concerned with those topics were added into the questionnaire that was developed for the survey. The municipalities need to provide insight into whether they are aware which dimming and control systems are used in their lighting systems and does their lighting management system support interfacing with other software, e.g. smart city systems.

III. Green Public Procurements

The EU defines Green public procurements (GPP) as processes, where public authorities procure goods, services and works with a reduced environmental impact throughout their entire life cycle compared to procurements carried out otherwise. GPPs rely on focusing on long-term impacts of each action, which also includes assessment whether a purchase is necessary in the first place [20]. The EU publishes criteria for GPPs, which is a voluntary instrument for public authorities and plays a key role in the EUs effort to increase overall resource-efficiency. The GPP criteria are maintained and updated constantly, to maintain clear and ambitious environmental targets, which are based on scientific evidence and follow an approach that is concerned with the entire product lifecycle. GPP criteria are divided into core and comprehensive criteria:

- **Core criteria** are designed for easy adoption of GPP principles, focusing on key aspects of environmental performance and aiming to maintain low administrative cost for companies.

- **Comprehensive criteria** account for additional aspects of environmental performance and are more detailed than core criteria. They are designed for use by authorities, which want to increase their effort in reaching environmental and innovation goals.

GPPs rely on key performance indicators (KPI) and measurable verification. For example, municipalities are encouraged to calculate their annual energy consumption indicators (AECI) and power density indicators (PDI). The AECI is the total amount of electricity consumed by a lighting installation in proportion to the total area to be illuminated by it. The PDI is a value of the system power divided by the value of the product of the surface area to be lit and the calculated maintained average illuminance value on this area. Verification standards are provided for each GPP criteria and municipalities are encouraged to include verification in the tender to receive quantifiable or qualitative results for determining whether they got what they procured. Additionally, verification provides the possibility to adjust in the process.

In terms of urban lighting, GPP criteria for road lighting and traffic signals are provided in [21]. The main environmental impacts of road lighting and traffic signals, along with the proposed EU GPP road lighting approach, are outlined in TABLE III. , which provides an example on how these specific criteria are meant to affect the environment. To assess whether municipalities in the BSR are aware of GPP criteria when procuring public lighting systems, several

Key environmental impacts	EU GPP road lighting approach
CO_2 emissions from electricity consumption by lighting.	Procure luminaires that exceed minimum luminaire efficacies.
Emission of acidifying gases through electricity use of lighting.	Encourage use of dimming and metering for real-time optimisation and monitoring of lighting systems.
Decreased star visibility caused by upward light output and ground reflection.	Require all luminaires to have no upward light output and, ensure 97 % of light falls within a downward angle of 75,5°.
Disruption of nocturnal species' behaviour.	Encourage dimming in areas of concern; set limits on blue light proportion (G-index) of luminaire.
Poor resource efficiency caused by cheaper and low quality products, poor installation and reparability.	Procure durable and fit-for-use equipment, which is repairable and covered by (extended) warranty.
	Set minimum requirements for staff approving the installation.

TABLE IV.   DETAILED DESCRIPTION OF CATEGORIES DISPLAYED ON FIG. 1 AND FIG. 2.

Category	Description
Potential	Is the LED-ification and savings potential in terms of energy and CO2-emission reduction known.
Energy consumption	Is the AECI or PDI of lighting systems known?
Luminous efficacy	Is the increase of luminous efficacy known for reconstructed lighting systems?
Control system	Does the municipality have insight into control systems used in lighting systems?
Dimming system	Does the municipality know which dimming systems have been installed?
Pre-programmed dimming	For installed lighting systems, have the dimming levels been pre-programmed?
Programmability	For installed lighting systems, are the dimming levels freely programmable?
Interfacing	Do existing lighting management systems support interfacing with smart city systems?
Supporting technologies	Do existing lighting systems include supporting technologies (e.g. PV panels, batteries etc.).
Reliability	Does the municipality know the reliability and annual failure rates of installed lighting systems?
Maintenance costs	Does the municipality know the reduction of maintenance and/or repair costs of refurbished lighting systems?
Waste recovery	Are the components of lighting systems separated and sent for recovery in accordance with the WEEE directive?
Reparability	Are individual lighting system components reparable without damaging other components?
Labelling	Do LED luminaires of installed lighting systems have detailed labelling?
Protection rating	Do the luminaires on M- and C- class roads have an optical system with an ingress protection rating of IP65 or higher, and a rating of IP55 or higher on P- and SC- class roads?
Power quality	Does the municipality know the power factor of installed LED-lighting systems?
Life expectancy	Does the municipality know the expected lifetime of LED-light sources of installed lighting systems?
Warranty	Does the municipality know the warranty period of installed LED-lighting systems?
Metering	Does the municipality determine technical requirements for metering systems (e.g. according to Measuring Instruments Directive 2004/22/EC)?
Verification measurements	Does the municipality perform verification measurements before and after the (re)construction of lighting systems (e.g. quality indicators, average illuminance etc.)?

questions were included into the developed questionnaire. The procurement of energy efficient luminaires is of key importance, as is verification, thus the questions regarding energy consumption, luminous efficacy, metering and verification measurements were composed. One key approach in EU GPP road lighting is the use of dimming systems, which is studied using questions regarding dimming systems, pre-programmed dimming and, programmability. Assessing a holistic approach to system operation and entire life-cycle, issues regarding maintenance costs, waste recovery, system life expectancy, power quality and system reliability are addressed. The awareness towards the use of repairable and warranted products is covered by inquiries regarding reparability and labelling of products, ingress protection ratings and warranty periods.

IV. SURVEY

To assess the awareness of municipalities regarding the lighting of streets and recreational areas, a survey among five municipalities from different countries in the BSR was conducted. The survey was in the form of a written questionnaire and lighting experts from municipalities were selected as the target group. The questionnaire was made up of twenty questions about street and recreational lighting. Each question could be answered as either "YES" or "NO". For each "YES" as a reply, the subject also had to answer a follow-up question, which required some quantification to solidify the positive response. The questions of the questionnaire were divided into two categories: GPP criteria and state of the art lighting technology. The results of the questionnaire are depicted on Fig. 1 and Fig. 2. A detailed description of the depicted categories is shown in TABLE IV.

The chart displayed on Fig. 1 summarizes the results of the study regarding the awareness about state of art lighting and control technologies. There is a slight difference between awareness about technologies used for recreational and street lighting in favor of the latter. Very good level of awareness was displayed for dimming and control systems. The participants reported the use of time based, zone based, adaptive and other unspecified method of dimming. All responders described the implementation of central lighting

control systems, but two of the responders also described the use of decentralized and hybrid control. Based on the survey, knowledge about supporting technologies in participating municipalities was deemed poor. Only two responders noted the use of supporting technologies for urban lighting and described the use of batteries for either supporting the control system of the streetlights or providing a backup energy source for pedestrian crossings.

The chart displayed on Fig. 2 illustrates the awareness of participating municipalities about GPP criteria (the criteria of dimming system and reliability fall into both studied categories). Similar to the awareness towards lighting system technology, the municipalities display slightly higher levels of awareness about street lighting than for recreational lighting. High level of awareness was demonstrated about reparability, labelling, ingress protection rating, expected lifetime and warranty period. All municipalities confirmed that the installed lighting system components are clearly identifiable, accessible and removable without damaging other parts or the
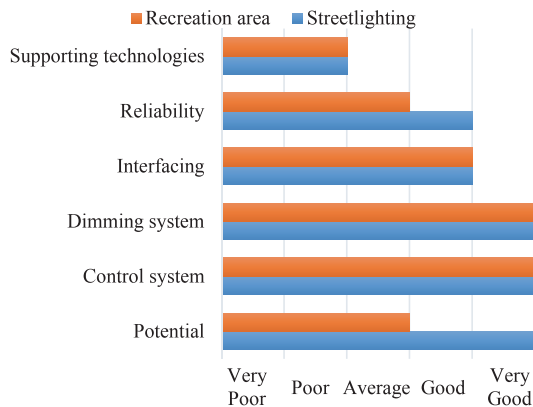
Fig. 1. Awareness of municipalities about state of art lighting and control technologies.

luminaire. The expected lifetime of installed LED–lighting systems ranges from 32 000 h up to 100 000 h. The warranty period for luminaires spun from 20 000 h to 100 000 h and the warranty period for the entire system was mostly 5 years, but also 3 or 10 years for special cases. Although all municipalities stated that their installed the labels varied significantly. The lowest awareness was demonstrated regarding the reduction of maintenance costs and energy consumption indicators. One responder reported the 10 % reduction of maintenance costs and a 60 % reduction of reparation cost. One municipality stated that there has been no reduction in either maintenance or reparation cost. Similar to maintenance, only one municipality reported the decrease of AECI from 1480 Wh/m2 per year and PDI from 0,095 W/lx*m to AECI value of 326 Wh/m2 and PDI values of 0,019 W/lx*m due to the replacement of conventional lighting systems with LED technology. One municipality indicated that they rely on theoretical calculations, but do not calculate the AECI and PDI values based on actual measurements.

V. CONCLUSIONS AND FUTURE WORK

This paper describes the development of a questionnaire for assessing awareness about public lighting technology and GPPs. Results of a survey, carried out using the developed questionnaire, which was conducted in the scope of project LUCIA is presented. Based on the survey, an assessment of awareness of public authorities in the BSR towards state of the art lighting and control technologies and green public procurement criteria is provided. It is found that the awareness of municipalities about dimming, control systems, reparability, labelling, ingress protection rating, expected lifetime and warranty period is high, while knowledge about supporting technologies, the reduction of maintenance costs and energy consumption indicators is lacking. Another finding is that public authorities display better knowledge about street than about recreational lighting technologies.

The presented findings can be used as guidelines for municipalities for creating staff training plans and education requirements. Also, providers of lighting technology can use the presented results for developing communication and business strategies when partnering with public authorities in the BSR. Further actions include the replication of the described survey on a larger scale, using a modified version of the described questionnaire, to increase the survey sample.
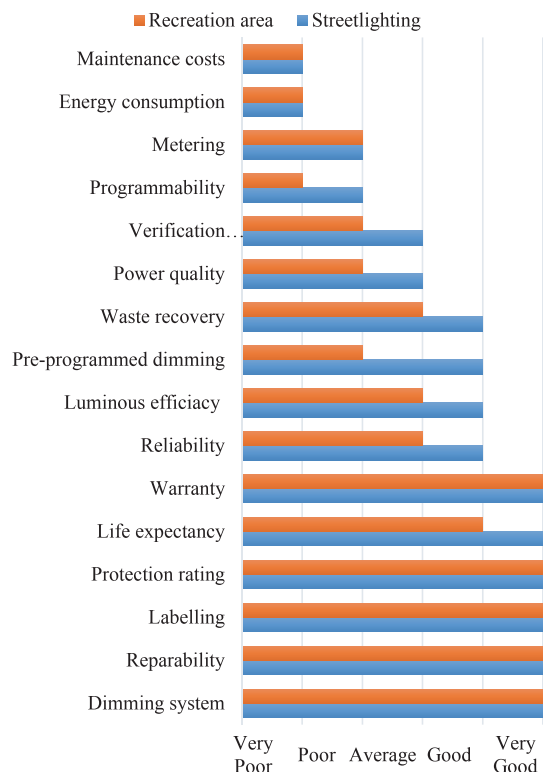

Fig. 2. Awareness of municipalities about GPP criteria.

REFERENCES

[1] Enrico Petritoli , Fabio Leccese , Stefano Pizzuti , Francesco Pieroni, "Smart lighting as basic building block of smart city: An energy performance comparative case study," Measurement, vol. 136 , p. 466–477, 2019.

[2] Kati Brocka, Elke den Ouden, Kees van der Klauw, Ksenia Podoynitsyna, Fred Langerak, "Light the way for smart cities: Lessons from Philips Lighting," Technological Forecasting & Social Change, pp. article in press, https://doi.org/10.1016/j.techfore.2018.07.021, 2018.

[3] Lighting Europe Secretariat, "Strategic Roadmap 2025 of the European Lighting Industry," 2016.

[4] Sei Ping Lau , Geoff V. Merrett, Alex S. Weddell, Neil M. White, "A traffic-aware street lighting scheme for Smart Cities using autonomous networked sensors," Computers and Electrical Engineering, vol. 45, p. 192–207, 2015.

[5] Andras Kovacs a,Roland Batai b, Balazs Csanad Csaji a, Peter Dudas b, Borbala Hay, "Intelligent control for energy-positive street lighting," Energy, vol. 114, pp. 40-51, 2016.

[6] T. Korõtko, A. Rosin and R. Ahmadiahangar, "Development of Prosumer Logical Structure and Object Modeling," 2019 IEEE 13th International Conference on Compatibility, Power Electronics and Power Engineering (CPE-POWERENG), Sonderborg, Denmark, 2019, pp. 1-6.

[7] Suntiti Yoomak, Chaiyan Jettanasen, Atthapol Ngaopitakkul, Sulee Bunjongjit,, "Comparative study of lighting quality and power quality for LED andHPS luminaires in a roadway lighting system," Energy and Buildings, vol. 159, p. 542–557, 2018.

[8] UN Environment – Global Environment Facility | United for Efficiency (U4E), "Accelerating the Global Adoption of ENERGY-EFFICIENT LIGHTING," U4E POLICY GUIDE SERIES, 2017.

[9] Lutz Thomas , Ritzer Markus, "Reliability and lifetime of LEDs," Osrom optp Semicpnductors, 2018.

[10] KR Shailesh , CP Kurian , SG Kini, "Understanding the reliability of LED luminaires," Lighting Res. Technology, vol. 50, p. 1179–1197, 2018.

[11] Warehouse-Lighting.com, 2018. [Online]. Available: www.warehouse-lighting.com/howdoes-led-lighting-reduce-co2-emissions.aspx. [Accessed 11.2019].

[12] Hinton AB, "LED STREETLIGHTS," 2020, [Online]. Available: "https://www.hinton.ca/890/LED-Streetlights [Accessed 02.2020].

[13] Energy Trust of Oregon, Inc., "Cities take savings to the streets," 2020, [Online]. Available: https://blog.energytrust.org/cities-take-savings-to-the-streets/. [Accessed 11.2019].

[14] P. Padmavathi and S. Natarajan, "A Survey on Efficient Converter Driver Techniques for LED LIGHTING Applications," 2019 Innovations in Power and Advanced Computing Technologies (i-PACT), Vellore, India, 2019, pp. 1-7.

[15] Premium Light pro Consertium, "LED Street Lighting Procurement & Design," Österreichische Energieagentur – Austrian Energy Agency, 2017.

[16] Sei Ping Lau ; Geoff V. Merrett ; Neil M. White, "Energy-efficient street lighting through embedded adaptive intelligence," in International Conference on Advanced Logistics and Transport, Sousse, Tunisia, 2013.

[17] Raffaele Carli , Mariagrazia Dotoli , Roberta Pellegrino, "A decision-making tool for energy efficiency optimization of street lighting," Computers and Operations Research , vol. 96, p. 222–234, 2018.

[18] Eveliina Juntunena, Esa-Matti Sarjanoja, Juho Eskeli,, "Smart and dynamic route lighting control based on movement tracking," Building and Environment, vol. 142, p. 472–483, 2018.

[19] M. Kuusik, T. Varjas and A. Rosin, "Case study of smart city lighting system with motion detector and remote control," 2016 IEEE International Energy Conference (ENERGYCON), Leuven, 2016, pp. 1-5.

[20] European Commission, "Public Procurement for a Circular Economy: Good Practice and Guidance," 2017. https://ec.europa.eu/environment/gpp/pdf/cp_european_commission_brochure_en.pdf [Accessed 25.02.2020]

[21] European Commission, "EU green public procurement criteria for road lighting and traffic signals," 2018. https://ec.europa.eu/environment/gpp/pdf/toolkit/traffic/EN.pdf [Accessed 18.02.2020]

Publication V
De Luca, F.; Sepulveda, A; Varjas, T. (2021). Static Shading Optimization for Glare Control and Daylight. Towards a New, Configurable Architecture, Proceedings of the 39th eCAADe Conference: eCAADe 2021 - Towards a New, Configurable Architecture, Faculty of Technical Sciences, University of Novi Sad, Novi Sad, Serbia, 8-10, September 2021. Ed. Stojakovic, V.; Tepavcevic, B. Education and research in Computer Aided Architectural Design in Europe, 419–428.

Static Shading Optimization for Glare Control and Daylight

Francesco De Luca[1], Abel Sepúlveda[2], Toivo Varjas[3]
[1,2,3] Tallinn University of Technology
[1,2,3] {francesco.deluca|absepu|toivo.varjas}@taltech.ee

Daylight and solar access influence positively building occupants` wellbeing and students' learning performance. However, an excess of sunlight can harm the visual comfort of occupants through disturbing glare effects. This study investigated, through multi-objective optimization, the potential of static shading devices to reduce glare and to guarantee daylight provision in a university building. The results showed that the reduction of disturbing glare was up to more than twice the reduced daylight, which nevertheless, was provided in adequate levels. View out and energy performance were also analyzed. Detailed results of optimal shading types and classrooms layout indications are presented.

Keywords: *Daylight, Visual comfort, Shading, Multi-objective optimization*

INTRODUCTION

Daylight and solar access are important factors for building occupants' comfort and wellness. Studies showed that sunlight and the perception of day-night alternation improve health facilitating the correct entrainment of humans' circadian rhythm (Lockley 2009). Research works proved that daylight increases the workers' satisfaction and productivity (Andersen et al. 2012) and improves the students' learning performance in educational buildings (Heschong 2002). Additionally, studies showed that through a correct design natural light in buildings reduce energy consumption through consistent cut of electric lighting energy and reduction of heating energy also at Northern latitudes (De Luca et al. 2016, Voll et al. 2016) without significant cooling energy increase (De Luca et al. 2018).

On the other hand, an excess of daylight and direct sunlight can significantly decrease the building occupants' visual comfort due to glare effects. A study conducted in a students' studio open space taking into account sun in the field of view, direct

sunlight on the desk and monitor contrast found that the space was considered intolerably uncomfortable for many occupied hours (Jakubiec and Reinhart 2016). Field studies conducted in office spaces underlined the importance of the occupant distance from the windows and view direction to control glare (Kong et al. 2018). The studies about the use of shading to eliminate visual discomfort mostly focused on operable internal shades or blinds investigating materials, geometrical configurations and controls (Chan and Tzempelikos 2013, Koo et al. 2010).

There is yet a limited focus in analyzing optimal configurations of building massing and envelope to admit daylight (De Luca 2017), and types of external shading devices to control glare. If on the one hand the static shading glare reduction is smaller compared to the internal operable ones, on the other hand they present the advantages of a constant though reduced view out and higher electric lighting energy reductions because not dependent on occupants' operation (Reinhart 2004). Static shading proved to be an efficient and economic strategy

to control daylight distribution (Hans and Voss 2011). Being visual comfort and daylight potentially conflicting performances, they need to be analyzed simultaneously in the early design stages to find optimal and trade-off shading solutions.

Glare analysis

Glare can be caused by an excessive luminous intensity and by the contrast between the different luminance level of the light sources and background. The level of glare is affected also by the location of the main light source inside the field of view of the observer. Two glare levels can be distinguished: discomfort glare which causes eye strain and disability glare which prevents a person to see the surrounding environment (Reinhart 2018). Discomfort glare metrics are based on the glare index which expresses the contrast between a glare source characterized by its size, luminance and position inside the field of view, and the average luminance of the background. According to the glare index, larger and or brighter light sources located in the center of the field of view increase glare, whereas a brighter background attenuates the glare effect (Jakubiec and Reinhart 2012).

Several glare metrics have been developed, such as the Daylight Glare Index (DGI) (Hopkinson 1972) and the Daylight Glare Probability (DGP) (Wienold and Christoffersen 2006). DGI advanced the initial metrics developed for the small sources of electric lighting taking into account large glare sources such as daylight through windows. DGP, which is one the most recent metrics, adds the measure of the scene brightness (saturation effect) as possible visual discomfort source in addition to the contrast used by the previous indices (Reinhart 2018). The DGP index is based on four levels of probability that a person would experience visual discomfort in the specific setting, i.e., imperceptible (DGP $\leq$ 34 %), perceptible (34 % < DGP $\leq$ 38 %), disturbing (38 % < DGP $\leq$ 45 %) and intolerable glare (DGP > 45 %).

Glare analysis is particularly important in educational and work premises because the occupants cannot change seating position and view direction.

Using computer simulations, glare is assessed at the height of the eyes and in the view direction of the occupant in a seating position at approximately 1.2 m. Input of the simulations are the interior surfaces, the glazed areas and the external obstructions, the materials reflectance and the visible transmittance values. Glare simulations are performed for a single moment (point-in-time) using a specific sky condition or a climate based sky, or for the entire year. The point-in-time simulation output is the fisheye view presenting the luminance values (cd/m^2) and the glare assessment through the metric used (Figure 1). Annual glare simulations require the additional inputs of the statistical weather data and occupancy hours. The output is a chart showing the visual discomfort levels for each hour of the year.

Daylight analysis

Daylight availability metrics date back to the end of 19th century. One of the most used metrics is the Daylight Factor (DF) which predicts interior natural light levels as a ratio of exterior illuminance. DF is a simple metric to use through formulas and computer simulations. Its reliability is limited because it considers only the geometrical characteristics of the room surfaces, glazed areas and external obstructions and the materials' reflectance and glazing transparency. Climate based daylight metrics such as Daylight Autonomy and Useful Daylight Illuminance have been developed to accurately predict through computer simulations the annual percentage of time during which an interior point meets the daylight thresh-
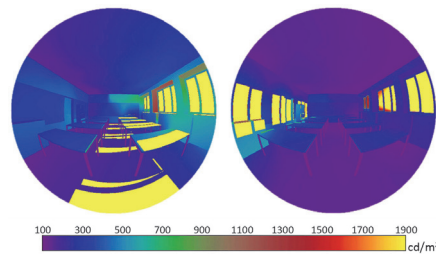
Figure 1
Point-in-time glare assessments in one classroom of the study using a clear sky with sun at 11 a.m. on April 4 – DGP 32 % (left) and at 11 a.m. on January 4 – DGP 43 % (right).

old, using also the building orientation and statistical weather data (Reinhart et al. 2006, Nabil and Mardaljevic 2006).

Spatial Daylight Autonomy (sDA) is a recently developed annual daylight metric introduced in the method LM-83-12 and adopted by leading international standards such as LEED (Illuminating Engineering Society 2013). sDA assesses annual daylight availability as the percentage of occupied floor area where the illuminance threshold of 300 lux is reached for at least 50 % of the time (sDA300/50%) between 8 a.m. and 6 p.m. regardless of the function of the building. LM-83-12 requires minimum 55 % of sDA300/50% to consider a room acceptably daylit.

Daylight is simulated on a horizontal plane (simulation grid) located at the desk height of approximately 0.75 m using sensor points. Other inputs of the annual daylight analysis are the room surfaces of floors, walls, ceiling, window glass and frames, main furnishing and the external obstructions, their reflectance and visible transmittance values, the illuminance threshold (lux), the occupancy hours and the annual weather data.

This study investigated through multi-objective optimization the potential of different types of external static shading devices to improve visual comfort while guaranteeing adequate daylight provision in two classrooms of Tallinn University of Technology (TalTech). The study was conducted using two simulation planes to provide useful information for the classrooms' layout. View out and energy performance using the shadings are also presented. The novelty of the study lies in the assessment of glare, to control together with daylight through static shading, for the entire room area and multiple views instead than for a single view as in existing literature.

METHODS

The study was conducted through three-dimensional modeling of the classrooms and buildings, measurement of the optical properties of the interior materials, parametric modeling of the shading devices, daylight modeling, multi-objective optimization, view out and energy modeling. The building used in the study is the Academy of Architecture and Urban Studies of TalTech located in Tallinn, Estonia (Lat. 59°26'N Lon. 24°45'E).

Building and classrooms model

The classrooms 46 of 45.9 m^2 southerly oriented and 41 of 52 m^2 easterly oriented, which have the same windows and tables layout, were selected to analyze glare and daylight for different orientations and opposite buildings' height and distance (Figure 2). The classrooms were located at a height of 13.25 m. Detailed three-dimensional models were realized in Rhinoceros (McNeel 2021) including tables, cupboards, cork wall boards and the main appliances as projector and whiteboard. The relevant surrounding buildings were also modeled (Figure 2).

Figure 2
The Academy building with location of the classrooms used in the study and the surrounding buildings. Grayscale rendering of classroom 46.
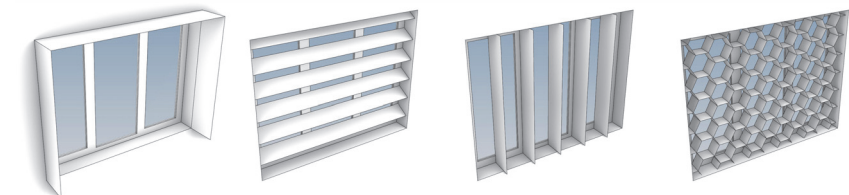
Surface	R (%)	VT (%)
Walls int./Ext./Cork pan.	80/30/60	-
Floor/Ceiling	24/20	-
Table top/Legs	83/5	-
Whiteb. screen/Frame	86/10	-
Projector bracket/Body	80/5	-
Window frame-Glazing	84	77

Material characterization

The optical properties of the interior surfaces and windows were measured to realize a reliable daylight model and to obtain accurate occupant visual comfort and daylight availability predictions. The light reflectance (R) of the opaque surfaces was obtained using the calibrated equipment 3nh - Spectrophotometer YS3060 (Figure 4). The visible light transmittance (VT) of the two-pane glazing was calculated as the ratio of the vertical illuminance measured with the window closed and open, which constitutes a simple method to approximate VT (Reinhart 2018). The VT measurements were conducted using the calibrated Luxmeter MSC-15. The R and VT values are presented in Table 1.

Shading parametric models

For the study four different shading device types were modeled: overhang with vertical fins; horizontal louver; vertical louver; and hexagonal pattern (Figure 3). For each type an algorithm was realized in Grasshopper (Rutten 2021) to generate the shading using different parameters.

The overhang with vertical fins shading only parameter was the depth, variable from 0 m to 2 m. The parameters of the horizontal louver were the slats spacing starting from 0.1 m to the full window height (no slats), the depth from 0 m to 0.3 m and the rotation with hinge on the top edge of the slat from 0° (open) to 89° downward (closed). The parameters of the vertical louver were the slats distance from 0.1 m to the window width (no slats), the depth from 0 m to 0.3 m and the rotation with hinge on the internal edge from -89° (closed cw) through 0° (fully open) to +89° (closed ccw). The parameters for the hexagonal pattern shading were the radius of the aperture from 0.1 m to the window width (no shading), and the depth from 0 m to 0.3 m.

The shadings were located on the exterior of the window frame inside the window recess of 0.22 m, except the overhang with fins which was attached to the building façade. The overhang had two fins for the south facing room and only the one toward south for the east facing room as recommended by rules-of-thumb. The windows were 2.28 m and 2.35 m (w), and 1.71 m and 1.74 m (h) in size in classrooms 46 and 41, respectively. Custom components were created and used in the parametric model for the glare and daylight simulations, the multi-objective optimizations, the view out and the energy assessments.

Daylight model

The daylight model was realized using the software ClimateStudio in Grasshopper (Solemma 2021). ClimateStudio is based on the validated daylight simulation software Radiance (Ward 1994) and the novel path tracing technology which allows daylight simulations hundreds or thousands of time faster than previous Radiance-based software without compromising the accuracy. The daylight model presented two sections, one for glare and the other for daylight availability simulations. Both used as inputs the classrooms' three-dimensional models and the materials definition realized using the measured interior surfaces' optical properties. For the surrounding buildings and ground were used standard reflectance values, i.e. 35 % and 20 %, respectively. The material used for the shading was a metal with reflectance 49.8 %. Additional inputs were the statistical annual weather data of Tallinn in *epw* format, the occupancy schedule from 8 a.m. to 6 p.m. during weekdays, which are the hours during which lessons take place in the classrooms and as well those recommended by the Estonian building regulations for energy and daylight analysis of educational buildings.

The simulations were conducted using grids of points spaced 0.5 m, with two offsets from the walls and windows, approx. 0.5 m and 1 m, to analyze the performance of different classroom used areas. For glare simulations the grid was located at 1.2 m and presented 8 view directions for each grid point, for a total of 1320 and 768 in room 46 and 1496 and 832

in room 41, for grid offsets 0.5 m and 1 m, respectively. ClimateStudio performed annual hourly glare simulation for every view. The output was the spatial discomfort glare (sDG) based on the metric DGP, i.e., the fraction of views which present a DGP level above 0.38 (disturbing glare) for more than 5 % of the occupied hours (Figure 5). The 5 % exceedance time in glare assessments is defined in the European daylight standard EN 17037 (CEN 2018).

For daylight availability simulations the grid was located at 0.75 m from the floor, and was constituted by single points with the normal facing upward. Among the several daylight metrics available in ClimateStudio, sDA300/50% was used as introduced by LM-83-12 (Figure 5). Although the current Estonian daylight standard requires daylight assessments through DF, sDA was used because existing literature proved that DF is not reliable to predict daylight levels in Estonia (Sepúlveda et al. 2020). The main Radiance parameters used in the simulations were: - ab 6 - lw 0.01 -ad 1. The path tracing parameters were: sample rays per sensor per pass 64 and max number of passes 100.

Multi-objective optimization

Multi-objective optimization was used to investigate optimal trade-off shading configurations to reduce glare while guaranteeing daylight availability. The software used was Opossum, a model-based optimization tool for Grasshopper (Wortmann 2017). The

Figure 5
The analysis grid for glare simulations with views (left) and for daylight availability (right) in classroom 46 (0.5 m from walls), as generated by ClimateStudio with results visualization.

%t DGP>0.38   0 — 5

DA300/50%   0 — 50 — 100
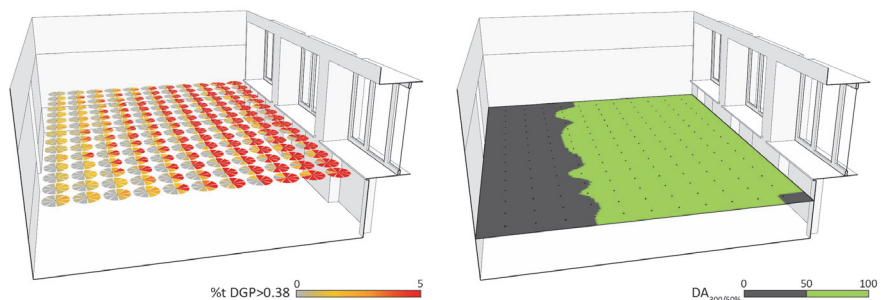
algorithm used was RBFMOpt (Radial Basis Multi-Objective Optimization). The objectives were the minimization of sDG and the maximization of sDA through minimization of the result of the subtraction of the simulation result from 1 (1=100 % of the sensor points receiving DA300/50%). The parameters of the shading devices were used as the variables of the optimization process.

Energy and view out models

Energy simulations were performed without and with the Pareto-optimal shading types with the best performances using the energy tools of ClimateStudio based on the software EnergyPlus (NREL 2019). The simulations parameters are presented in Table 2.

Zone settings		Envelope properties		
People density	0.2 (p/m²)		EW	IW-F-C	W
Lighting density	7 (W/m²)	U_t	0.14	A	0.9
Heat./Cool. setp.	21/25 (°C)		W-VT 77%	W-SHGC 0.4	

The scope was to investigate the effect of the different shading devices on the energy performance. The occupancy schedule, the climatic data and the daylight setpoint were the same used for the daylight model. The view out allowed by the shadings was analyzed through the Sky Exposure Factor (SEF) using the plug-in Ladybug Tools (Sadeghipour and Pak 2013). The SEF metric calculates the visible portion of the sky from points of surfaces as a ratio of the sky hemisphere visible without any obstruction.
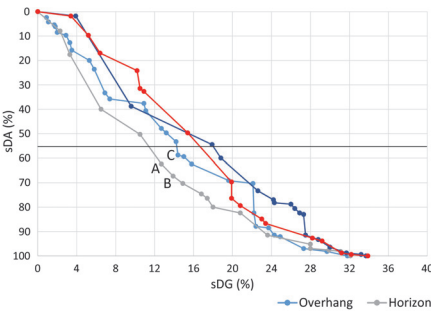
RESULTS

The results of the study are presented in three sections. In the first the optimal types of shading devices to reduce glare and provide adequate daylight are presented and the performances are discussed. In the second the influence of the shadings on the view out is presented. In the third the energy consumption variations using the shadings are analyzed.

Optimal shading devices

To find the optimal trade-offs allowed by the different types of shading multi-objective optimization was used for each shading type in the two classrooms 46 and 41 using the two simulation grids as presented in the section Methods. To compare the performance, the Pareto front solutions of each shading type were used because these represented the optimal trade-offs of glare protection and daylight availability. The most performative shading types of each classroom were those which permitted the largest sDG reduction and at the same time an sDA of minimum 55 %.

Taking into account classroom 46 the sDG and sDA in the actual condition (no shading) were 38.4 % and 99.4 % respectively, using the simulation grid at 0.5 m offset from the walls, and 41.7 % and 100 % respectively, using the grid with 1 m offset from the walls. The results are presented in Figure 6. The two most performative shading types were the horizontal louver and the overhang with vertical fins. Considering the simulation grid with the maximum extension,
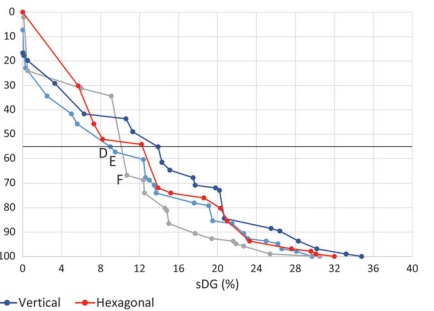
the best shading was a horizontal louver (A) which reduced the sDG to 12.7 % while guaranteed an sDA of 62.4 %. The geometrical parameters of the slats were 0.13 m spacing, 0.14 m depth and 4.8° rotation. The second best performance was recorded also for the type horizontal louver (B) characterized by the slats parameters of 0.14 m spacing, 0.14 m depth and 3.5° rotation. This shading allowed to reduce sDG to 13.9 % and at the same time to provide an sDA of 67.3 %. The third most performative shading was of the type overhang with fins (C) which allowed to reduce sDG to 14.4 % while guaranteed an sDA of 58.8 %. The depth of the shading was 1 m.

Considering the simulation grid with the largest distance from walls and windows, the most performative shading type was the overhang with vertical fins with two configurations. The first (D) had a depth of 1.19 m and permitted to reduce glare in the classroom so that only 9 % of all the views recorded a disturbing glare (sDG) and at the same time guaranteed a daylight provision of sDA 55.2 %. The second (E) had a depth of 1.24 m and allowed a reduction of sDG to 9.5 % and an sDA of 57.3 %. The third most performative shading was a horizontal louver (F). It allowed a reduction of sDG to 10.7 % and at the same time guaranteed an sDA of 66.7 % using the slats geometrical parameters of 0.25 m spacing, 0.21 m depth and 13.9° rotation angle.

Taking into account classroom 41 the sDG and sDA without shading were 18.8 % and 85.0 % respectively, using the analysis grid at 0.5 m from the walls, and 21.1 % and 91.4 % respectively, using the grid at 1 m from the walls. The most performative shading types were the overhang with fin, the hexagonal pattern and the vertical louver. The results are presented in Figure 7. Considering the grid closer to the walls, the first and the third best shading types (G-I) were overhang with fin which allowed to reduce the sDG to 6.6 % and 6.8 % while guaranteed an sDA of 55.6 % and 56.7 %, respectively. Their depths were 0.60 m and 0.61 m, respectively. The second best shading (H) was of the type hexagonal pattern with an aperture radius of 0.46 m and a depth of 0.3 m. It allowed to reduce sDG to 6.8 % as the third best shading of type overhang with fin but allowed slightly more daylight provision with an sDA of 58.3 %.

Considering the grid at 1 m from the walls, the three most performative shading types were all overhang with fin (J-K-L). They permitted to reduce the sDG to 2.9 %, 3.5 % and 3.9 %, respectively, while they allowed an sDA of 57.7 %, 58.6 % and 61.5 %, respectively. Their depth were 0.75 m, 0.71 m and 0.67 m, respectively. For classroom 41 and considering the small grid, two other shadings had performance similar to the third best. A hexagonal pattern shading (M) with 0.1 m of aperture radius and 0.07 m of depth reduced sDG to 4 % and allowed an sDA of 62.5 %. A vertical louver (N) with slats spacing of 0.9 m, a depth of 0.24 m and a rotation of 58.7° CCW reduced the sDG to 4.1 % while allowed a sDA of 55.8 %.

Figure 7
Plots of the Pareto front trade-off solutions of the shading devices of classroom 41 for analysis grid with distance from walls 0.5 m (left) and 1 m (right).
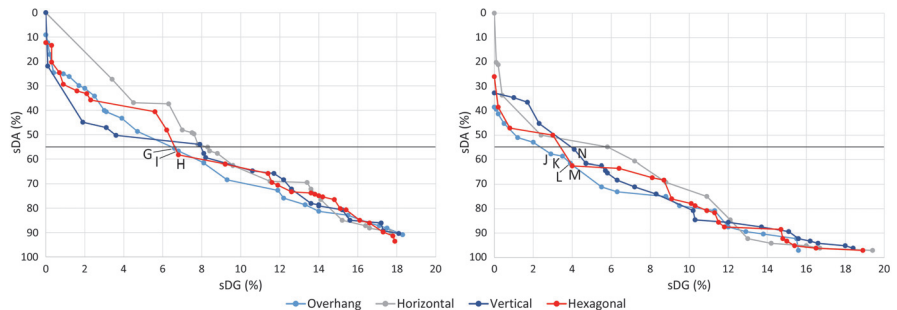
Grid		46 reduction (%)			41 reduction (%)				
		A	B	C	G	H	I		
0.5	sDG	66.9	63.8	62.5	64.9	63.8	63.8		
	sDA	37.2	32.3	40.8	34.6	31.4	33.3		
		D	E	F	J	K	L	M	N
1	sDG	78.4	77.2	74.3	86.3	83.4	81.5	81.0	80.1
	sDA	44.8	42.7	33.3	36.9	35.9	32.7	31.6	38.9

Table 3 summarizes the shading devices performance for glare reduction and consequent decrease of daylight which was anyway adequate according to the most advanced standards. In classroom 46, due to its southerly orientation, the most performative shadings were the horizontal louver (A), which reduced annual glare by 66.9 % and daylight by only 37.2 % when the large grid was used, and the overhang with fins (D), which reduced glare by 78.4 % and daylight by a much lesser 44.8 % when the small grid was used. In classroom 41, due to its easterly orientation, the most performative shadings were the overhang with fin and the vertical louver, with close performances. However, the first was the most performative using both the large and the small grid (G-J) reducing glare by 64.9 % and by 86.3 % and daylight by a much lesser 34.6 % and 36.9 %, respectively.

Thus evidence showed that using static shading the reduction of visual discomfort outperformed the decrease of daylight availability. Results also showed that the analysis grid, representing a possible tables' layout, further from the walls presented higher glare and daylight without shading, being the further sensors closer to the windows, but also recorded the larger glare reduction using the shadings.
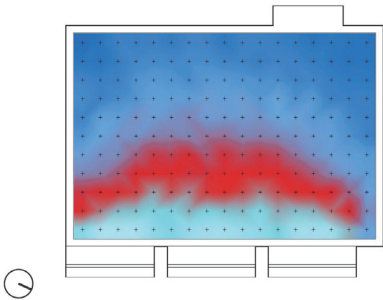
View out analysis

The view out analysis as well as the energy analysis were used in the study to evaluate the influence of the shading devices on other aspects of occupant comfort and building performances. For the view out analysis SEF was calculated for the same sensor points as for the glare simulations (Figure 8), using both analysis grids. The average SEFs of the classrooms without shading and with the 14 most performative shadings analyzed were compared (Table 4).

Grid	46 av. SEF (%)				41 av. SEF (%)				
	ns	A	B	C	ns	G	H	I	
0.5	6.1	3.5	3.8	3.36	6.3	4.8	4.5	4.8	
	ns	D	E	F	ns	J	K	L	M	N
1	6	3.1	3.1	3.6	6	4.4	4.5	4.6	4.4	4.1

In classroom 46 using the larger analysis grid (0.5) the three most performative shadings (A-B-C) reduced the view to the sky by values between 38.5 % and 44.8 %. Similar reductions, between 40 % and 48.3 %, were recorded when the smaller analysis grid was used (1) and with the related most performative shadings (D-E-F). In classroom 41 the reduction of SEF was between 24.1 % and 28.7 % when the large grid was used (0.5) with the related optimal shadings (G-H-I), and was between 23.3 % and 31.6 % when the smaller grid was used (1) and the related most performative shadings (J-K-L-M-N). The smaller SEF reduction in classroom 41 was due to the possibility to use smaller and more open shadings because the easterly orientation caused smaller visual discomfort.
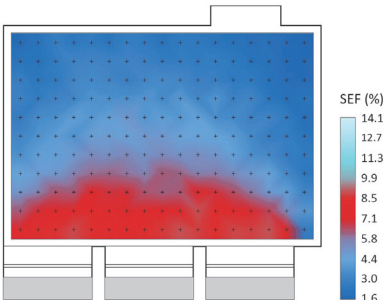
SEF (%)
14.1
12.7
11.3
9.9
8.5
7.1
5.8
4.4
3.0
1.6

Energy analysis

The energy simulations were performed for the main types of consumption which can be influenced by the external static shading, i.e., heating, cooling and electric lighting (Figure 9). The results showed that the use of the shading caused a small increase of total energy consumption in comparison with the much larger visual comfort increase. In both classrooms the 14 most performative static shading types analyzed (A-N) increased the heating energy and decreased the cooling energy due to reduced solar gains, and increased the electric lighting consumption due to reduced daylight.

In classroom 46 the average increase of total energy was 8 %. The average increase of heating energy was 9.8 %, the average decrease of cooling energy was 70.5 %, and the average increase of electric lighting was 8.3 %. In classroom 41 the average increase of total energy was 2.5 %. The average heating and electric lighting energy increase was 2.6 % and 4.9 %, respectively and the average cooling energy decrease was 25.5 %. Being heating the largest consumption, the difference of energy increase between the two classrooms was due to the smaller solar gains of classroom 41, due to its easterly orientation.

CONCLUSION

The research investigated the potential of static shading to reduce visual discomfort and to guarantee adequate natural illumination in two classrooms of TalTech Academy of Architecture and Urban Studies with different orientations. Parametric variations of four types of shading (overhang with fins, horizontal and vertical louver, hexagonal pattern) were used to minimize disturbing glare and maximize daylight autonomy through multi-objective optimization. View out and energy analyses were used to further evaluate the optimal shadings. Two analysis grids with different offsets from the walls were used to obtain useful information for the classroom tables' layout.

The results showed that the shadings allowed a reduction of disturbing glare by up to 78.4 % and 86.3 % and at the same time reduced daylight availability of 44.8 % and 36.9 % in the southerly and easterly oriented classrooms, respectively. Nevertheless, adequate daylight levels were provided. Thus the study proved the potential of static shading in improving visual comfort while guaranteeing daylight provision. However, the most performative shadings reduced the average view out by 48.3 % and 26.6 %, and increased the energy consumption by 7.9 % and 2.3 % in the two classrooms, respectively.

The outcomes also showed that using the smaller grid, which represented a compact tables' layout, the shadings performed better in reducing glare. Moreover, the shadings horizontal louver and overhang with fins were the most performative for the southerly oriented classroom and the latter also for the easterly oriented classroom together with the vertical louver.

Future work will analyze classes with different sizes and orientations and will use multi-objective optimization of pairs of performances between glare, daylight, view out and energy. The resulting sets of data will be used to develop prediction formulas to be applied as the basis of a coupled method to inform design decisions about optimal shading types and sizes for specific room sizes, orientation and layout, during the early design phase.

Figure 9
Energy simulation results for the classrooms without shading (ns) and with the shadings analyzed (A-N).
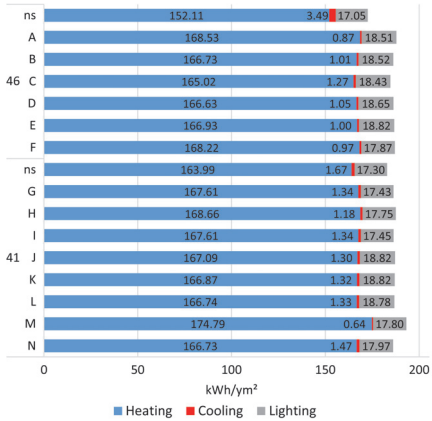
REFERENCES

Andersen, M, Mardaljevic, J and Lockley, SW 2012, 'A framework for predicting the non-visual effects of daylight – Part I: photobiology-based model', *Lighting Research & Technology*, 44(1), pp. 37-53

CEN, European Committee for Standardization 2018, *EN 17037:2018: Daylight in Buildings*, CEN, Brussels

Chan, YC and Tzempelikos, A 2013, 'Efficient venetian blind control strategies considering daylight utilization and glare protection', *Sol. En.*, 98, p. 241–254

Hans, O and Voss, K 2011 'OPTIShade potentials in optimization of passive climate protection for buildings', *In Proc. Climate and Construction*, Karlsruhe, pp. 1-10

Heschong, L, Wright, RL and Okura, S 2002, 'Daylighting Impacts on Human Performance in School', *J. of the Illuminating Engineering Society*, 31(2), pp. 101-114

Hopkinson, R 1972, 'Glare from daylighting in buildings', *Applied Ergonomics*, 3, pp. 206-215

Jakubiec, JA and Reinhart, CF 2012, 'The 'adaptive zone' – A concept for assessing discomfort glare throughout daylit spaces', *Light. Res. & Tech.*, 44, p. 149–170

Jakubiec, JA and Reinhart, CF 2016, 'A Concept for Predicting Occupants' Long-Term Visual Comfort within Daylit Spaces', *Leukos*, 12(4), pp. 185-202

Kong, Z, Utzinger, MD, Freihoefer, K and Steege, T 2018, 'The impact of interior design on visual discomfort reduction: A field study integrating lighting environments with POE survey', *Building and Environment*, 138, pp. 135-148

Koo, SO, Yeo, MS and Kim, KW 2010, 'Automated blind control to maximize the benefits of daylight in buildings', *Building and Environment*, 45, pp. 1508-1520

Lockley, SW 2009, 'Circadian Rhythms: Influence of Light in Humans', in Squire, LR (eds) 2009, *Encyclopedia of Neuroscience*, Elsevier Academic Publishing, Amsterdam, pp. 971-988

De Luca, F 2017 'From Envelope to Layout. Buildings Massing and Layout Generation for Solar Access in Urban Environments', *In Proc. of 35th eCAADe*, Rome, vol. 2, pp. 431-440

De Luca, F, Voll, H and Thalfeldt, M 2016, 'Horizontal or Vertical? Windows' layout selection for shading devices optimization', *Management of Environmental Quality: An International Journal*, 27(6), pp. 623-633

De Luca, F, Voll, H and Thalfeldt, M 2018, 'Comparison of Static and Dynamic Shading Systems for Office Buildings Energy Consumption and Cooling Load Assessment', *Management of Environmental Quality: An International Journal*, 29(5), pp. 978-998

McNeel, R 2021, *Rhinoceros*, https://www.rhino3d.com

Nabil, A and Mardaljevic, J 2006, 'Useful Daylight Illuminances: A Replacement for Daylight Factors', *Energy and Buildings*, 38(7), pp. 905-913

NREL, National Renewable Energy Laboratory 2021, *EnergyPlus*, https://energyplus.net

Reinhart, CF 2004, 'Lightswitch-2002: a model for manual and automated control of electric lighting and blinds', *Solar Energy*, 77(1), pp. 15-28

Reinhart, CF 2018, *Daylighting Handbook II. Daylight Simulations. Dynamic Facades*, Building Technology Press, Cambridge (MA), USA

Reinhart, CF, Mardaljevic, J and Rogers, Z 2006, 'Dynamic Daylight Performance Metrics for Sustainable Building Design', *Leukos*, 3(1), pp. 7-31

Sadeghipour Roudsari, M and Pak, M 2013 'Ladybug: a parametric environmental plugin for grasshopper to help designers create an environmentally-conscious design', *In Proc. of BS 2013*, Chambery, p. 3128–3135

Rutten, D 2021, *Grasshopper*, Algorithmic modeling for Rhino, https://www.grasshopper3d.com

Sepúlveda, A, De Luca, F, Thalfeldt, M and Kurnitski, J 2020, 'Analyzing the fulfillment of daylight and overheating requirements in residential and office buildings in Estonia', *Building and Environment*, 180, p. 107036

Illuminating Engineering Society, IES 2013, *Approved Method: IES Spatial Daylight Autonomy (sDA) and Annual Sunlight Exposure (ASE)*, IES

Solemma, LLC 2021, *ClimateStudio*, Solemma, https://www.solemma.com

Voll, H, Thalfeldt, M, De Luca, F, Kurnitski, J and Olesk, T 2016, 'Urban planning principles of nearly zero-energy residential buildings in Estonia', *Management of Environmental Quality: An International Journal*, 27(6), p. 634–648

Ward, GJ 1994 'The RADIANCE lighting simulation and rendering system', *In Proc. of the 21st SIGGRAPH Conference*, Orlando (FL), USA, p. 459–472

Wienold, J and Christoffersen, J 2006, 'Evaluation methods and development of a new glare prediction model for daylight environments with the use of CCD cameras', *Energy and Buildings*, 38, pp. 743-757

Wortmann, T 2017, "Model-based Optimization for Architectural Design: Optimizing Daylight and Glare in Grasshopper', *Tech. Arch. + Des.*, 1(2), pp. 176-185

Publication VI
Sepulveda, A.; De Luca, F.; Varjas, T. (2021). Influence of daylight modeling decisions on daylight provision and glare protection. Proceedings of the Symposium on Simulation for Architecture and Urban Design (SimAUD): 2021 Symposium on Simulation for Architecture and Urban Design, A. Chronis, G. Wurzer, W.E. Lorenz, C.M. Herr, U. Pont, D. Cupkova, G. Wainer, Online, 15-17 April 2021. ACM Digital Library.

Influence of daylight modeling decisions on daylight provision and glare protection

Abel Sepúlveda [1], Francesco De Luca [1] and Toivo Varjas[1]

[1]Tallinn University of Technology
Tallinn, Estonia
absepu@taltech.ee, francesco.deluca@taltech.ee,
toivo.varjas@taltech.ee

ABSTRACT

This paper aims to investigate the influence of frequent decisions within climate-based daylight modeling (CBDM) on daylight and glare assessment. The analyzed factors are the sky model, opaque surfaces' reflectance, level of detail of the three-dimensional model, and shading model. A hybrid methodology based on illuminance/luminance measurements and Radiance simulations is applied. An uncertainty analysis based on four steps and a final daylight/glare annual assessment considering the European standard EN17037 are presented. The use of calibrated reflectance values instead of standard reflectance values can decrease illuminance relative deviations from 62% to 15%. The deviations for view direction with view contact with the outside can decrease of 30% the accuracy of daylight glare calculations when improving the three-dimensional model of the exterior environment. We recommend quantifying uncertainty of daylight glare calculations for each studied occupant view direction before to use the shading model for annual simulations. The use of standard reflectance values instead of calibrated ones can underestimate annual daylight performance up to 30%.

Author Keywords

daylighting; climate-based daylight modeling; daylight glare; calibration; visual comfort; complex fenestration system

ACM Classification Keywords

1 INTRODUCTION

Human-centric design is nowadays one of the central criteria in architectural design. Visual comfort in buildings is a key component of the overall comfort of occupants [1]. The level of visual comfort in buildings depends on daylight provision, view out, solar access, and glare protection [2]. Daylight is the most preferred source of light [3] and improves building's users' health and performance [4] [5] [6]. However, high daylight levels can provoke glare discomfort [7]. The daylight aspects of the buildings are in constant conflict, usually representing a challenge for designers whether in early stages of design or refurbishment plans [8] [9].

Daylight modeling started being reliable when ray-tracing-based software Radiance was developed [10]. Along the last decade, several friendly-use applications such DAYSIM [11], LadyBug/HoneyBee [12] [13], DIVA-for-Rhino [14], and Fener [15] were created in order to increase availability of Radiance-based simulations in the building design community. The use of climate-based daylight modeling (CBDM) is key for –reliable assessment of daylight provision in buildings [16] [17]. Many factors influence the accuracy of daylight simulations. Previous investigations compared CBDM techniques and proposed ranges for simulation parameters to ensure the accuracy of daylight assessments [18] [19] [20].

Nevertheless, daylight calculation methods and simulation parameters are not the only factors affecting simulation results. Other researches highlighted the importance of a suitable modeling of glazing units in combination with external/internal shading systems known as complex fenestration systems (CFSs) [21] [22]. Thus, the use of Bidirectional Scattering Distribution functions (BSDF) data sets to represent the angular-dependent behavior of the CFS is critical to not underestimate daylight glare risk [23]. Additionally, small changes in diffuse reflectance of opaque surfaces of the interior [24] [25] [20] or exterior [26] scene have significant effects in lighting levels of indoor spaces. Material properties also play a relevant role in electric lighting consumption when daylight control are assumed [27].

There is a lack of studies about how decisions in daylight modeling relative to three-dimensional model, surface properties, CFS model, and sky model could affect the accuracy of daylight and glare assessment within the context of the European standard EN17037 in high latitudes. This paper aims to investigate the impact on the accuracy of the most usual modeling decisions that architects and practitioners must conduct in CBDM. The objectives of this research can be summarized as follows:

- To quantify the impact on illuminance levels and discomfort glare of measured irradiance by non-

calibrated pyranometers to model clear and intermediate skies,

- To evaluate the agreement in terms of illuminance and luminance distributions between experiments and simulations when considering different material's reflectance,

- To study how different levels of detail in the geometrical model (interior scene and surroundings) affect accuracy of simulation results,

- To determine the influence of different CFSs on the accuracy of the daylight and glare simulations.

- To investigate the effects of calibrating the daylight model on annual daylight provision and glare performance within the context of the standard EN17037,

The practical implications of this paper can help architects and designers to be more conscious about the consequences of their decisions in daylight modeling. Thus, designers could prioritize decisions during daylight the modeling process, which is fundamental within an efficient human-centric design practice.

2 METHODOLOGY

2.1. CASE STUDY

We used a hybrid methodology based on field measurements and simulations. Illuminance and luminance experiments were conducted at the nZEB TalTech test facility [28] located in Tallinn, Estonia, (59.394737° N, 24.658502° E) (Figure 1) [29].
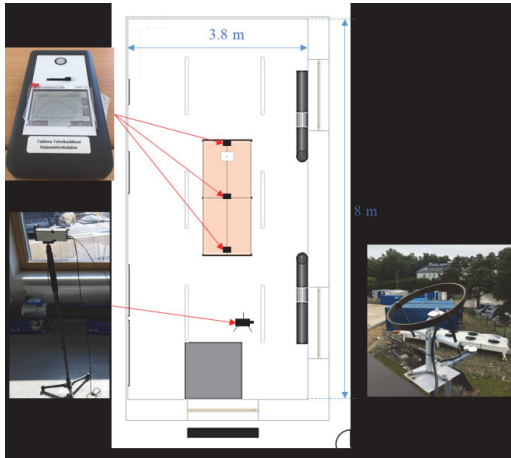

Figure 1. Top view scheme of the nZEB test facility with the used equipment for the illuminance, luminance, and solar radiation measurements.

The room used for the test is 3.8 m deep and 8 m wide, and has 3 external windows. Two are east-oriented windows and another is facing south. East-oriented windows have internal roller fabrics installed and the south-oriented window has external louvers. We kept louvers in closed position during the experiments to study the availability of daylight and glare risk due to only east-oriented windows.

The experimental session were on June 5, 2020 (fully clear sky conditions) and on June 29, 2020 (partially clear sky conditions). The analyzed times were from 8:00 to 12:00 during morning with time steps of 20 minutes. Thus, 13 time steps were measured in each session. Two view directions were considered as the most probable by a building occupant: east (E) and north (N).

2.2. ERROR ANALYSES AND METRICS

We considered the field measurements as benchmark for the research . Thus, this study consists in three error analyses and one annual daylight/glare assessment regarding different aspects of daylight modeling explained in section 1.

We evaluated daylight glare risk using the Daylight Glare Probability (DGP), which is the most robust glare metric nowadays [30] [31]. We also analyzed the horizontal illuminance on the table located in the middle of the room. The final analysis consists in an annual evaluation of daylight and glare according to the European standard 17037. The analyzed factors were the sky models, the materials' reflectance, the level of detail of the geometrical model (exterior and interior scene), and those related with the CFSs.

For annual assessments, we used the widely used Spatial Daylight Autonomy (sDA) [32] and percentage of discomfort glare hours ($fDGP_t$) where DGP_t is the threshold for the DGP value [2]. According to the standard EN17037, the maximum percentage of discomfort glare hours must not exceed 5 % of the occupied time. Using the recommended threshold of 300 lx (during at least 50% of occupied time), the minimum sDA should be 50%. In addition, at least 95% of the reference plane should be lit with a minimum target illuminance of 100 lx during at least 50% of daylight hours. DGP thresholds values and glare protection classes are shown in Table 1.

DGP threshold (DGP_t)	0.35	0.40	0.45
Level of glare protection	High	Medium	Minimum

Table 1. Glare protection classes recommended by the European standard EN17037 [2].

The metrics to quantify absolute and relative deviation between measured and simulated variables were the Mean Relative Error (MRE) (1) and the relative Root Mean Squared Error (rRMSE) (2).

$$RME = \left(\sum_{i=1}^{N}(x_{i,sim} - x_{i,exp})/x_{i,exp} \right)/N \qquad (1)$$

$$rRSME = \sqrt{\left(\sum_{i=1}^{N}(x_{i,sim} - x_{i,exp})^2/\left(x_{i,exp}\right) \right)/N} \qquad (2)$$

Where $x_{i,sim}$ and $x_{i,exp}$ are the illuminance/DGP values obtained from simulations and experiments, respectively. N is the number of values compared.

2.3. EXPERIMENTAL SET UP

Illumination tests were performed with a calibrated Gigahertz-Optik luxmeter MSC-15 (calibration laboratory that is accredited by DAkkS), which allows accurate measurement of luminance spectrum, color and color rendering. Accurate measurements of the illuminance of natural and artificial lighting are important to ensure the most accurate cosine response possible (for the MSC-15 meter it is f2≤ 3%). We used the calibrated luminance camera LMK98-3 color with lens TT8 and software LMK Labsoft for the luminance measurements [33]. The technical data of the experimental devices are presented in Table 2.

Measuring instrument	Technical specification
Luxmeter MSC-15	Measurable parameter - illuminance (lx); Measurement range 1 lx to 350,000 lx, 360 nm to 830 nm
Luminance camera LMK98-3 color with lens TT8 and software LMK Labsoft	Image luminance measurement device (ILMD) camera is equipped with a filter wheel adapted to the color matching functions of the 2° CIE standard observer (CIE 1931) for light and color measurement. Resolution 1380 x 1030 pixel Measurement values – luminance L (cd/m^2); Fixed focus lens TT8, aperture 2.8

Table 2. Technical data of the experimental set up.

The illuminance sensors were located at points p, s1, s2, s3 displayed in Figure 2.
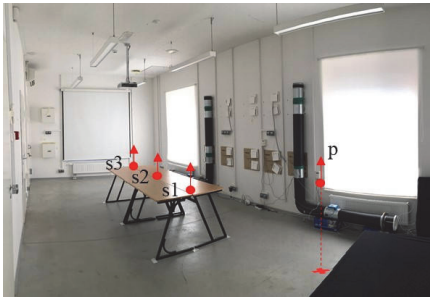

Figure 2. Interior view of the test room with lowered interior fabrics.

2.4. VIRTUAL MODEL IN RADIANCE

For point-in-time calculations we used the traditional ray-tracing-based *rtrace* method. For annual simulations we used the validated matrix-based five phase method (5pm) which can represent accurately the direct component of the sun [34]. All the Radiance parameters are presented in Table 3. These are recommended Radiance parameters by Radiance tutorials and previous investigations [35][36].

DGP calculations were conducted using Radiance command *evalglare* [37]. The evaluation of the DGP requires information about the luminance distribution of the scene (.HDR files) and (optionally) the vertical illuminance at eye level (E_v). We input in evalglare measured and simulated E_v to generate DGP_{exp} and DGP_{sim}, respectively.

We modeled the double-pane clear glazing with *trans* material in Radiance using a visual transmittance of 70% (according to previous calibrated thermal model of the test room). Reflectance values and Radiance materials used to model opaque surfaces are presented in Table 4. The angular-dependent behavior of the interior fabric was measured at Fraunhofer ISE using a scanning photogoniometer pgII [38]. Transmittance and reflectance profiles of the fabric (openness factor of 0.5%) are shown in Figure 3. The direct-diffuse transmittance and reflectance ranges are 24-35% and 60-70%, respectively.

5pm	3pm	Sky generation: -m 1 (MF=1)
		Daylight matrix: -c 1500 -ab 4 -ad 1024 -lw 9.76e-4
		View matrix: -c 10 -ab 10 -ad 65536 -lw 1.53e-5 -pj 0.7 -x 600 -x 600
	3pmD	Sky generation: -m 1 (MF=1) -d (direct component of the sun)
		Daylight matrix: -c 1500 -ab 0 -ad 1024 -lw 9.76e-4
		View matrix: -c 10 -ab 1 -ad 65536 -lw 1.53e-5 -pj 0.7 -x 600 -x 600
	cds	Sky generation: MF=3 (1297 sky subdivisions)
		Daylight coefficient matrix: -ab 1 -ad 1024 -pj 0.7 -dc 1 -dt 0 -dj 0 -x 600 -x 600
rtrace		-ab 5 -ad 1024 -lw 1/1024 -aa 0.15 -st 0.15 -as 512 -x 1200 -y 900 [39]

Table 3. Radiance parameters used for glare simulations using *rtrace* and 5pm. cds=direct coefficient sun simulation, 3pm=3-phase method, and 3pmD=3-phase method Direct calculation.

Surface	Radiance Material	Min	Ref. case	Max
Ceiling [2]	Plastic	0.7	0.7	0.9
Interior walls [2]	Plastic	0.5	0.5	0.8
Floor [2]	Plastic	0.2	0.2	0.4
Exterior walls [2]	Plastic	0.2	0.3	0.4
Exterior ground [2]	Plastic	-	0.2	-
Table, Frames [40]	Plastic	-	0.4	-
Black textile, table legs/Pipe	Metal/ Plastic	-	0.1	-
Exterior venetian	Plastic		0.3	

| Aluminum rings [41] | Metal | - | 0.65 | - |
| Doors, other interior objects | Plastic | - | 0.8 | - |

Table 4. Radiance material and reflectance values for opaque surfaces of the virtual model.
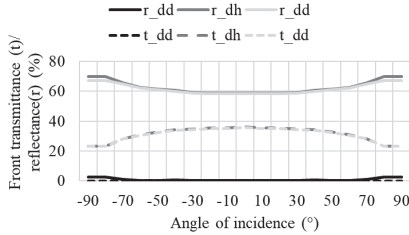

Figure 3. Optical properties of the fabric depending on the angle of incidence. d=direct, h=hemispherical, and d=diffuse.

3   RESULTS

3.1. SKY MODEL AND MATERIALS' REFLECTANCE

The objective of this error analysis is to find a combination of reflectance values of the main opaque surfaces and the most reliable sky model to use in our full virtual model (Figure 5). This need arises when reflectance of materials are unknown. We varied the reflectance of ceiling, interior walls, floor and exterior walls/sourronding buildings. We calculated the relative deviations in terms of illuminance for all the sensors at 8:00, when the room space receives more sunlight. No shading is used in order to minimize the uncertainty of the virtual model when using different set of reflectance values. The selected reflectance ranges for this analysis are shown in Table 5.

Surface	Min	Step	Max
Ceiling	0.7	0.05	0.9
Interior walls	0.5	0.05	0.8
Floor	0.2	0.05	0.4
Exterior walls	0.2	0.05	0.4

Table 5. Reflectance ranges for the opaque surfaces studied in this analysis. Where Min=minimum value and Max=maximum value.
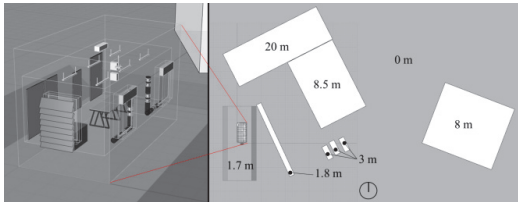

Figure 5. Detailed (left) and top (right) view of the room study in Rhinoceros. Exterior environment are constitued by buildings

under renovation (of 8.5 and 20 m height) construction objects (up to 3 m height), and Mektrory building of 8 m height.

A general comparison between sky models is presented in Figure 6. The maximum relative deviation was higher when using Perez than when using clear CIE sky model in 99.9% of the cases. In previous investigations, Perez has been proved a reliable model to represent real sky conditions and that CIE clear sky model tends to underestimate indoor levels of light [42]. Illuminance deviations are higher when using Perez sky to model clear and intermediate sky conditions than CIE model for clear sky conditions. This fact is due to the non-calibrated measurements of global and horizontal diffuse irradiance. Although Perez models are more accurate than CIE models to represent real climate sky conditions, we cannot trust on our Perez model neither under clear nor intermediate sky conditions because the inaccurate irradiance measurements. For the study, only clear sky conditions are considered for the error analyses explained in subsections 3.2 and 3.3.

The rRMSE of the cases with lowest relative deviations per ceiling reflectance are displayed in Figure 7. The optimal combination of reflectance values (C70, with rRMSE=15%) are 70%, 80%, 40% and 40% for ceiling, interior walls, floor, and exterior walls, respectively. Considering these reflectance values, the model in Radiance when no shading is used and under clear sky conditions, has an uncertainty in terms of rRMSE of 15%. For the rest of the paper the presented reflectance values are considered.
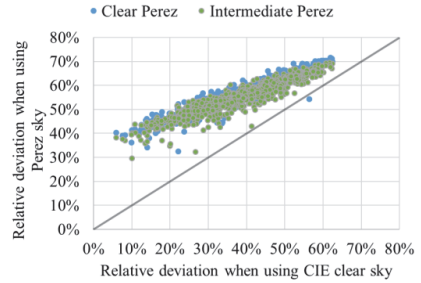

Figure 6. Relation between the maximum relative deviation of illuminance sensors when using Perez and Clear CIE skies.
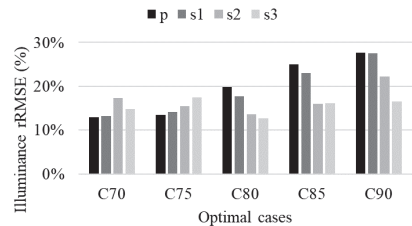

Figure 7. Relative root square mean error (rRMSE) for the optimal cases.

3.2. THREE-DIMENSIONAL MODEL

In this subsection, we quantify the influence of different levels of detail of the three-dimensional model on relative deviations of illuminance and DGP. Two representative view directions are analyzed: room occupant's sight towards N and E. We used the calibrated model from the previous subsection. We considered no shading in order to minimize the uncertainty of the error analysis.

The first step is to analyze relative deviations in terms of illuminance. The rRMSEs for different geometrical models are presented in Figure 8. The maximum absolute variation in terms of rRMSE is from 15% to 20% for any level of detail of the three-dimensional model. Unexpectedly, the deviations between simulated and measured values do not decrease with the level of detail (including interior and/or exterior scene) of the geometrical model. The authors argue that this is due to the small influence of both, interior and exterior scene during the day of study: June 25, 2020. In addition, higher specularity of real surfaces of the interior/exterior scene could have significant impact on rRMSE.

The second step of this analysis is to quantify the rRMSE in terms of DGP for two different view directions and the mentioned three-dimensional models. For view N the DGP rRMSE does not change more than 4%. However, the deviations for view E direction decreases 30% when adding the exterior scene (Figure 9) .
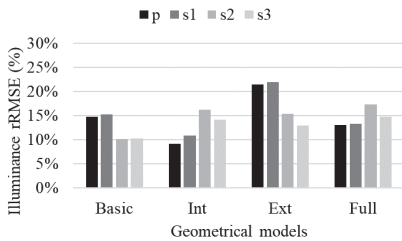

Figure 8. Relative Root Mean Squared Error (rRMSE) for the different geometrical models: Basic=without interior/exterior objects, Int= only interior objects, Ext= only exterior objects, and Full= detailed model shown in Figure 5.
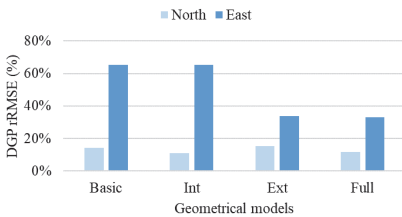

Figure 9. Relative root square mean error (rRMSE) of DGP for the different geometrical models: Basic=without interior/exterior objects, Int= only interior objects, Ext= only exterior objects, and Full= detailed model shown in Figure 5.

The most representative luminance distributions for view direction N are presented in Figure 10. The DGP decreases when interior/exterior scene is added to the model. The main differences between the measured distribution and the calibrated virtual model are the order of magnitude of the luminance of the window area (10:00 and 12:00) and the peak of luminance on the wall at 8:00. These differences might be associated to actual uncertainty of the full virtual model quantified in the previous subsection. The luminance distributions for view direction E are presented is Figure 11. The DGP decreases with the level of detail of the exterior scene: there are more exterior surfaces with medium-low luminance values (750-300 cd/m^2) associated to the zones in shadow. The consideration of the exterior scene corrected the overestimation of discomfort glare: from DGP approximately 0.4 (perceptible) to 0.30 (imperceptible). The overestimation of glare risk could have crucial influence when using shading control algorithms based on DGP: the decrease of indoor daylight levels for the excessive use of the interior fabric due to an overestimated DGP calculation.
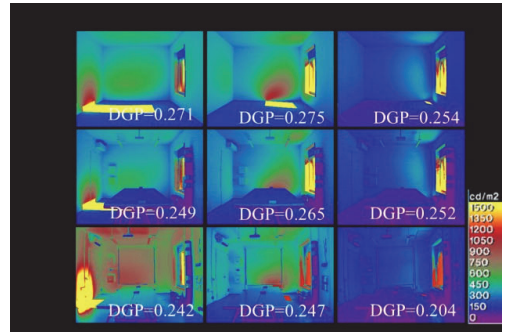

Figure 10. Luminance maps and DGP values for view towards N at different time steps on June 25, 2020.
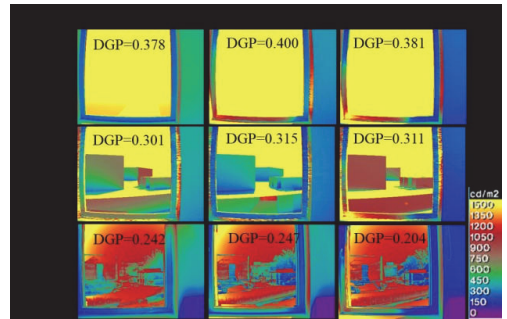

Figure 11. Luminance maps and DGP values for view towards E at different time steps on June 25, 2020.

3.3. UNCERTAINTY DUE TO FABRIC SHADING

The aim of this subsection is to quantify the deviations introduced when the interior fabric blind is used as shading system (Figure 2). The metrics used are the illuminance and DGP rRMSEs. Two view directions are analyzed: E and N.

The full and calibrated virtual model was considered in order to minimize the uncertainty of simulation results. Thirteen time steps under clear sky conditions were analyzed. The fabric is model in Radiance using the aBSDF material (witth Klems basis angular resolution) wich improves the virtual representation of the transmittance peak shown in Figure 3.

The illuminance rRMSEs for different façade states is presented in Figure 12. The use of the fabric as shading system increases the maximum deviation from 17% to 37% while the average maximum deviation increases of 14% in absolute values. The highest rRMSE is associated to sensor p. The authors argue that this is due to the inaccuracies related to the exterior scene and Klems basis angular resolution. An improvement of the angular resolution might decrease illuminance deviations. Finally, for view N the DGP rRMSE is 8% against 76% for view E (Figure 13). This high discrepancy can be a sufficient criterion to not trust the fabric model for glare calculations in our case study, when view direction towards E is considered. On the contrary, the DGP uncertainty due to the fabric shading for view N direction is acceptable.
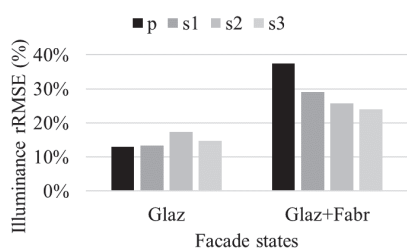

Figure 12. Illuminance relative root square mean error (rRMSE) for façade states: Glaz= glazing modeled with trans material and Glaz+Fabr= Glaz case adding fabric modeled with aBSDF material and Klems angular resolution.
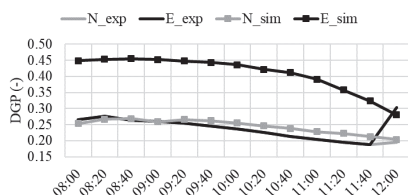

Figure 13. DGP variation with time for clear sky conditions and using interior fabric. exp= experiment and sim=simulation.

3.4. ANNUAL ASSESSMENT OF DAYLIGHT AND GLARE

The objective of this subsection is to compare daylight and glare annual performance when using a virtual model with standard reflectance values and a calibrated model. We calculated the annual metrics sDA and fDGP. Thresholds were set according to the European standard EN17037 (Table 1).We used Perez sky based on the weather file related to Tallinn, Estonia, year 2018. We used the five-phase

method to calculate hourly illuminance and DGP. The sensor grid is located at 0.85 m from the floor and the separation between sensors is 0.5 m. For DGP calculations, only the view direction towards N is considered because it showed an acceptable agreement with measured and simulated values in subsection 3.4.

The results of annual simulations are presented in Table 5. The annual daylight performance in terms of sDA increases in absolute value of 6% (relative deviation of 27%) when using calibrated reflectance values. Nevertheless, sDA does not meet the minimum requirements (50%). Therefore, louvers of the south-oriented window might be changed to open position to increase the indoor lighting levels. The annual glare protection performance does not depend on whether the reflectance values are calibrated or not. The maximum absolute difference in terms of illuminance is 225 lux in timesteps where glare sources are not relevant. Furthermore, the room used in the study does not have glare problems for the most probable view directions (E and N) (fDGPt< 5%, maximum glare protection) and the fabric shading might be used exclusively for privacy needs.

Reflectance values	$sDA_{300,50\%}$	$fDGP_t$ (%)		
	(%)	$f0.35$	$f0.40$	$f0.45$
Standard EN17037	22.1	0.39	0.36	0.36
Calibrated	28.1	0.39	0.36	0.36

Table 5. Annual daylight and glare protection performance for different sets of materials' reflectance when shading is not used.

4 CONCLUSION

This paper analyzed key decisions in daylight modeling and their impact on daylight and glare calculations. The analyzed decisions are: 1) the sky models; 2) the materials' reflectance; 3) the level of detail of the three-dimensional model; 4) and the shading model. Measured and simulated illuminance and DGP values were compared. Thus, three error analyses and one final annual daylight and glare assessment were conducted. These error analyses represent steps of a workflow to calibrate daylight models in practice. The main outcomes of this research as practical recommendations for architects and practitioners are the following:

- Intermediate CIE sky model could not represent the partial sunny conditions in Tallinn. For clear sky conditions, the use of clear CIE sky model is more accurate than Perez sky model based on non-calibrated irradiance measurements.

- A suitable selection of the reflectance of opaque surfaces is crucial to achieve accurate simulation results: the use of calibrated instead of standard reflectance values could decrease illuminance relative deviations from 62% to 15%. The lack of consideration of calibrated models could

underestimate annual daylight performance of up to 30%. The effect on annual glare protection performance is not significant in our case study. Furthermore, we recommend conducting an error analysis as we presented in subsection 3.1 when reflectance values are unknown and accurate daylight calculations are desired.

- The level of detail of the three-dimensional model could vary the illuminance rRMSE of approximately 5%. Nevertheless, the deviations for view E direction (view to the outside) could decrease of up to 30% the DGP rRMSE when a more detailed exterior environment is used. For view direction towards the interior (with lower luminance levels) a detailed three-dimensional model has less impact on DGP uncertainty (ΔrRMSE=4%). Furthermore, we recommend using a detailed three-dimensional model of the exterior environment when studying view to the outside in order to obtain more accurate DGP and illuminance calculations.

- The use of interior fabrics modeled with Radiance materials such as aBSDF and Klems BSDF data sets could increase the illuminance rRMSE from 17% to 37%. In addition, the use of shading model for some view directions could increase rRMSE from satisfactory approximations such as rRMSE of 8% to very large deviations such as rRMSE of 76%.

- Therefore, we recommend quantifying DGP uncertainty for occupant view directions of interest before using the shading model for annual simulations.

This research focuses on a case study in Estonia for limited number of weather conditions. Future work is to study uncertainty of daylight modeling decisions for different sky conditions and locations. We did not study the impact of the modeling of exterior vegetation. The impact of decisions on daylight modeling regarding different types of exterior scene such as rural and natural environments should be further investigated. Moreover, different CFS models could have different influence on daylight and glare calculations. Thus, further investigations could quantify model uncertainty when using different CFS models. Findings of these future investigations would help designers to create reliable daylight models to find sustainable design solutions in early stages of the design of new buildings and refurbishment plans.

REFERENCES
1. Shafavi, N. S., Zomorodian, Z. S., Tahsildoost, M., & Javadi, M. (2020). Occupants visual comfort assessments: A review of field studies and lab experiments. Solar Energy, 208, 249-274.

2. European comission, BS EN 17037:2018: Daylight in buildings, (2018). https://www.en-standard.eu/bs-en-17037-2018-daylight-in-buildings/.

3. Knoop, M., Stefani, O., Bueno, B., Matusiak, B., Hobday, R., Wirz-Justice, A., ... & Appelt, S. (2020). Daylight: What makes the difference?. Lighting Research & Technology, 52(3), 423-442.

4. Ko, W. H., Brager, G., Schiavon, S., & Selkowitz, S. (2017). Building envelope impact on human performance and well-being: experimental study on view clarity.

5. Lockley, S.W. (2009). Circadian Rhythms: Influence of Light in Humans. In Squire L.R. (edited by) Encyclopedia of Neuroscience, vol. 2, Academic Press, Cambridge (USA), 971-988.

6. Samuels, R. (1990). Solar efficient architecture and quality of life: The role of sunlight in ecological and psychological well-being. In Proceedings of the 1st World Renewable Energy Congress: Energy and the Environment (Sayigh/ed.)(p-2653-2659). Pergamon Press.

7. Pierson, C., Wienold, J., & Bodart, M. (2017). Discomfort glare perception in daylighting: influencing factors. Energy Procedia, 122, 331-336.

8. Bueno, B., Cejudo-López, J. M., Katsifaraki, A., & Wilson, H. R. (2018). A systematic workflow for retrofitting office façades with large window-to-wall ratios based on automatic control and building simulations. Building and Environment, 132, 104-113.

9. Bueno, B., & Ozceylan, F. (2019, January). A workflow for retrofitting façade systems for daylight, comfortable and energy efficient buildings. In IOP Conference Series: Earth and Environmental Science, 225, conference 1.

10. Ward, G. J. (1994, July). The RADIANCE lighting simulation and rendering system. In Proceedings of the 21st annual conference on Computer graphics and interactive techniques (pp. 459-472).

11. Reinhart, C., & Breton, P. F. (2009). Experimental validation of Autodesk® 3ds Max® Design 2009 and DAYSIM 3.0. Leukos, 6(1), 7-35.

12. Ladybug 2020.https://www.ladybug.tools/ladybug.html

13. Honeybee 2020. https://www.ladybug.tools/ladybug.html

14. Solemma LLC. DIVA. 2020. https://www.solemma.com/Diva.html

15. Bueno, B., Wienold, J., Katsifaraki, A., & Kuhn, T. E. (2015). Fener: A Radiance-based modeling approach to

assess the thermal and daylighting performance of complex fenestration systems in office spaces. Energy and Buildings, 94, 10-20.

16. Kong, Z., Utzinger, D. M., & Humann, C. (2018). Evaluation of a hybrid photo-radiometer sky model compared with the Perez sky model. Energy and Buildings, 178, 318-330.

17. Mardaljevic, J. (1999). Daylight simulation: validation, sky models and daylight coefficients. Leicester: De Montfort University.

18. Brembilla, E., & Mardaljevic, J. (2019). Climate-Based Daylight Modeling for compliance verification: Benchmarking multiple state-of-the-art methods. Building and Environment, 158, 151-164.

19. Brembilla, E., Chi, D. A., Hopfe, C. J., & Mardaljevic, J. (2019). Evaluation of climate-based daylighting techniques for complex fenestration and shading systems. Energy and Buildings, 203, 109454.

20. Kharvari, F. (2020). An empirical validation of daylighting tools: Assessing radiance parameters and simulation settings in Ladybug and Honeybee against field measurements. Solar Energy, 207, 1021-1036.

21. Tzempelikos, A., & Chan, Y. C. (2016). Estimating detailed optical properties of window shades from basic available data and modeling implications on daylighting and visual comfort. Energy and Buildings, 126, 396-407.

22. Thanachareonkit, A., & Scartezzini, J. L. (2010). Modeling complex fenestration systems using physical and virtual models. Solar Energy, 84(4), 563-586.

23. Inanici, M., & Hashemloo, A. (2017). An investigation of the daylighting simulation techniques and sky modeling practices for occupant centric evaluations. Building and Environment, 113, 220-231.

24. Brembilla, E., Hopfe, C. J., & Mardaljevic, J. (2018). Influence of input reflectance values on climate-based daylight metrics using sensitivity analysis. Journal of Building Performance Simulation, 11(3), 333-349.

25. De Luca, F., Kiil, M., Simson, R., Kurnitski, J., & Murula, R. (2019, September). Evaluating Daylight Factor Standard through Climate Based Daylight Simulations and Overheating Regulations in Estonia. In Proceedings of the 16th IBPSA Conference (Vol. 2, p. 4).

26. Bugeat, A., Beckers, B., & Fernández, E. (2020). Improving the daylighting performance of residential light wells by reflecting and redirecting approaches. Solar Energy, 207, 1434-1444.

27. Hoffmann, S., Lee, E. S., McNeil, A., Fernandes, L., Vidanovic, D., & Thanachareonkit, A. (2016). Balancing daylight, glare, and energy-efficiency goals: An evaluation of exterior coplanar shading systems using complex fenestration modeling tools. Energy and Buildings, 112, 279-298.

28. nZEB technological test facility 2020.

https://old.taltech.ee/institutes/department-of-civil-engineering-and-architecture/labs-and-services-3/nzeb-technological-test-facility/

29. Google maps 2020.

https://goo.gl/maps/PTzqPJ7mYH1wYMuY9

30. Wienold, J., Iwata, T., Sarey Khanie, M., Erell, E., Kaftan, E., Rodriguez, R. G., ... & Kuhn, T. E. (2019). Cross-validation and robustness of daylight glare metrics. Lighting Research & Technology, 51(7), 983-1013.

31. Wienold, J., & Christoffersen, J. (2006). Evaluation methods and development of a new glare prediction model for daylight environments with the use of CCD cameras. Energy and buildings, 38(7), 743-757.

32. LM, I. (2013). Approved method: IES spatial Daylight autonomy (sDA) and annual sunlight exposure (ASE).

33. Manualzz 2020. https://manualzz.com/doc/31466295/luminance-and-color-measuring-camera-lmk-98

34. A. McNeil, The 5--phase method, (2013). https://www.radiance-online.org/community/workshops/2013-golden-co/McNeil-5phase.pdf.

35. A. McNeil, BSDFs, Matrices and Phases, (2014) 158. https://www.radiance-online.org/community/workshops/2014-london/presentations/day1/McNeil_BSDFsandPhases.pdf.

36. S. Subramaniam, Daylighting Simulations with Radiance using Matrix-based Methods, 2017. https://www.researchgate.net/publication/325248488_Daylighting_simulations_with_Radiance_using_matrix-based_methods

37. evalglare 2020. https://www.radiance-online.org/learning/documentation/manual-pages/pdfs/evalglare.pdf/view

38. TestLab Solar Façades, Fraunhofer ISE 2020. https://www.ise.fraunhofer.de/en/rd-infrastructure/accredited-labs/testlab-solar-facades.html

39. Mainini, A. G., Zani, A., De Michele, G., Speroni, A., Poli, T., Zinzi, M., & Gasparella, A. (2019). Daylighting performance of three-dimensional textiles. Energy and Buildings, 190, 202-215.

40. Leaderflush Shapland 2020.http://www.leaderflushshapland.co.uk/Integrated-doorsets/Technical-Resources/Light-reflectance-values-PVC-laminates

41. Taveres-Cachat, E., Bøe, K., Lobaccaro, G., Goia, F., & Grynning, S. (2017). Balancing competing parameters in search of optimal configurations for a fix louvre blade system with integrated PV. Energy Procedia, 122, 607-612

Publication VII

Varjas, T.; Laaneots, R.; Rosin, A. (2021). European Patent Application no EP3839482 (A1) Method and Device for Measuring Charcteristics of Refelection of Light on Surfaces. Available: https://espacenet.com. Publication 2021-06-23.

(54) **METHOD AND DEVICE FOR MEASURING CHARCTERISTICS OF REFELECTION OF LIGHT ON SURFACES**

(57)   The invention is within the area of optical electronics and can be used for measuring and assessing of values characteristic of reflection of light on all kinds of road surfaces, such as the luminance, luminance coefficient, reduced luminance coefficient, colour temperature, chromaticity coordinates. As a result of the measurement method and the application of the measuring device used for it, the measurement conditions of the lighting characteristics shall be adjusted and the characteristic values taken as reference values. Based on those values actual values of reflection of light from modern LED lighting solutions used on road surfaces of asphalt and concrete and different additives used in those can be assessed. The application of the invention takes into account the effect of the visual light's spectral composition on the assessment of the reflection of light from the surfaces and thereby offers safer and more efficient solutions for the traffic environment.
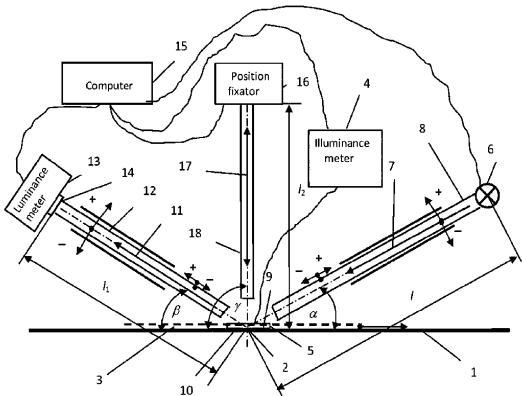
FIG 1

Description

Technical field

5　[0001]　The invention is within the area of optical electronics and can be used for measuring and assessing of quantities of reflection of light on all kinds of road surfaces, such as the luminance, luminance coefficient, reduced luminance coefficient, colour temperature, chromaticity coordinates of light falling on a road surface and reflecting from the surface.

Background art

10

[0002]　Measurement methods for lighting characteristics are usually intended for the spectre-based measurement of lighting and reflection quantities of the cover surfaces of illuminated objects. Basically, these are the possible measurement procedures for measuring the luminous intensity emitted from the light source, the illuminance of light directed at the measurement object and the luminance of the light reflected from that object, and the measuring instruments ap-

15　propriate for realising them.
[0003]　The demand for measuring the quantities of light reflected from the surfaces of objects, including the road surfaces or pavements, such as luminance, luminance coefficient, reduced luminance coefficient, colour temperature and chromaticity coordinates, has risen from the need to apply the obtained measurement results in designing and building road surfaces and the lighting installations belonging to the roads, but also for performing operations in the

20　required lighting simulation programmes. The measurement results obtained are also necessary for updating the standardised luminance coefficient and reduced luminance coefficient values for designing and building road surfaces and lighting installations. Even the lighting quantities of existing roads already in use need to be measured when they are being checked.
[0004]　The way road surfaces reflect light in the surrounding space is a characteristic quantity of road surfaces which

25　the human eye can detect, and which plays a key part in designing and building road lighting installations. Values characteristic quantities of light reflected from road surfaces are crucial for the functional quality and safety of roads, not only due to mechanical and dynamic performance but also due to the visual perception and night-time safety of all road users.
[0005]　The properties of current roadway and walkway surfaces and the road materials used to produce them (additives,

30　fillers and binders) have gradually changed. Therefore, the measurements obtained based on the measurement operations used for road surface luminance have a measurement uncertainty of up to 30 % of the measurement result and sometimes even 50 % of the measurement result (Road Surface Photometric Characterisation and Its Impact on Energy Savings. Coatings 2019, 9, 286). Luminous intensity distribution of the new type of light sources, especially the SSL-type light sources, is very sharp, which increases the impact of light characteristic quantities reflected from the surface.

35　Even the current LED technology supports smart road surface lighting and the opportunity to adapt the luminous flux at any time in terms of intensity and direction according to the characteristic quantities of the road surfaces and the luminance requirements. These circumstances require developing new modern measurement methods and mobile measuring instruments in order to design more efficient, more economic and safer road surfaces and road lighting installations.
[0006]　A significant need has risen to simplify and improve the measurement methods currently used for measuring

40　the characteristic quantities of reflection of light in order to be able to measure on site with a mobile measuring instrument the luminance of the cover surface directly surrounding the measuring point of the measuring grid defined on the cover surface, and other light characteristics reflected from this surface and the diversity of these values, thus reducing measurement capacity and increasing measurement accuracy.
[0007]　Characteristic quantities of reflection of light on surfaces of objects are measured using the following methods

45　and devices.
[0008]　The luminance of the surface of road surfaces is primarily measured by standardised measurement methods and devices (EN 13201-3:2015 and EN 13201-4:2015), according to which, road surface luminance is measured at the given points of the measuring field (calculation field) on the road surface defined by the standard. According to this standard, the measuring points of the measuring field defined for measuring the luminance of the surface of a road

50　section are distributed evenly, forming a grid of measuring points. At that, the grid of measuring points must be the same as when measuring the illuminance of the same road section, which occurs before measuring the luminance of the surface. When measuring the luminance of the light reflected from the road surface, the measuring instrument, e.g., a luminance meter, is placed on a tripod, usually at a height of 1.5 m from the road surface and 60 m away from the first (closest) measured points of the grid of measuring points on the measuring field (calculating field) of the road surface

55　in the traffic region being looked at. Measurements in each measuring point can also be taken from a shorter distance, but in that case the extent of the surface of the road probed by the luminance meter around the measuring point and the height of the measuring instrument from the surface of the road must be proportionally smaller. The direction (angle of observation) of the luminance meter itself in relation to the surface normal must be kept within 89° $\pm$ 0.5°. In the

transverse direction, the luminance meter must in turn be placed at the centre line of the selected measuring field on each lane. The average luminance of the road surface, the general uniformity of luminance and the elevation factor of the luminance threshold is calculated based on the measured values obtained at the measuring points given during the measurement of road section surface luminance. At that, the longitudinal uniformity of the luminance of the road surface is calculated based on the measured values obtained upon measuring the luminance of a road surface with many lanes at the centre line of all lanes.

[0009] A disadvantage of this measurement method is that it is very measurement-intensive, expensive and has a relatively low accuracy. When realising the method using all possible types of illuminance and luminance meters, the impact of the location of light sources next to the measuring points and grid outside the given measuring field of the road surface and the light produced by them to the luminance of the road surface must be taken into account. Also, with all used luminance meters, upon measurement the luminance of a random point in the grid of measuring points, the angle between two tangents of the measured road surface cannot be bigger than 2 arcminutes in the vertical position and no bigger than 20 arcminutes in the horizontal position. At the same time, this angle cannot be less than 1 arcminute, which is the normal angle of human visual acuity. To get results for measuring the road surface luminance, luminance coefficient, reduced luminance coefficient, colour temperature and chromaticity coordinates, first, the illuminance of the road surface at each of the measuring points must be measured, which for all kinds of road surfaces is usually in the range of 1 lx to 50 lx. Illuminance is measured by placing a measuring instrument, such as an illuminance meter, at the measuring point of the road surface grid. Thus, with this measurement method, the measured values of illuminance and luminance obtained by measurement at a random point on the grid of measuring points in a measuring field are influenced by momentary properties of road lighting installations, weather and surrounding conditions, and extraneous and obtrusive light. Also, the measured surface of the road may be newly completed, due to which the reflective properties of this surface of the road surface have not stabilised. The reflective properties of this surface of the road surface may not stabilise until a couple of months.

[0010] A road traffic sign luminance measurement method and the luminance meters applied for it are known from the document US9,171,360B2, DBI/Cidaut Technologies, LLC, 27.10.2015.

[0011] According to this measurement method, road traffic sign surface luminance is measured indirectly based on the difference between two characteristic quantities of the level of reflection of light. Luminance meters are fixed to the front side of the vehicle between the lights. The characteristic quantity of one level of reflection of a road traffic sign surface are fixed based on road surface lighting installations by one luminance meter and the characteristic quantity of the other level of reflection are determined based on the luminous flux coming from the vehicle's lights by the other luminance meter. The difference between the obtained characteristic quantities to the light reflection levels is fixed by an indicating device attached to the vehicle, which has a system for recording the reflection of light, positioning and synchronisation, and which displays the final data from the measurement of road traffic sign luminance.

[0012] A disadvantage of this method and the used luminance meters is their relatively high cost. The method and devices are applicable by using a respective moving vehicle. Thereat, the method and the luminance meters used for its implementation only enable measuring the luminance of road traffic signs.

[0013] A device for measuring the luminance of the surface of the road surface is known from the document WO2013/133033A1, IWASAKI ELECTRIC CO LTD, 12.09.2013. This device enables measuring luminance around the measuring points (grid points) of the measuring field of the road surface by using a tripod and directing the light from the measurement device with an image capturing unit onto the surface of the road, which is analogous to the above-mentioned standard measuring method. Luminance of a road section is measured at the determined measuring points of a measuring field and is then assessed by image processing. Road surface luminance is measured using the spot-lighting of a large number of, e.g., 100, measuring points, which are used for assessing the average luminance. To shorten the measurement time, the target region's image is taken with an imaging device, such as a semiconductor sensor camera, and processed with image processing equipment. Based on the measured values obtained in the given measuring points upon measuring the luminance of the surface of a road section, the average luminance and uniformity of luminance of the target area are calculated in the given grid. The measurement device has a display unit for capturing an image and it displays the measuring range mask, which is located on top of the image captured in the image capturing unit.

[0014] A disadvantage of the described measuring device is its high price and relatively low accuracy. For calculating the luminance values, the measuring instrument uses grayscale, and due to its light reflecting characteristics (according to spectral distribution), it cannot be calibrated. The measuring device uses imaging software, which increases meas-urement capacity and the inaccuracy of measuring. In addition, this measurement device enables measuring the lumi-nance of the surface of road surface illuminated by only certain determined lighting installations and also does that relatively inaccurately, i.e., with an approximately 30% measurement uncertainty from the measurement result.

[0015] The method and device used for measurement the surface luminance coefficient and reduced luminance coefficient of measurement objects, including samples of road surfaces prepared from different materials, are known from the document US7,872,753B2, Schreder, 18.01.2011. According to this measurement method, a bundle of light

rays is directed in an open environment from the light source to the surface of the studied measurement object with a diameter of 113 mm gradually fixed at 0-, 30-, 50- or 70-degree angles from the surface normal of the measurement object. The measured luminance values of the light reflected from this 113 mm diameter surface of the measurement object are fixed by respective sensitive elements based on the horizontal of the surface in the direction of 5, 10, 20, 30, 40, 50, 60, 70 or 80 angular degrees. The measured values fixed by the sensitive elements are the basis for calculating the luminance coefficient and reduced luminance coefficient. As a result, values of light reflected from the surface of the measurement object are obtained, which is a basis for calculating the luminance coefficient and reduced luminance coefficient of the surface of liquids as well as the surface of objects of fibrous material (road surface samples) depending on the angle of incidence of light and the direction of the luminance fixing element in relation to the surface of the measurement object. According to the method, the illuminance of the light directed to the measurement object is in the range of 5,000 lx to 15,000 lx, wherein illuminance is not measured.

[0016]   The mobile device used for realising the method, which is placed above the measurement object, consists of a curved housing open from below and from the sides. Light source assemblies and sensitive elements fixing luminance have been attached to the surface of the curved housing positioned at an angle. At that, the light source assemblies are fixed at a 0-, 30-, 50- and 70-degree angle from the vertical direction. The luminance fixing sensitive elements used for measuring the reflective characteristics of the 113 mm diameter surface of the illuminated measurement object in an open environment have been fixed in place and are directed to the surface of the measurement object at a 5-, 10-, 20-, 30-, 40-, 50-, 60-, 70- and 80-degree angle from the horizontal.

[0017]   The described technical solution is the closest solution to the present invention and has thus been taken as a prototype.

[0018]   The disadvantage of the technical solution is the fact that the method is only intended for determining the luminance coefficient and reduced luminance coefficient of the surface of measurement objects. The measurement method is measurement-intensive (measurement is performed at several different angles directing light and fixing the reflection of light) and does not enable measuring any of the characteristics of lighting reflected from the surface of the road surface which are detectable to the human eye in a vehicle or when walking, as the illuminance of the surfaces of road surfaces is usually between 1 lx and 50 lx. This measurement method is effective in the measurement object surface illuminance range of 5,000 1x to 15,000 1x. The method has a relatively low accuracy level, as upon calculating luminance coefficients, their values are not associated with the measured illuminance of the light falling onto the surface of the measurement object. The light sources used in this technical solution lack spectral definition and the possibility of adjustment. Uncertainty of the luminance values fixed by sensitive elements is unknown. Also, the light directed at the measurement object is diffused and there is no possibility for it to be precisely targeted to a measuring point on the measurement object surface.

Disclosure of invention

[0019]   The object of the present invention submitted for protection of the measurement method and device for measuring values characteristic of reflection of light on the surface of the object is to increase universality, decrease measurement capacity and ensure the opportunity for measuring the values of light reflected from the surface of the road surface, with an increase in their measurement accuracy by eliminating the influence of the momentary properties of road lighting installations, weather and surrounding conditions, and extraneous and obtrusive light.

[0020]   This objective is achieved by the method and device of this invention for measuring the values characteristic of reflection of light on a surface. At that, when using the measurement method, the measurement object is the road surface or pavement such as asphalt, concrete, gravel, composite coverings, etc., and when implementing the method, should the need arise, the first thing to be done, is to check whether the method is adjusted to the measurement conditions for measuring lighting values. For that, the bundle of light rays coming from the calibrated light source without any external influence is directed at an angle to the surface of the sensor of the illuminance meter that is placed at the measuring point on the surface of the road surface, the position of the centre of the sensor surface is aligned with the measuring point on the surface of the road surface, and illuminance, spectral distribution of light and colour temperature are measured. If the measured values show that the measurement conditions are not compatible with the lighting measurement method, the light source luminous flux, the angle of incidence of the bundle of light rays of the light source (direction in relation to the surface of the road) and the distance of the light source are adjusted until the measurement conditions are met, i.e., the method is adjusted for measuring lighting characteristics, and then the values of illuminance of the sensor surface, spectral distribution of light and colour temperature are fixed as reference values. These reference values are necessary, as without them, it is not possible to determine the values of light characteristics reflected from the road surface, excluding the luminance coefficient and reduced luminance coefficient values, which can be determined at a relatively low level of accuracy, which significantly increases the universality of the measurement method and decreases measurement capacity. Next, the holder and the sensor are removed from the measuring point of the measuring grid on the road surface and a bundle of light rays at the adjusted measurement conditions of lighting and free

from the effects of external influences is directed to the measuring point on the surface of the road surface being measured, and from this surface, as a result of the impact of the bundle of light rays free from the impact of external influences to the sensing element of the luminance meter, the measured values of the lighting characteristics reflected from the surface surrounding the measuring point on the surface of the road surface are fixed, such as luminance, luminance coefficient, reduced luminance coefficient, colour temperature, chromaticity coordinates and other measure values. These measured values are fixed under the adjusted measurement conditions for measuring the values of light reflected from the surface of the road surface. If a situation should arise where the measurement conditions of the named light values do not comply with the adjusted measurement conditions, then the observation angle of the luminance meter and the distance of the sensor of the luminance meter from the centre of the measured surface (measuring point) are adjusted to ensure this. After adapting the measurement conditions, the measurement data/measured values obtained via measuring are directed into a programme-based calculation model, and the measurement results for the characteristics of light reflected from the surface of the road surface are obtained from the calculation model together with the uncertainty of these results and are presented on an indicating device or on a computer screen.

[0021]   As the implementation of the method removes the impact the location of the light sources next to the grid of measuring points in the measuring field of the road surface and the light produced by them have on the measurement of the luminance of the road surface, this significantly increases the measurement accuracy of all the characteristics of light reflected from the road surface.

[0022]   The method also allows measuring the characteristics of light reflected from the surface of the road surface in a situation where the bundle of light rays directed from the light source is perpendicular with the surface of the measurement object. In that case, the position of the centre of the sensor surface is aligned with the measuring point on the road surface in an inclined direction, by swapping the places of the light source assembly and the measuring point position fixator, which in turn increases the universality of the method.

[0023]   To implement the measurement method, a measurement device is used, which is composed of a curved housing with an open bottom, and a light source assembly and luminance-fixing sensitive element attached to this curved top part at an angle. A curved segment-shaped side panel has been fixed in place on both sides of the housing, two longitudinally and angularly adjustable opposite tubular protective elements have been attached to the inside of the adjustable curved surface part of the housing, which eliminate the impact of external influences, and a third tubular protective element has been rigidly fixed in the symmetry plane of the housing to the inside of the curved housing, which helps eliminate external influences and has a centreline perpendicular to the support surface of the housing. Adjustment of the two tubular protective elements longitudinally and angularly is enabled by the circular grooves passing through the side panels with fastening parts. A luminance meter with an axially adjustable and fixable sensing element is attached to the external end element on one of the tubular protective elements as the luminance-fixing sensitive element. To the external end element of the two other tubular protective elements is attached in an adjustable and fixable way a light source assembly with supply, adjustment and guiding parts, and a position fixator, and to the external surface of the rear side panel are attached two swivel joints with the swivel elements attached to the rotatable holder carrying the sensor of the illuminance meter. Furthermore, the light source assembly, measuring point position fixator, luminance meter, the illuminance meter attachable to the side panel of the measuring instrument housing and the illuminance meter sensor in the holder are connected to a computer with a wire or wirelessly, and the light source assembly and the measuring point position fixator attached in an adjustable and fixable way to the end surfaces of the tubular protective elements are interchangeable.

[0024]   By enabling the adjustability of the two tubular protective elements longitudinally and at an angle, the necessary adjustment of the measurement conditions for the lighting characteristics directed to the road surface as well as the characteristics of light reflected from this surface is achieved, which increases the universality of the measurement device, reduces measurement capacity and enables more accurate fixing of the obtained measured values.

[0025]   By attaching the rotatable holder carrying the illuminance meter sensor to the side panel of the measurement device housing, constant control over the adjustment of the measurement conditions for illuminance and values related to it is achieved, which increases the accuracy of the fixed reference values and thus also the accuracy of the measurements of the characteristics of light reflected from the road surface.

[0026]   Connecting the light source assembly, measuring point position fixator, luminance meter, the illuminance meter attachable to the side panel of the measurement device housing and the sensor of the illuminance meter to a computer significantly reduces the time the measurement device requires for measuring, facilitates managing the measurement procedure, performs necessary calculations and other necessary operations related to measuring, which in turn reduces measurement capacity and increases universality.

Brief description of drawings

[0027]   The functioning of the method according to the present invention and the construction of the device realising its functioning are explained in the description with reference to the following figures, wherein

Figure 1 shows the conceptual operating scheme of the measurement method for values characteristic of reflection of light on a surface.

Figure 2 shows a front view of a measurement device for measuring values characteristic of reflection of light on a surface in a situation where the method is being applied.

Figure 3 shows a front view of the measuring instrument of figure 2 in an enlarged form (luminance meter 13 has been removed, which is why the contours of the luminance meter have been depicted with a thinner line).

Figure 4 shows the front view of the measurement device according to the invention with a half-section and the holder lowered.

Figure 5 shows a section of the measurement device along line A-A on figure 4.

Figure 6 shows the rear view of the measurement device with the holder raised.

Figure 7 shows the graphic presentation of the dependence between the road surface luminance values obtained from measuring the luminance of different road surfaces with the help of the device (prototype of the device) and colour temperature.

Detailed description of the embodiment

[0028]   The conceptual operational scheme of the measurement method according to the invention shown in Figure 1 consists of the following: measurement object, which is the road surface 1, measuring point 2 of the measuring field grid formed on the surface of the road surface, holder 3, illuminance meter 4, sensor 5 of the illuminance meter 4, light source 6, bundle of light rays 7, first tubular protective element 8, surface 9 of sensor 5, surface 10 surrounding the measuring point 2 on the surface of the road surface 1 used for measuring luminance, to which a bundle of light rays 7 is directed and which is touchable when measuring luminance, bundle of light rays 11 reflected from the surrounding surface 10, second tubular protective element 12, luminance meter 13, sensing element 14 of the luminance meter 13, computer 15, position fixator 16 of the measuring point 2, third tubular protective element 18 used for attaching the position fixator 16 and directing the beam of touch 17, wherein the beam of touch 17 is directed perpendicularly to the surface 10 surrounding the measuring point 2. The bundle of light rays 7 of the light source 6 depicted on the scheme is directed to the measuring point 2 at an angle α luminance of the light reflected from the surface 10 surrounding the measuring point 2 is viewed at an angle β based on the bundle of light rays 11 and the accurate fixation of the position of the centre of the surface 9 of the sensor 5 of the illuminance meter 4 is checked and specified upon adjusting the measurement method as well as upon measuring the values characteristic of the luminance of the surface 10 surrounding the measuring point on the road surface 1 (in that case, the feature being fixed is the position of the measuring point 2 on the road surface 1 at the angle γ in the direction of the beam of touch 17). The light source 6 is attached at a distance l from the measuring point 2 on the road surface 1, the sensing element 14 of luminance meter 13 is at a distance l_1 from the measuring point 2 and the distance of the beam of touch 17 of the position fixator 16 from the surface 10 surrounding the measuring point on the road surface 1 is l_2. For controlling the measurement operation according to the presented method and processing the received measured values, the illuminance meter 4, sensor 5 of the illuminance meter 4, light source 6, luminance meter 13 and position fixator 16 can be connected to a computer 15 by a wire or wirelessly. If necessary, the method also allows to switch the positions of the light source 6 and the position fixator 16.

[0029]   The measurement device presented in figure 2 or 4 consists of the following components: holder 3; sensor 5; housing 19, which consists of two parallel segment-shaped side panels 20, between which are attached, on opposite sides, the first and second tubular protective element 8, 12 that are longitudinally and angularly adjustable, and in the transverse direction, a third tubular protective element 18, which is fixed in place and perpendicular with the lower end surface of the housing 19; the longitudinal and angular adjustment of the first and second tubular protective elements 8 and 12 is enabled by circular grooves 21 formed in the side panels 20 passing through the side panels 20 together with fastening parts or mounting members 22; assembly 23 of the light source 6 with feed, adjustment and guiding parts; a luminance meter 13 and a position fixator 16, which are respectively attachable to the external end elements of the tubular protective elements 8, 12 and 18 with the possibility of axial adjustment and fixing thanks to a transition fit; two swivel joints 24, which are fixed to the outer surface of one of the side panels 20 of the housing 19, e.g., in Figure 3, this is the left side panel 20, and the swivel elements of these joints are fixed to the rotatable holder 3 carrying the sensor 5.

[0030]   Figure 3 consists of the following components: housing 19 composed of two side panels 20 (on the figure, the left side panel and right side panel), tubular protective element 12 fixed between the side panels, grooves 21 passing through the side panels 20 together with fastening parts 22 enabling the adjustment and fastening of the tubular protective

element 12, illuminance meter 4 and swivel joints 24 fixed to the outer surface of one side panel 20 (on the figure, the left side panel). In figure 3, the solid line denotes the position of the sensor 5 holder 3 during the adjustment of the measuring instrument (adjustment of the measurement method), and the dashed line denotes the position of the holder 3 carrying the sensor 5 of the illuminance meter 4 with the help of swivel joints 24, the position being fixed for the duration of measuring the values characteristic of the reflection of light on the surface of the road surface 1 (see figure 1) after the measuring instrument is adjusted for taking measurements.

[0031]　The measurement method for values characteristic of the reflection of light on a surface is performed with the device as follows.

[0032]　Swivel joints 24 are fixed to the bottom part of one of the side panels 20 (on figure 3, the left side panel) of the device housing 19, which allow the holder 3 of the sensor 5 of the illuminance meter 4 to be rotated from being supported on the measuring instrument to the bottom end surfaces of the side panels 20 of the measuring instrument housing 19 and be fixed to this position, as shown in figures 2 and 3. After fixing the holder 3, the measuring instrument, being supported with the lower end surfaces of the side panels 20 to the upper surface of the holder 3, is lifted to the measuring point 2 of the grid on the surface of the road surface 1, so that the lower surface of the holder 3 lies on top of the road surface 1 and the centre of the surface 9 of the sensor 5 is aligned with the measuring point 2 on the road surface 1, after which the setup of the measuring instrument, i.e., the adjustment of the measurement method for light characteristics, commences. The centreline of the first tubular protective element 8 is set at the angle α in relation to the surface of sensor 5 and the distance l of the light source 6 of the assembly 23 from the centre of the surface 9 of sensor 5 is set, whereafter the named values are fixed. In the assembly 23, the calibrated light source 6 is switched on, which has a stabilisation time for conducting measurements that is known, and the warming of the assembly 23 of the light source 6 is taken into account. Next, light (bundle of light rays 7) from the light source 6, e.g., a calibrated spectral distribution (LED) light source, which has an adjustable luminous flux, and which is itself replaceable, is now directed to the surface 9 of sensor 5 at the angle α from the distance l, which by calculations, corresponds to the measurement conditions of lighting. Then, the illuminance, spectral distribution and the colour temperature of light on the surface 9 of the sensor 5 are measured with the illuminance meter 4, e.g., a spectral illuminance meter (lux meter), attached to the outer surface of one of the side panels 20 (on figure 3 or 5, the left side panel) of the measuring instrument 19 protected from external influences as the bottom end surfaces of the side panels 20 of the measuring instrument housing 19 are also tightly against the upper surface of the holder 3, and the obtained values are fixed. Based on these values, the lighting measurement conditions of the method according to the invention are checked. If compliance has been ensured according to the fixed values, the measured values of light characteristics are taken as reference values. If compliance of the measurement conditions is not satisfactory, the method is applied again, i.e. new adjustment of the measuring instrument, based on which the angle α of the bundle of light rays 7 (angle α of the centreline of the tubular protective element 8) and the distance l of the light source 6 of assembly 23 is changed to the extent appropriate, as a result of which, as accurate lighting measurement conditions of the surface of the road surface as possible are assured according to the real conditions of the road surface. Based on the measured values obtained thereafter, the values for illuminance, spectral distribution and colour temperature of light directed to the surface 9 of the sensor 5, which during measurement is the surface 10 surrounding the measuring point 2 on the road surface 1, are determined with the output device of the illuminance meter 4 or a computer 15, and these values are taken as reference values, which are taken into account for measurements and which are the basis for measuring the values characteristic of the reflection of light directed to the surface 10 surrounding any measuring point 2 of the grid on the road surface 1. Measurement device is lifted, the holder 3 is released and swivelled together with the sensor 5 with the help of swivel joints 24 against the back panel 20 of the measuring instrument housing 19 and is fixed to this position (see figure 3 and 6). The measuring instrument is then placed back above the measuring point 2 of the grid on the road surface 1, supported on the bottom end surfaces of the side panels 20, and the light (bundle of light rays 7) separated through the tubular protective element 8 from the light source 6 of the assembly 23 is now directed to the surface 10 surrounding the measuring point 2 of the grid on the road surface 1, and the values characteristic to reflection are now going to be probed by the luminance meter 13, e.g., spectroradiometric luminance meter. The direction, i.e., adjusted angle of observation, of the luminance meter 13 in relation to the road surface 1 is β. Thus, the reflection of the light produced from the surface 10 as a bundle of light rays 11 through the tubular protective element 12, which eliminates the impact of external influences, is fixed by the sensing element 14 of the luminance meter 13 under the observation angle β, which is usually, but may not be precisely equal to the angle α adjusted for measuring lighting. If the luminance measurement conditions are insufficient, then in order to ensure the measurement conditions are as accurate as possible, the observation angle β of the luminance meter 13 or the distance l_1 of the sensing element 14 of the luminance meter 13 from the centre of the sensor 5 surface is changed to the extent appropriate, if necessary. However, if the adjustment is in accordance with luminance measurement, the measured values of light reflected from the surface 10 surrounding the surface of the road surface 1 obtained by the luminance meter 13 are transferred by wires or wirelessly to a computer 15. In the computer 15, using the respective programme JETI LiVal® (https://www.jeti.com/cms/index.php/jeti-software/lival) for radiometric data/measured values, the values characteristic of reflection of light on the road surface, such as luminance, luminance coefficient, reduced

luminance coefficient, colour temperature, chromaticity coordinates, spectral distribution of reflected light or other values characteristic to luminance, final measurement results and the uncertainty of these results are obtained in accordance with the measurement task given.

[0033]   Furthermore, using the measuring device, the measurement method allows to fix precisely and also adjust the position of the centre of the surface 9 of the sensor 5 of the illuminance meter 4 upon setting up the measuring instrument, adjusting the measurement conditions for light characteristics, before measuring and after swivelling the holder 3 in the measuring instrument with the help of the swivel joints 24, the precise position of the measuring point 2 and its alignment with the bundle of light rays 11, but also with the centreline of the tubular protective element 12, and the intersection point with the surrounding surface 10 with the help of the position fixator 16 removably attached to the third tubular protective element 18 of the measuring instrument, from the top of the third tubular protective element 18 removing the impact of external influences at the angle γ in relation to the beam of touch 17 and the surface 10 surrounding the measuring point of the road surface 1 or perpendicularly, i.e., at a 90-degree angle or close to it, with the bottom end surfaces of the side panels 20 of the measuring instrument housing 19. If the values characteristic of the light reflected have been measured in the first measuring point 2 on the road surface 1, the device is moved to a following random measuring point 2 on the road surface 1 grid. To a side panel 20 of the device housing 19 has been attached a rotatable holder 3 with the sensor 5 of the illuminance meter 4 by swivel joints 24, such that when setting up the measuring instrument, adjusting the measurement conditions, the surface 9 of the sensor 5 when measuring with this instrument aligns with the surface 10 surrounding the measuring point 2 on the road surface 1. As the random measuring point 2 on the road surface 1 grid is on the same plane as the surface 9 of the sensor 5 as during the previous adjustment of the method, the position fixator 16 can easily be used to align the position of the centre of the sensor 5 when setting up the measuring instrument with the position of the random measuring point 2 on the road surface 1 when measuring with the measuring instrument.

[0034]   In each following random measuring point 2 on the road surface 1 grid, the measurement of the values characteristic to the reflection on the surface with an already set up measuring instrument, under adjusted measurement conditions, is performed without any setting or adjustment operations, similarly to the above, wherein the exact position of the random measuring point 2 on the road surface 1 grid is fixed with the position fixator 16. This is how the values characteristic to reflection of the surface are measured in all measuring points 2 on the road surface 1 grid.

[0035]   If there is a need for measuring values characteristic of the reflection of light on a surface in a situation where light is directed only perpendicularly with the road surface 1 being measured, then this situation can be solved with the measuring instrument by switching the positions of the assembly 23 with the light source 6 and the position fixator 16 (see figure 2). Next, similarly to the above, the measuring instrument is set up, measurement conditions are applied, with the sensor 5 of the illuminance meter 4, by directing the light from the light source 6 perpendicularly with the surface 9 of the sensor 5 and performing the measurement of illuminance perpendicularly to the surface 9 of the sensor 5 with adjusting the distance of the light source 6 and the luminous flux. In this case, after the measuring instrument is set up, measurement conditions are applied, the measurement of the values characteristic to the reflection of light on the road surface 1 is performed similarly to the above, except that fixing the position of the centre of the surface 9 of the sensor 5 during user adjustments, applying measurement conditions, and fixing the measuring point 2 on the road surface 1 during measurement with the measuring instrument are now performed in an inclined position, at the angle α.

[0036]   A holder 3 with the sensor 5 of the illuminance meter 4, that can be swivelled, is fixed to the lower part of the measuring instrument housing 19 in such a way that when setting up the measuring instrument, the surface 9, when measuring with the measuring instrument, aligns with the surface 10 surrounding the measuring point 2 on the road surface 1. After checking the measurement conditions, the sensor 5 and the holder 3 can be swivelled to the side via the swivel joints 24 for the duration of the measuring, and after that, the lower part of the device housing 19 will be supported on the surface 10 surrounding the measuring point on the road surface 1 and the previous performance of device adjustment, application of measurement conditions, remains valid.

[0037]   The new measurement method and device according to the present invention developed for values characteristic of the reflection of light are one way of realising the above. Furthermore, the developed invention enables getting new reliable values for the values characteristic of the luminance (reflection of light) of modern road surfaces, such as luminance coefficient, reduced luminance coefficient, colour temperature and chromaticity coordinates, at the same time enabling the monitoring of all measurement results of values characteristic to luminance.

[0038]   The effect of using the method and device is, that resulting from its application, for example in case of asphalt surfaces of modern roads, which have traditional gas-discharge lighting or lighting solutions already based on the modern LED technology, it is possible to operationally evaluate changes in values characteristic to reflection of light in case of changes arising from the wearing of surfaces and the environment, and to propose safer and more effective solutions depending on changes in the traffic environment.

[0039]   The effect of the measurement method and device according to the present invention is also that resulting from their application, the human scotopic and mesopic vision in a dark and dim environment will be taken into account, which has thus far not been implemented, and it is possible to really evaluate the values characteristic to the reflection of light

on road surfaces in the case of lighting solutions based on LED technology used for lighting modern roads, and in the case of modern asphalt and concrete surfaces and different additives used in them. The application of the method takes into account the spectral composition of visible light or the effect of colour temperature on the assessment of the reflection of light from the surfaces, thereby offering safer and more efficient solutions for the traffic environment. Thus, according to the experiment performed using the measurement method and device (prototype of the device) for values characteristic of the reflection of light on a surface, different road surfaces have been evaluated, where if the light falling to the surface has an illuminance of 20 lx, the luminance of light reflected from the same surface has the different values of colour temperature shown on the diagram in figure 7.

[0040]   As the measurement method according to the invention for values characteristic of the reflection of light on a surface is simple and the mobile device used for its application can be used to measure on site, at the measuring point of the measurement grid defined for the road surface, the lighting characteristics reflected directly from the surface of the road surface surrounding this point and the diversity of these values, then this allows to reduce measurement capacity and increase measurement accuracy. The above is also supported by a comparative analysis of the measurement of values characteristic of reflection of light on road surfaces performed with the currently used standard measurement method for road surfaces and the measuring instruments in regular use, as well as with the measurement method and device (prototype of the device) presented in the description of the invention, in terms of some characteristics, which have been presented in the following table.

[0041]   The table presents a comparative analysis of the measurement of values characteristic of the reflection of light performed with the measurement methods and measuring instruments for road surfaces in regular use and with the measurement method and device (prototype of the device) presented in the description of the invention.

Values characteristic of reflection of light on the road surface

Used measurement method	Illuminance	Luminance	Luminance coefficients	Colour temperature	Chromaticity coordinates
Measurement methods of EN 13201-3 and EN 13201-4	Measurable by lux meter with V-lambda correction	Measurable by luminance meter placed on a tripod	Calculable using data from the example of the luminance meter and lux meter and data presented in the standard	Measurable by colour temperature meter	Chromaticity coordinates of light cannot be measured
Measurement method according to the invention	All values characteristic of reflection of light on the road surface are measurable and calculable				

Time required for measuring the values characteristic of reflection of light on the road surface and for calculating their values depends on the time specified in the manual of the used measuring instrument for performing the measurement procedure

Used measuring instruments	Illuminance	Luminance	Luminance coefficients	Colour temperature	Chromaticity coordinates
Measuring instruments in regular use	Lux meter with spectrometric component BTS256 EF	Spectroradiometer with spectrometric component JETI specbos 1211UV	Calculable using data from the example of the luminance meter and lux meter and data presented in the standard	Spectroradiometer with spectrometric component JETI specbos 1211UV	Spectroradiometer with spectrometric component JETI specbos 1211UV
Measuring device according to the invention	All values characteristic of reflection of light on the road surface are measurable and calculable within 2 hours				

The average achievable value of the expanded uncertainty of the measurement and calculation results of the values characteristic of reflection of light on the road surface in per cents from the measurement or calculation results at a level of probability of 95% (the achievable value of the expanded uncertainty of colour temperature and chromaticity coordinates is given with a unit of measurement)

Used measurement method	Illuminance	Luminance	Luminance coefficient	Reduced luminance coefficient	Colour temperature	Chromaticity coordinates
Measurement method of EN 13201-3 and EN 13201-4	10	15	18	20		
Measurement method according to the invention	5	10	12	12	100 K	0.001

[0042] As seen from the data in the table, the method and device according to the present invention help increase measurement accuracy. For the standard measurement method, the table includes data for the average value of the expanded uncertainty of the measurement result obtained at the measuring point on the road surface in per cents from the measurement result (Mõõtetulemuse määramatuse hindamise lähendmeetod valgustehnilistel mõõtmistel. TTU, Inseneriteaduskond, Tallinn, 2019). It turns out that approximately 1/3 of the expanded uncertainty value presented using the standard measurement method is composed of uncertainty components arising from external influences. As the described new measurement method of the invention enables to minimise the proportion of external influences, this allows to significantly reduce the expanded uncertainty of the results from the measurement of lighting characteristics of the road surface (values characteristic to reflection). The possible average values of the expanded uncertainties of the measurement results obtained by using the measurement method according to the present invention presented in the table were confirmed as a result of testing the prototype of the device used for realising the measurement method.

<u>List of details</u>

[0043]

1 - road surface (pavement *in American English*)
2 - measuring point of the grid
3 - holder
4 - illuminance meter; lux meter
5 - sensor
6 - calibrated light source
l - distance between the light source and the centre of the sensor surface
7 - bundle of light rays from a light source
8 - first tubular protective element
α - angle of the centreline of the tubular protective element compared to the surface of the sensor
9 - sensor surface
10 - surface surrounding the measuring point on the road surface
11 - bundle of light rays reflected from the surface of the road surface
12 - second tubular protective element
13 - luminance meter
14 - sensing element of the luminance meter
l_1 - distance between the luminance meter sensing element and the centre of the sensor surface
β - direction of the luminance meter in relation to the surface of the road surface, angle of observation of the luminance meter
15 - computer
16 - position fixator, positioner
17 - beam of touch or surface scanning ray or tactile beam
18 - third tubular protective element
γ - angle between the beam of touch and the road surface
l_2 - distance of the position fixator's beam of touch from the road surface surrounding the measuring point on the road surface
19 - housing of the measuring instrument or measuring instrument body
20 - side panels; on Figure 3, left side panel and right side panel
21 - circular grooves passing through the side panels
22 - fastening parts or mounting members
23 - set of assembled parts or assembly
24 - swivel joints or pivoting hinges

Claims

1. A method for measurement characteristic quantities of reflection of light on road surface (1), during which a luminous flux from a light source (6) is directed at the angle α to the road surface (1), after which the luminance of the light reflected from the road surface (1) is measured at the angle β, and based on the data obtained, a luminance coefficient and a reduced luminance coefficient are calculated, which is **characterised in that** a bundle of light rays (7) free from influences is directed, according to adjusted measurement conditions of lighting, to a measuring point (2) on the road surface (1) from the light source (6) and as a result of the impact of the bundle of light rays free from the

influences quantities of reflection of light on the road surface (1), under the luminance measurement conditions adjusted for a sensing element (5) of an illuminance meter (4), measured characteristic quantities of reflection of light on the road surface (1) surrounding the measuring point (2) on the road surface (1) are fixed, thereafter the measured quantity values are transferred to a programme-based calculation model and the measurement results for characteristic quantities of reflection of light on road surface (1) are obtained from the calculation model together with the uncertainty of the results, results are presented on an indicating device or a computer screen.

2. The method according to claim 1, **characterised in that** before directing light to the road surface (1), lighting measurement conditions are adjusted, pursuant to which the bundle of light rays (7) free from influences from the light source (6) is directed at an angle α to the surface of the sensor (5) of the calibrating illuminance meter (4) placed at the measuring point (2) on the road surface (1), the position of the centre of the surface (9) of the sensor (5) is aligned with the measuring point (2) of the road surface (1), the luminous flux of the light source (6), the falling angle α of the bundle of light rays (7) of the light source (6) and the distance l between the light source and the centre of the sensor (5) surface are adjusted, lighting measurement conditions are ensured, and then, the values obtained for the illuminance, spectral distribution of light and colour temperature on the surface of the sensor (5) are taken as reference values.

3. The method according to claim 1, **characterised in that** before obtaining the measured quantity values of reflection of light on the road surface (1), luminance measurement conditions are adjusted, if needed, which means that the angle of observation β of the luminance meter (13) and the distance l_1 between the sensing element (14) of the luminance meter (13) and the measuring point (2) on the road surface (1) are adjusted.

4. A device for measurement characteristic quantities of reflection of light on a road surface, which comprises a curved measuring instrument housing (19) open from the bottom and an assembly (23) of a light source (6) attached to its surface and positioned at the angle α, and an element (13) fixing luminance, **characterised in that** a curved segment-shaped side panel (20) has been fixed in place on both sides of the housing (19), from the curved surface to the inside of the housing (19) are adjustably attached first and second tubular protective elements (8) and (12) opposite each other adjustable in the direction of angle α and angle β and in terms of distance l and l_1, respectively, wherein their adjustment longitudinally and at the angles α and β, respectively, is enabled due to circular grooves (21) passing through panels (20) formed in the side panels (20) with fastening parts (22), and a third tubular protective element (18) fixed in place from the curved surface to the inside of the housing (19) in the symmetry plane of the housing (19), its centreline (17) being perpendicular with the support surface of the housing (19), wherein the luminance-fixing element (13) is a luminance meter (13) with an axial adjustment and fixing possibility attached to the outer end element of the second tubular protective element (12), and to the outer end element of the third and first tubular protective elements (18) and (8), respectively, a position fixator (16) and a light source (6) assembly (23) with feed, adjustment and guiding parts are attached in an adjustable and fixable way, and to the external surface of one side panel (20) is fixed an illuminance meter (4) and a swivel joint (24) with a rotatable holder (3) carrying the sensor (5) of the illuminance meter (4).

5. The device according to claim 4, **characterised in that** the light source assembly (23), measuring point position fixator (16), luminance meter (13), illuminance meter (4) attached to one of the side panels (20) of the measuring instrument housing (19) and the sensor (5) of the illuminance meter are connected by a wire or wirelessly to a computer (15).

6. The device according to claim 4, **characterised in that** the light source (6) assembly (23) and the measuring point (2) position fixator (16) attached in an adjustable and fixable way to the end surfaces of the first and third tubular protective elements (8) and (18), respectively, are interchangeable.
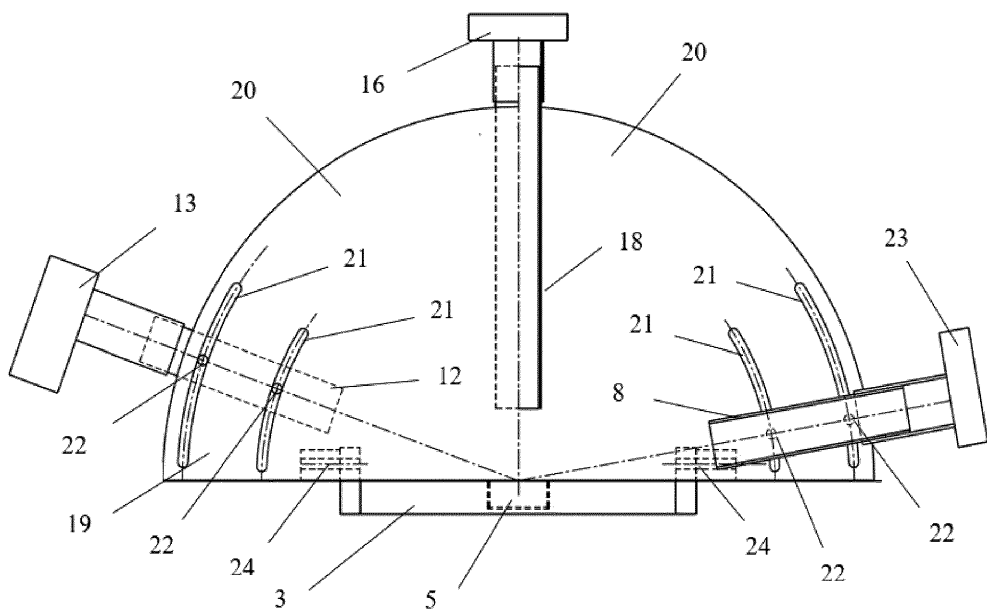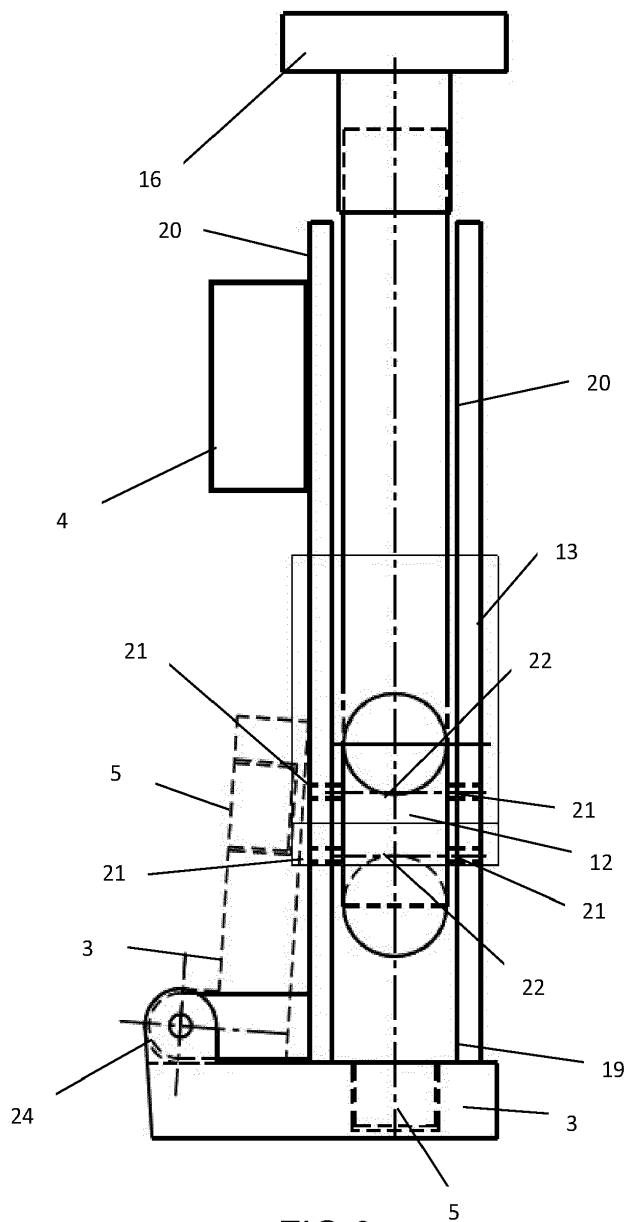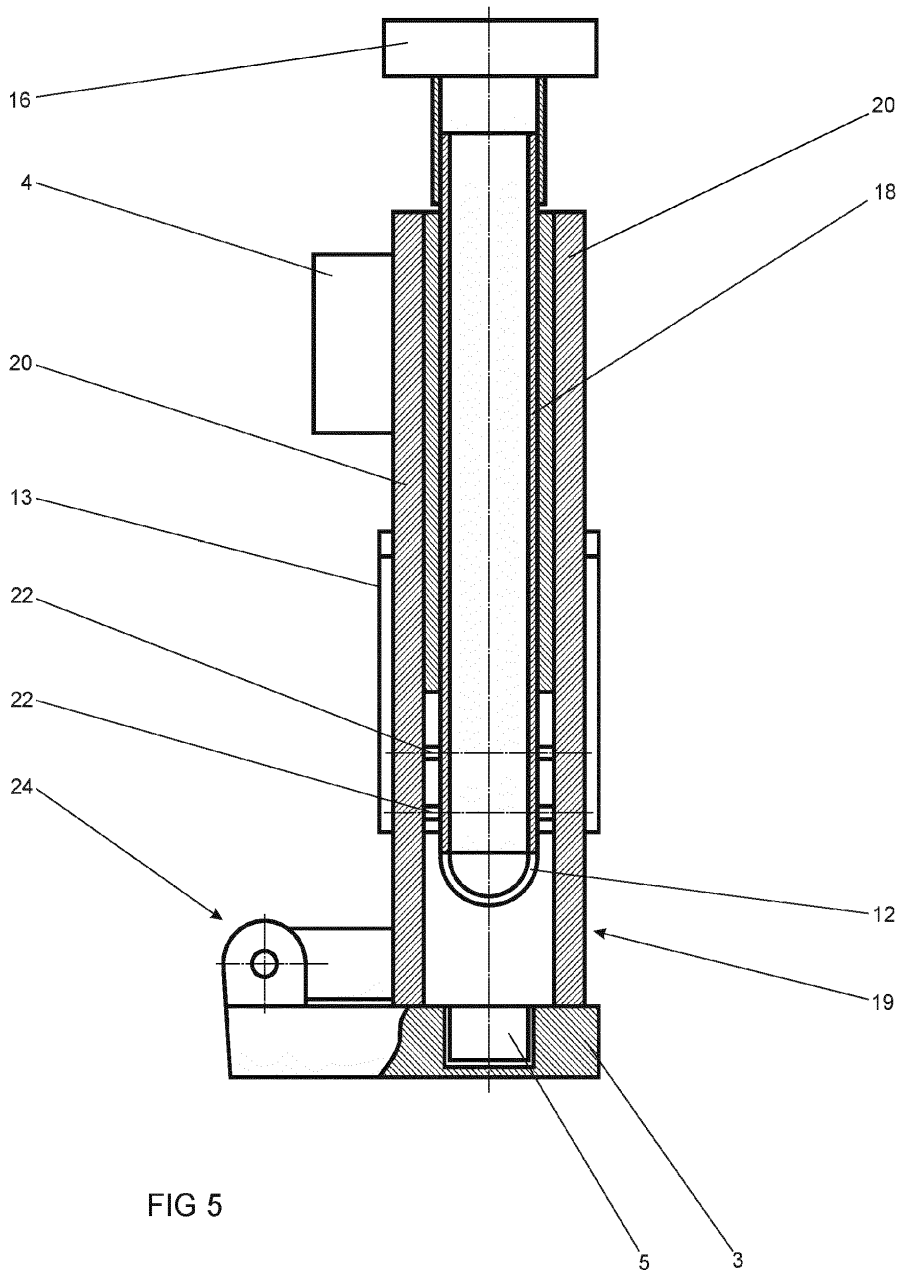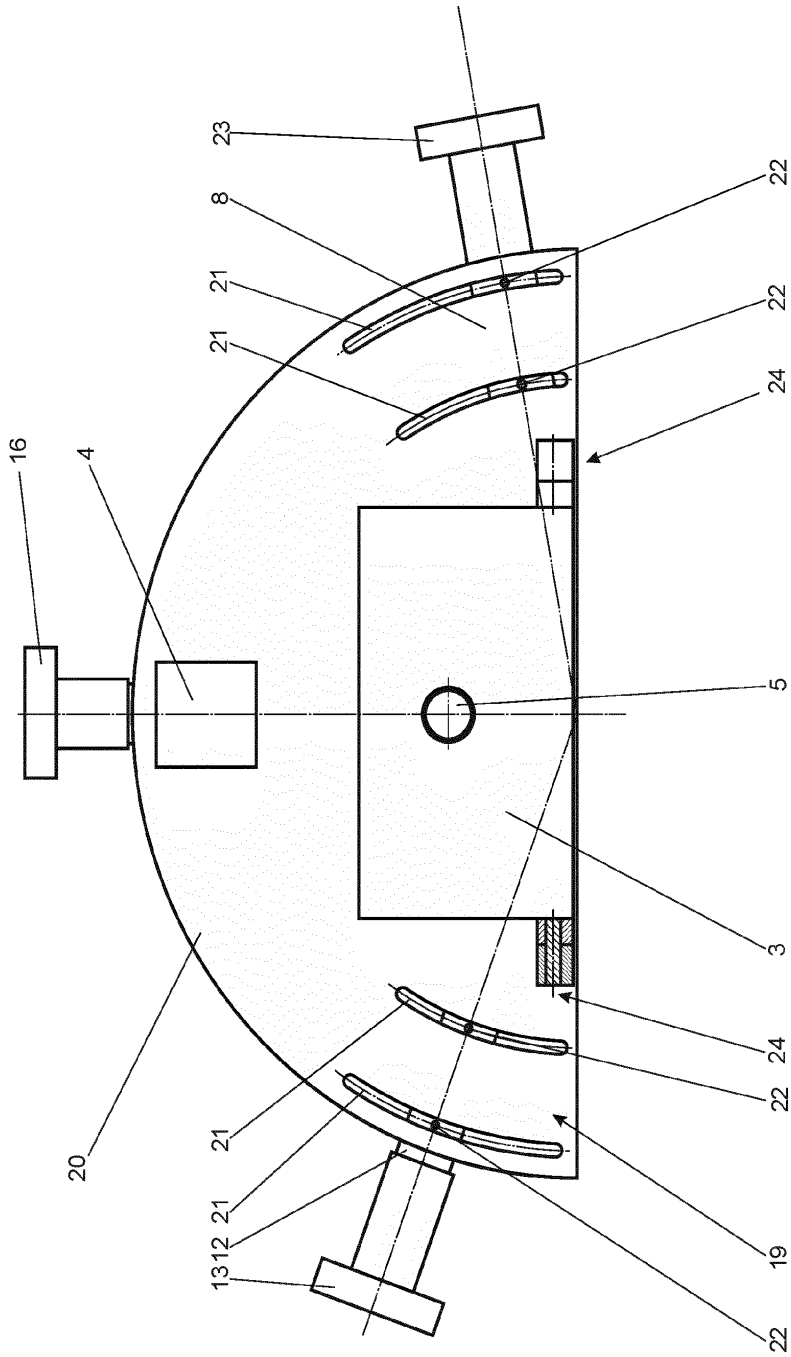
FIG 2

16

20

20

4

13

21

22

5

21

21

12

21

3

22

19

24

3

5

FIG 3

A - A

FIG 5

FIG 6

FIG 4

FIG 1

FIG 7

Europäisches
Patentamt

European
Patent Office

Office européen
des brevets
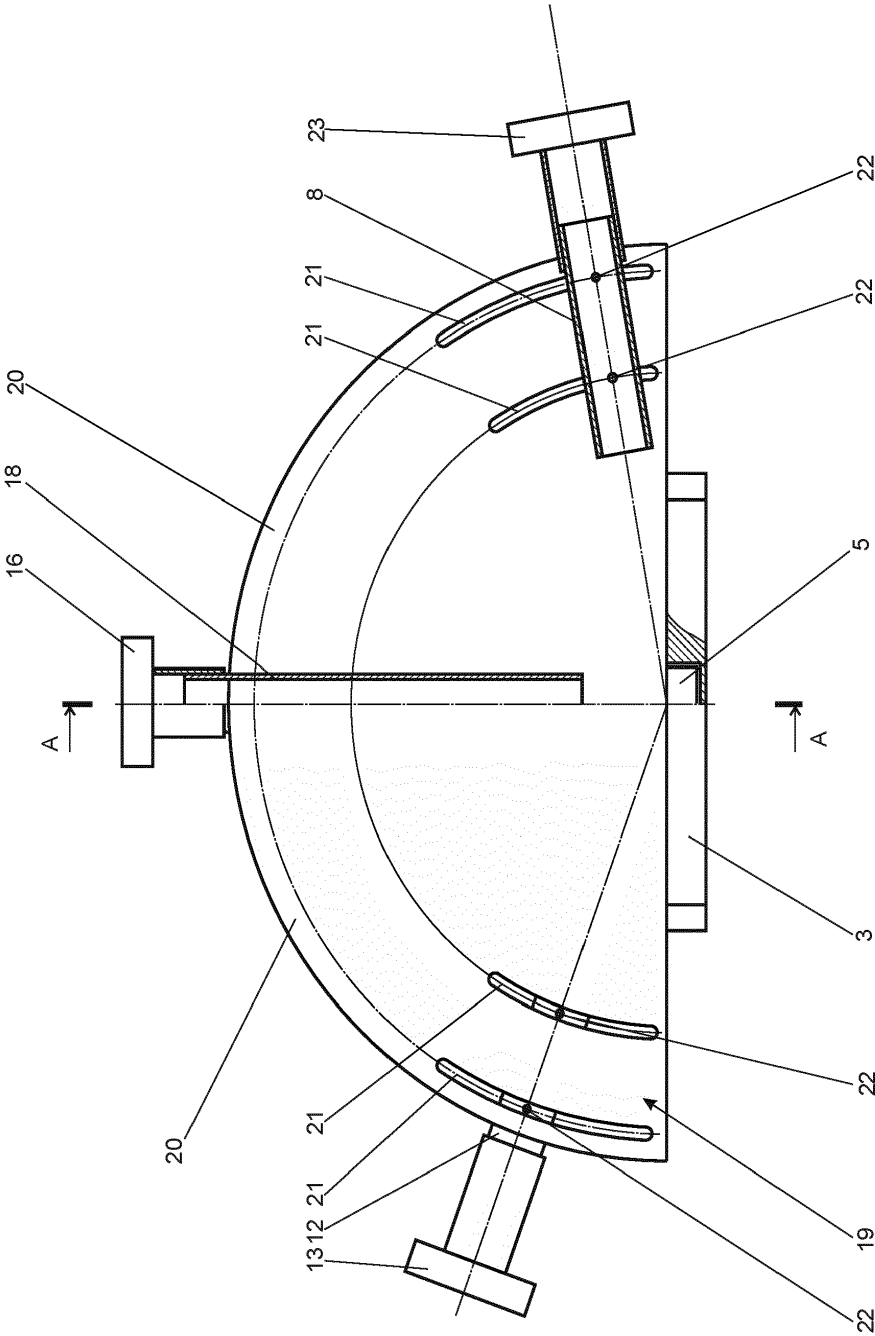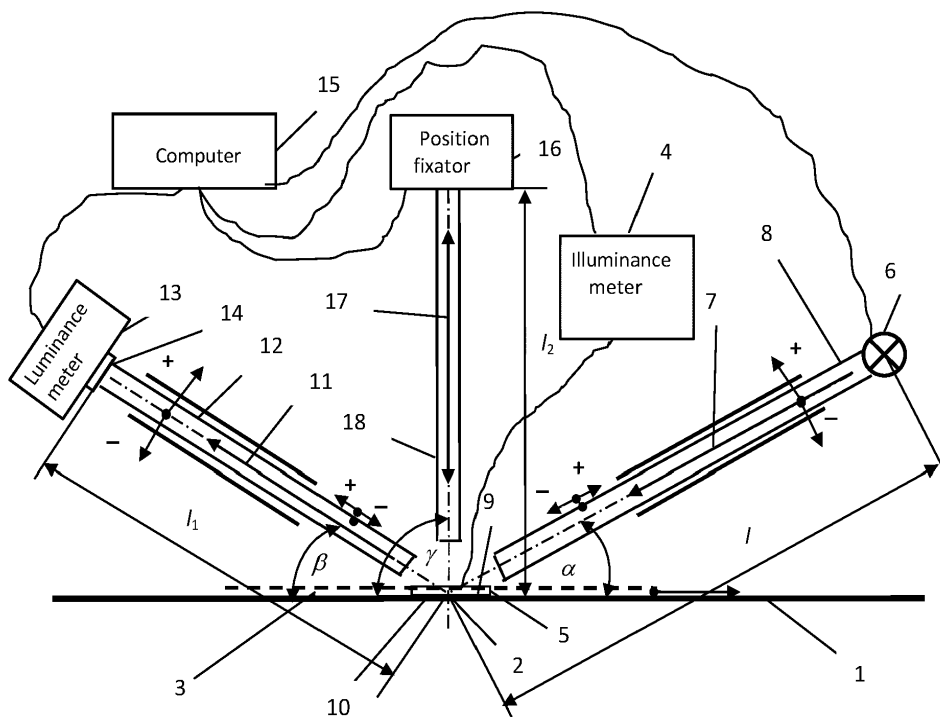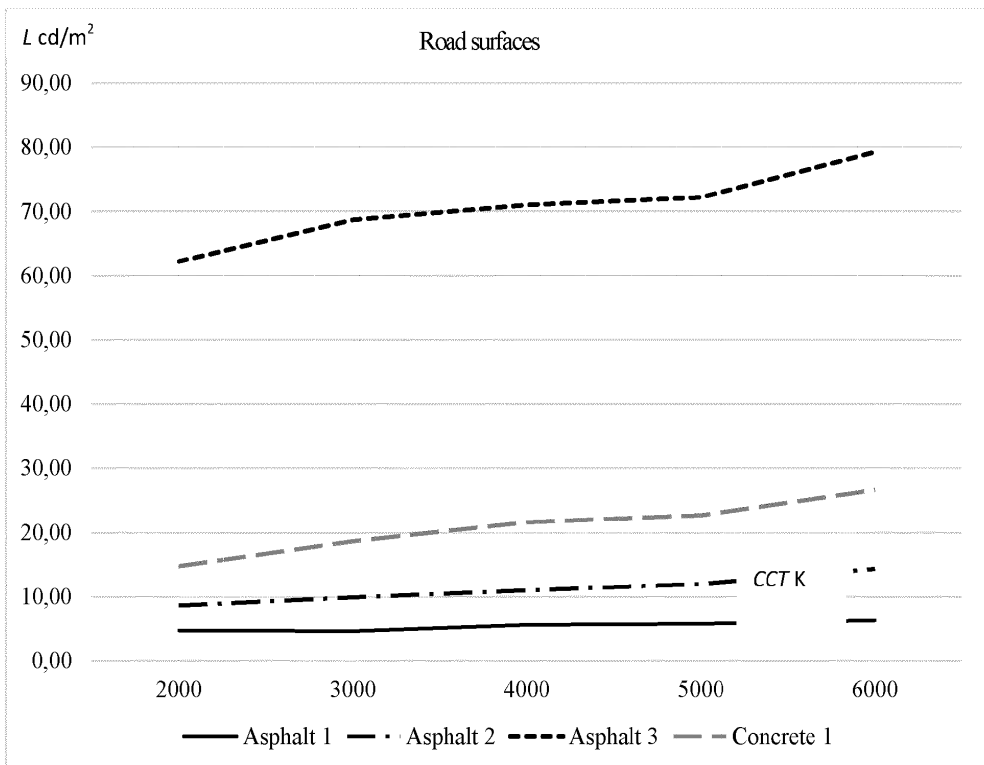
EUROPEAN SEARCH REPORT

Application Number

EP 20 21 4860

DOCUMENTS CONSIDERED TO BE RELEVANT

Category	Citation of document with indication, where appropriate, of relevant passages	Relevant to claim	CLASSIFICATION OF THE APPLICATION (IPC)
Y	US 2008/309942 A1 (FRANKINET MARC [BE]) 18 December 2008 (2008-12-18) * abstract; figure 2 * * paragraphs [0001] - [0047] * -----	1-6	INV. G01N21/47 G01N21/55
Y	US 2012/307041 A1 (FUJIWARA NARIAKI [JP] ET AL) 6 December 2012 (2012-12-06) * figures 1-4 * -----	4-6	
Y	CN 103 674 897 A (UNIV CHINA MINING) 26 March 2014 (2014-03-26) * figure 1 * -----	1-6	
Y	BOMMEL ET AL: "Road Surfaces and lighting", JOINT TECHNICAL REPORT CIE/PIARC, XX, XX, vol. 66, 1 January 1984 (1984-01-01), XP002258261, * abstract; figure 2 * -----	2	

		TECHNICAL FIELDS SEARCHED (IPC)
		G01N

The present search report has been drawn up for all claims

Place of search	Date of completion of the search	Examiner
Munich	9 April 2021	Meacher, David

EPO FORM 1503 03.82 (P04C01)

ANNEX TO THE EUROPEAN SEARCH REPORT
ON EUROPEAN PATENT APPLICATION NO.

EP 20 21 4860

Patent document cited in search report		Publication date	Patent family member(s)		Publication date
US 2008309942	A1	18-12-2008	BR	PI0618977 A2	20-09-2011
			CA	2630231 A1	31-05-2007
			CN	101313208 A	26-11-2008
			EC	SP088576 A	30-07-2008
			EP	1790972 A1	30-05-2007
			EP	1952126 A1	06-08-2008
			US	2008309942 A1	18-12-2008
			WO	2007060181 A1	31-05-2007
US 2012307041	A1	06-12-2012	CN	102809567 A	05-12-2012
			KR	20120135038 A	12-12-2012
			TW	201305554 A	01-02-2013
			US	2012307041 A1	06-12-2012
CN 103674897	A	26-03-2014	NONE		

For more details about this annex : see Official Journal of the European Patent Office, No. 12/82

REFERENCES CITED IN THE DESCRIPTION

This list of references cited by the applicant is for the reader's convenience only. It does not form part of the European patent document. Even though great care has been taken in compiling the references, errors or omissions cannot be excluded and the EPO disclaims all liability in this regard.

Patent documents cited in the description

- US 9171360 B2 **[0010]**
- WO 2013133033 A1 **[0013]**

- US 7872753 B2 **[0015]**

Non-patent literature cited in the description

- Road Surface Photometric Characterisation and Its Impact on Energy Savings. *Coatings,* 2019, vol. 9, 286 **[0005]**

Curriculum vitae

Personal data

    Name: Toivo Varjas
    Date of birth: 28.09.1967
    Place of birth: Estonia
    Citizenship: Estonian

Contact data

    E-mail: toivo.varjas@taltech.ee

Education

2014 – 2020	Tallinn University of Technology – PhD
1985 – 1992	Tallinn University of Technology – Mechanical Engineer (Cum Laude)
1982 – 1985	Tallinn 3rd Secondary School (Lilleküla Gymnasium)

Language competence

Estonian	Native speaker
Finnish	Fluent
English	Advanced
Russian	Advanced

Professional employment

2020 – …	Tallinn University of Technology, doctoral student-engineer, measurement specialist of an accredited lighting technology
2017 – 2020	Tallinn University of Technology, Early Stage Researcher
1997 – …	MINOTEC DC OÜ, Chairman of the board
2014 – 2017	Tallinn University of Technology, Administrative Officer
1994 – 1997	MINOTEC AS, Chairman of the board
1993 – 1994	AS SPIN DATA, Project Manager/ Sales Engineer
1992 – 1993	AS Mammut, Engineer
1990 – 1991	Pekolan PTO-Markinointi OY, Automation Engineer for wood processing lines

Scientific work and Research and Development projects

2019 – 2022	INTERREG LUCIA #R096, "Lighting the Baltic Sea Region - Cities Accelerate the Deployment of Sustainable and Smart Urban Lighting Solutions"
2019 – 2020	"Lighting measurements of Tallinn street lighting (7.09.2020–4.01.2021)"
2019 – 2020	"Applied research of problematic components of Kiuto smart building system and product development (1.04.2019–31.07.2020)"
2019 – 2020	LEP19093 "Technical expertise of the War of Independence Victory Column"
2017 – 2018	Lep18002 "Report evaluation of Comlight streetlighting pilot project"
2015	LEP 15023 Expertise "Street lighting analysis and trends in Harku parish"
2012 – 2014	Lep12184 "Investigation of existing outdoor lighting for prospective improvements. Proposals and recommendations for implementation of new light sources, luminaires and their control systems"

Elulookirjeldus

Isikuandmed

Nimi:	Toivo Varjas
Sünniaeg:	28.09.1967
Sünnikoht:	Eesti
Kodakondsus:	Eesti

Kontaktandmed

E-post:	toivo.varjas@taltech.ee

Hariduskäik

2014 – 2020	Tallinna Tehnikaülikool – PhD
1985 – 1992	Tallinna Tehnikaülikool – mehaanika insener (Cum Laude)
1982 – 1985	Tallinna 3. Keskkool (Lilleküla Gümnaasium)

Keelteoskus

Eesti keel	Emakeel
Soome keel	Kõrgtase
Inglise keel	Edasijõudnu
Vene keel	Edasijõudnu

Teenistuskäik

2020 – …	Tallinna Tehnikaülikool, doktorant-insener, akrediteeritud valgustehnikalabori mõõtespetsialist
2017 – 2020	Tallinna Tehnikaülikool, doktorant-nooremdeadur
1997 – …	MINOTEC DC OÜ, Tegevjuht/ Juhatuse liige
2014 – 2017	Tallinna Tehnikaülikool, haldusspetsialist
1994 – 1997	MINOTEC AS, Tegevjuht/ Juhatuse liige
1993 – 1994	AS SPIN DATA, Projektijuht/ Müügiinsener
1992 – 1993	AS Mammut, Insener
1990 – 1991	Pekolan PTO-Markinointi OY, puidutöötlusliinide automaatikainsener

Teadus- ning arendusprojektid

2019 – 2022	INTERREG LUCIA #R096, "Valgustades Läänemere piirkonda – Linnad mis kiirendavad jätkusuutlike ja nutikate valgustuslahenduste rakendamist"
2019 – 2020	LEEEE20099 "Tallinna tänavavalgustuse valgustehnilised mõõtmised (7.09.2020–4.01.2021)"
2019 – 2020	LEP19033 "Kiuto hooneautomaatika süsteemi probleemsete komponentide rakendusuuring ja tootearendus (1.04.2019–31.07.2020)"
2019 – 2020	LEP19093 "Vabadussõja Võidusamba tehnilise ekspertiisi teostamine"
2017 – 2018	Lep18002 "Comlight tänavavalgustuse juhtimise piloootprojekti tulemuste aruande hindamine"
2015	LEP 15023 Analüüs-ekspertarvamuse "Tänavavalgustuse arengusuunad Harku Vallas koostamine"
2012 – 2014	Lep12184 "Tallinna olemasoleva välisvalgustuse parendamisvõimaluste uurimine ning ettepanekute väljatöötamine uute valgusallikate ja valgustite ning juhtimissüsteemide rakendamiseks"